https://www.mdc-berlin.de/de/veroeffentlichungstypen/clinical-journal-club

Als gemeinsame Einrichtung von MDC und Charité fördert das Experimental and Clinical Research Center die Zusammenarbeit zwischen Grundlagenwissenschaftlern und klinischen Forschern. Hier werden neue Ansätze für Diagnose, Prävention und Therapie von Herz-Kreislauf- und Stoffwechselerkrankungen, Krebs sowie neurologischen Erkrankungen entwickelt und zeitnah am Patienten eingesetzt. Sie sind eingeladen, uns beizutreten. Bewerben Sie sich!

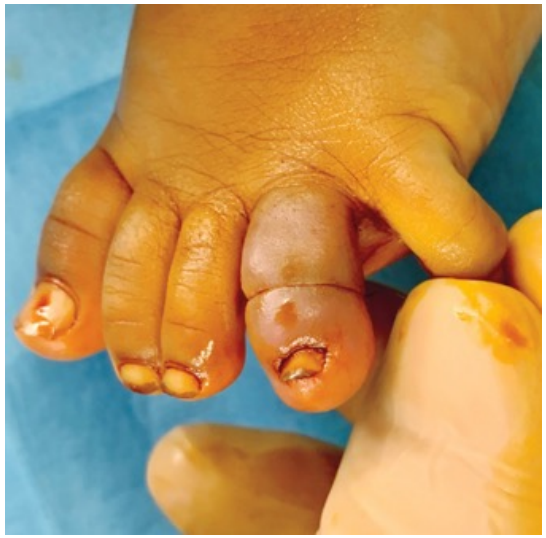

A 6-month-old girl was brought to the emergency department with a 3-day history of redness and swelling of a toe. A physical examination is shown. Which of the following is the most likely underlying cause of the findings?

Allergic reaction
Cellulitis
Hair tourniquet
Non-accidental trauma
Insect bite

A diagnosis of hair tourniquet was made. This condition is characterized by a tightly wound hair or thread coiled around an appendage, most commonly a toe. The constriction may lead to pain, swelling, and ultimately ischemia. Treatment involves application of a chemical depilatory agent or manual removal of the hair for superficial cases, or surgery for deeper tourniquets.

Ein Haartourniquet (auch als Haartourniquet-Syndrom oder Haarfadentourniquet-Syndrom bezeichnet) ist eine seltene Erkrankung, bei der ein Haar oder Faden so fest um einen Körperteil (meist Finger, Zehen oder Genitalien) gewickelt ist, dass die Durchblutung unterbrochen wird. Dies kann zu Schmerzen, Schwellungen und im schlimmsten Fall zu Gewebeschäden oder Nekrose führen.

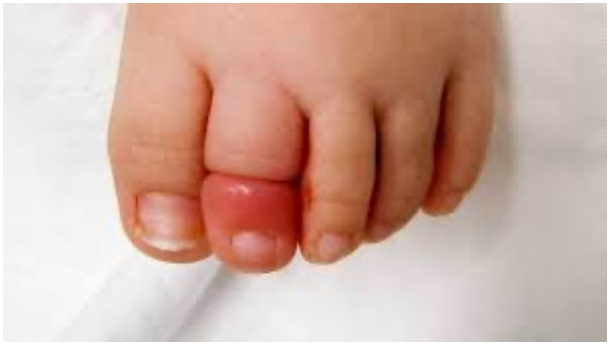

Ursachen und Symptome:

Ein Haar oder Faden kann sich um einen Finger, Zeh oder ein anderes Körperteil wickeln und eine Art Schnürung bilden, die die Blutzirkulation einschränkt.

Symptome:
Typische Symptome sind Schmerzen, Schwellungen, Rötungen und in fortgeschrittenen Fällen bläulich-dunkle Verfärbungen des betroffenen Körperteils. Kinder, insbesondere Säuglinge, zeigen oft inconsolable crying als Zeichen von Unwohlsein.

CD38 ist ein Glykoprotein und ein Enzym, das auf der Oberfläche vieler Immunzellen, insbesondere Plasmazellen, vorkommt. Es spielt eine wichtige Rolle bei der Aktivierung und Proliferation von Immunzellen und wird als Marker für Zellaktivierung und als Ziel für immuntherapeutische Maßnahmen verwendet.

Daratumumab ist ein humaner monoklonaler Antikörper (IgG1κ) der zur Behandlung von multipler Myelom, einer malignen Erkrankung des Knochenmarks, eingesetzt wird. Er bindet an das Glykoprotein CD38, welches auf Myelomzellen stark exprimiert wird, und löst dadurch verschiedene Mechanismen aus, die zum Zelltod der Myelomzellen führen. Daratumumab ist unter dem Handelsnamen Darzalex erhältlich.

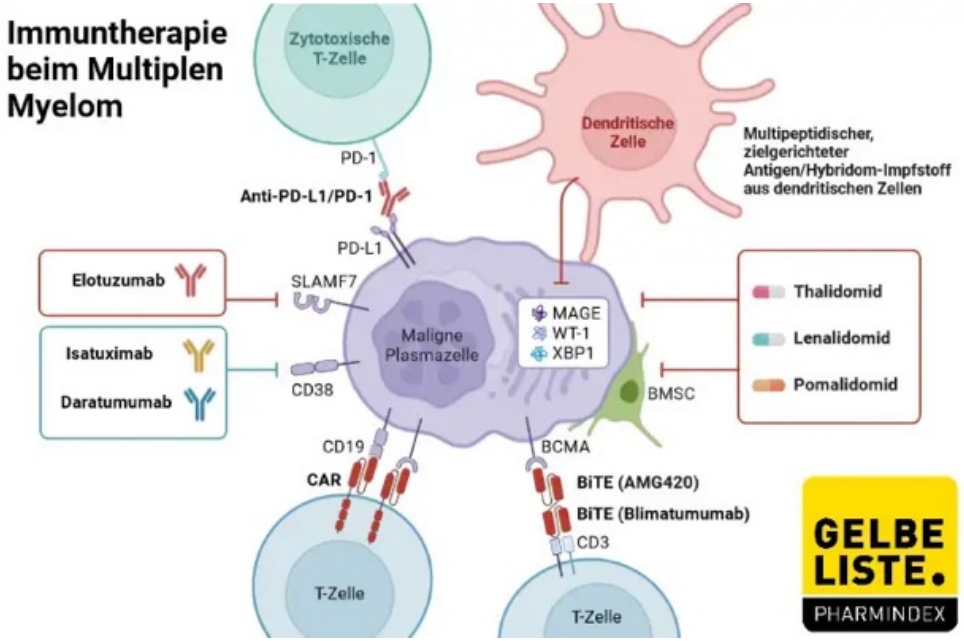

Daratumumab or Active Monitoring for High-Risk Smoldering Multiple Myeloma

(schwelend; glimmen)

Daratumumab, an anti-CD38 monoclonal antibody, has been approved for the treatment of multiple myeloma. Data are needed regarding the use of daratumumab for high-risk smoldering multiple myeloma, a precursor disease of active multiple myeloma for which no treatments have been approved.

In this phase 3 trial, we randomly assigned patients with high-risk smoldering multiple myeloma to receive either subcutaneous daratumumab monotherapy or active monitoring. Treatment was continued for 39 cycles, for 36 months, or until confirmation of disease progression, whichever occurred first. The primary end point was progression-free survival; progression to active multiple myeloma was assessed by an independent review committee in accordance with International Myeloma Working Group diagnostic criteria.

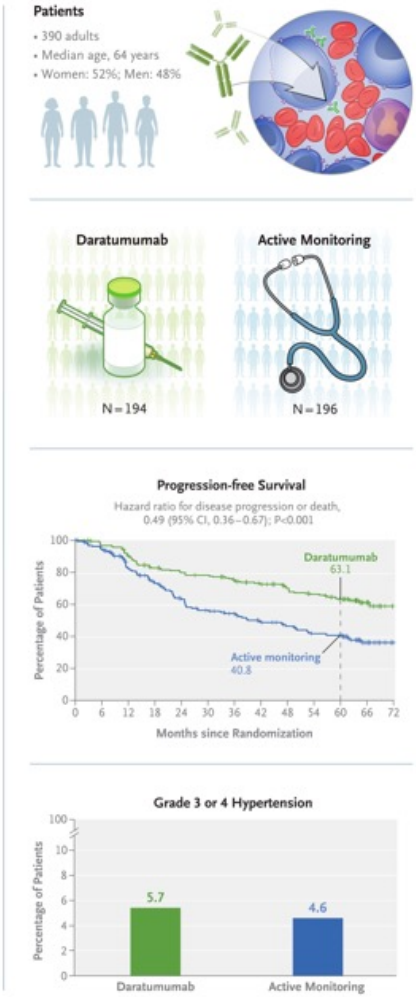

Smoldering multiple myeloma is an asymptomatic precursor disease of active multiple myeloma, and the current standard care is observation. However, patients with smoldering multiple myeloma who are at high risk for progression to active multiple myeloma may benefit from early treatment, although no treatments have been approved for this indication.

Daratumumab, a human IgGκ monoclonal antibody targeting CD38, has been approved for use as monotherapy or in combination with standard regimens for multiple myeloma. The phase 2 CENTAURUS study showed that daratumumab had single-agent activity in patients with intermediate-risk or high-risk smoldering multiple myeloma.

Patients

Patients were required to be at high risk for progression to active multiple myeloma, with a percentage of clonal plasma cells in bone marrow of at least 10% and the presence of at least one of the following risk factors (which were based on data available at the time of trial development): a serum M-protein level of at least 30 g per liter, IgA smoldering multiple myeloma, immunoparesis with reduced levels of two uninvolved immunoglobulin isotypes, a ratio of involved free light chains to uninvolved free light chains (FLC ratio) in serum of 8 to less than 100, or a percentage of clonal plasma cells in bone marrow of more than 50% to less than 60%.

End Points and Assessments

The primary end point was progression-free survival, which was evaluated in an analysis of the time from randomization to the initial documentation of progression to active multiple myeloma or death from any cause, whichever occurred first.

Characteristic	Daratumumab (N=194)	Active Monitoring (N=196)
Age		
Median (range) — yr	63.0 (31–86)	64.5 (36–83)
Distribution — no. (%)		
18 to <65 yr	106 (54.6)	98 (50.0)
65 to <75 yr	67 (34.5)	74 (37.8)
≥75 yr	21 (10.8)	24 (12.2)
Male sex — no. (%)	95 (49.0)	93 (47.4)
Race or ethnic group — no. (%)†		
White	161 (83.0)	162 (82.7)
Asian	18 (9.3)	13 (6.6)
Black	4 (2.1)	7 (3.6)
American Indian or Alaska Native	0	3 (1.5)
Native Hawaiian or other Pacific Islander	0	2 (1.0)
Multiple	1 (0.5)	0
Not reported	10 (5.2)	9 (4.6)
ECOG performance-status score — no. (%)‡		
0	165 (85.1)	160 (81.6)
1	29 (14.9)	36 (18.4)
Type of myeloma — no. (%)		
IgG	127 (65.5)	138 (70.4)
IgA	55 (28.4)	42 (21.4)
Other	12 (6.2)	16 (8.2)
Clonal plasma cells in bone marrow — no. (%)		
<10%	1 (0.5)	0
10% to ≤20%	124 (63.9)	102 (52.0)
>20% to <40%	50 (25.8)	66 (33.7)
≥40%	19 (9.8)	28 (14.3)
Risk factors for progression to multiple myeloma — no. (%)§		
<3	154 (79.4)	156 (79.6)
≥3	40 (20.6)	40 (20.4)
Cytogenetic risk profile — no./total no. (%)¶		
≥1 High-risk cytogenetic abnormality	29/167 (17.4)	22/170 (12.9)
del(17p)	3/166 (1.8)	8/166 (4.8)
t(4;14)	19/151 (12.6)	11/157 (7.0)
t(14;16)	7/146 (4.8)	3/145 (2.1)
Risk of progression according to Mayo 2018 risk criteria‖		
Low	45 (23.2)	34 (17.3)
Intermediate	77 (39.7)	76 (38.8)
High	72 (37.1)	86 (43.9)
Median time from diagnosis of smoldering multiple myeloma to randomization (range) — yr	0.80 (0–4.7)	0.67 (0–5.0)

Summary of Progression Events (Intention-to-Treat Population).

Event	Daratumumab (N=194)	Active Monitoring (N=196)
Disease progression or death — no. (%)	67 (34.5)	99 (50.5)
Disease progression — no./total no. (%)*	62/67 (92.5)	94/99 (94.9)
CRAB criteria		
Calcium level elevation	0/62	2/94 (2.1)
Renal insufficiency	0/62	0/94
Anemia	2/62 (3.2)	14/94 (14.9)
Bone disease	10/62 (16.1)	18/94 (19.1)
SLiM criteria		
≥60% Clonal plasma cells in bone marrow	5/62 (8.1)	16/94 (17.0)
Serum FLC ratio ≥100	33/62 (53.2)	33/94 (35.1)
>1 Focal lesion on magnetic resonance imaging	12/62 (19.4)	16/94 (17.0)
Death without disease progression — no./total no. (%)	5/67 (7.5)	5/99 (5.1)

Adverse events

Event	Daratumumab (N=193)	Active Monitoring (N=196)
	number of patients (percent)	
Any adverse event	187 (96.9)	162 (82.7)
Most common adverse events*		
Fatigue	66 (34.2)	26 (13.3)
Upper respiratory tract infection	58 (30.1)	15 (7.7)
Diarrhea	53 (27.5)	10 (5.1)
Arthralgia	52 (26.9)	35 (17.9)
Nasopharyngitis	49 (25.4)	23 (11.7)
Back pain	46 (23.8)	38 (19.4)
Insomnia	43 (22.3)	5 (2.6)
Grade 3 or 4 adverse event	78 (40.4)	59 (30.1)
Most common grade 3 or 4 adverse event: hypertension	11 (5.7)	9 (4.6)
Serious adverse event	56 (29.0)	38 (19.4)
Most common serious adverse event: pneumonia	7 (3.6)	1 (0.5)
Adverse event that led to death†	2 (1.0)	4 (2.0)
Second primary cancer	18 (9.3)	20 (10.2)

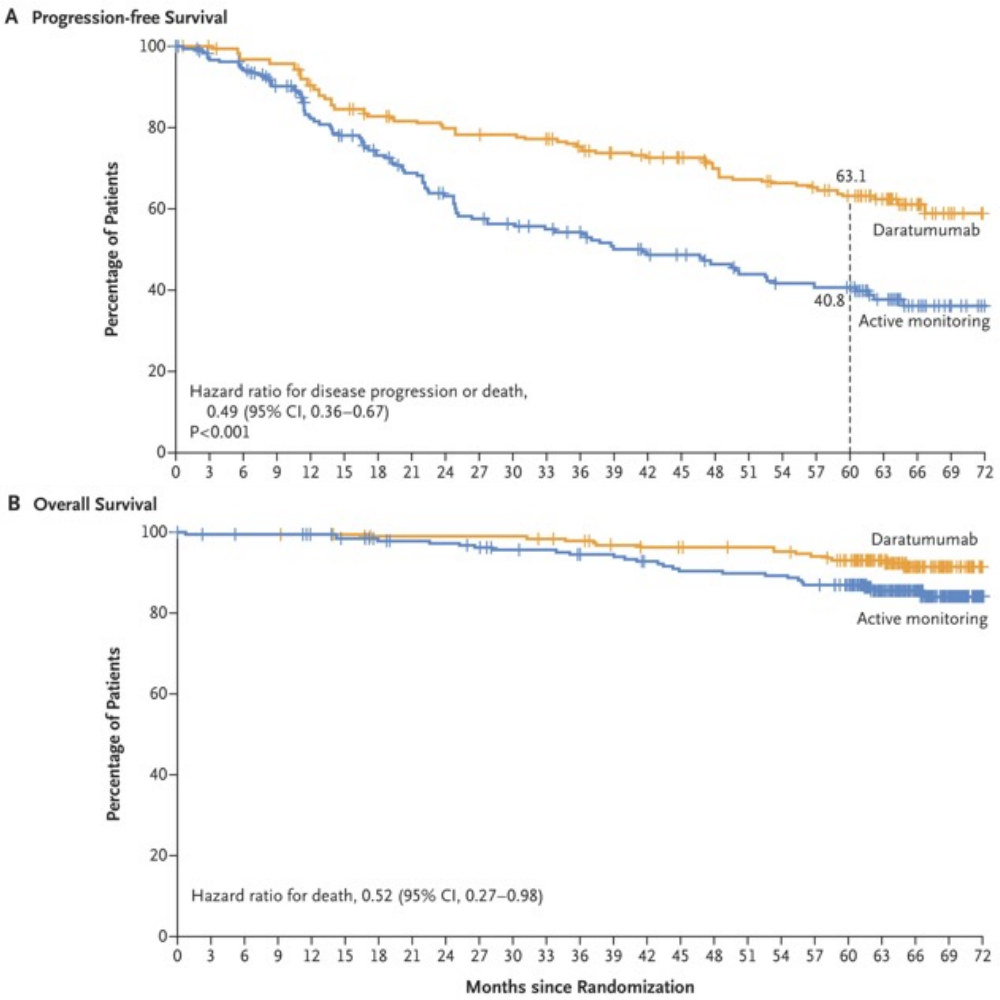

Progression-free Survival and Overall Survival. Panel A shows Kaplan–Meier estimates of progression-free survival in the intention-to-treat population. Progression-free survival was evaluated in an analysis of the time from randomization to the initial documentation of progression to active multiple myeloma or death from any cause, whichever occurred first. Disease progression was assessed by an independent review committee in accordance with the International Myeloma Working Group SLiM–CRAB diagnostic criteria for multiple myeloma.[6] The primary analysis of progression-free survival was performed after 166 events had occurred. Tick marks indicate censored data. The dashed line indicates the 5-year estimate. Panel B shows Kaplan–Meier estimates of overall survival in the intention-to-treat population.

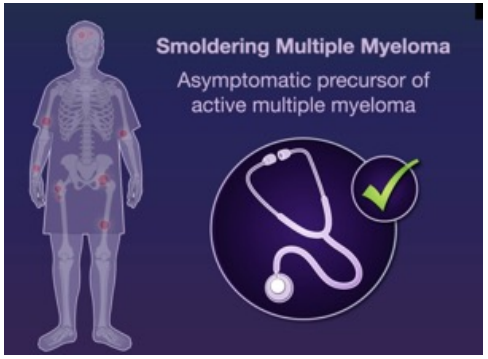
Smoldering Multiple Myeloma
Asymptomatic precursor of active multiple myeloma

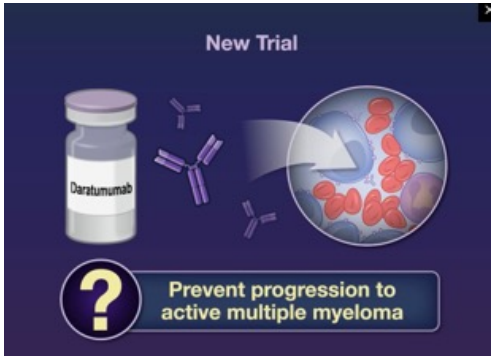
New Trial
Daratumumab
Prevent progression to active multiple myeloma

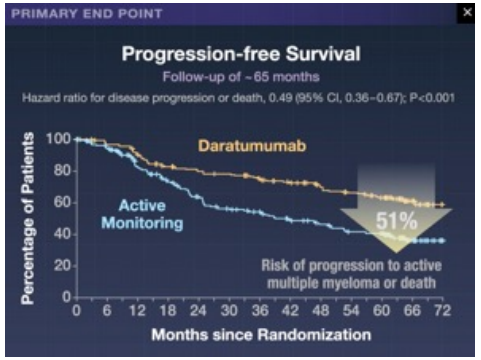
PRIMARY END POINT
Progression-free Survival
Follow-up of ~65 months
Hazard ratio for disease progression or death, 0.49 (95% CI, 0.36–0.67); P<0.001
Percentage of Patients
100
80
60
40
20
0
Daratumumab
Active Monitoring
51%
Risk of progression to active multiple myeloma or death
0 6 12 18 24 30 36 42 48 54 60 66 72
Months since Randomization

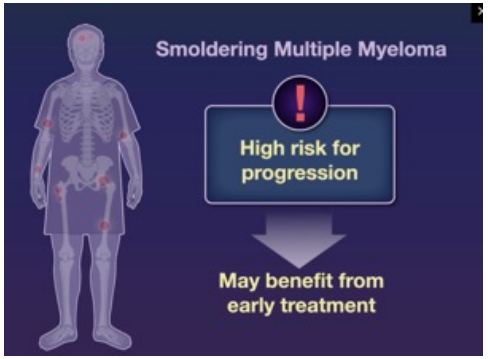
Smoldering Multiple Myeloma
High risk for progression
May benefit from early treatment

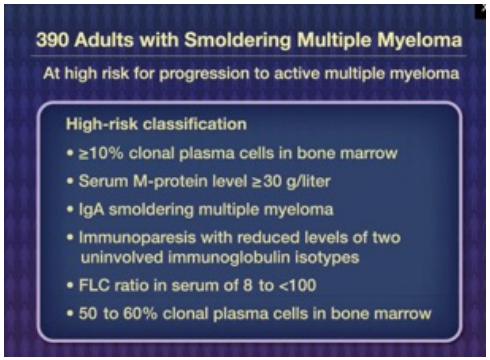
390 Adults with Smoldering Multiple Myeloma
At high risk for progression to active multiple myeloma
High-risk classification
• ≥10% clonal plasma cells in bone marrow
• Serum M-protein level ≥30 g/liter
• IgA smoldering multiple myeloma
• Immunoparesis with reduced levels of two uninvolved immunoglobulin isotypes
• FLC ratio in serum of 8 to <100
• 50 to 60% clonal plasma cells in bone marrow

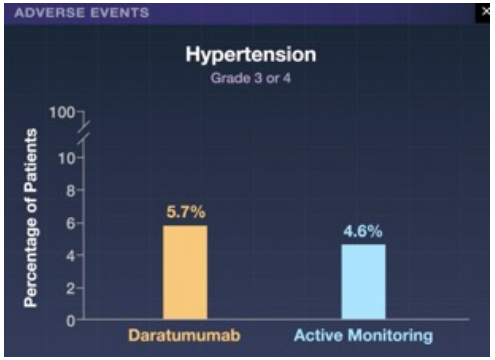
ADVERSE EVENTS
Hypertension
Grade 3 or 4
Percentage of Patients
100
10
8
6
4
2
0
5.7%
4.6%
Daratumumab
Active Monitoring

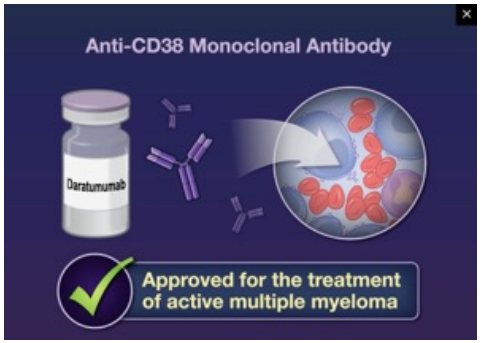
Anti-CD38 Monoclonal Antibody
Daratumumab
Approved for the treatment of active multiple myeloma


390 Adults with Smoldering Multiple Myeloma
At high risk for progression to active multiple myeloma
Daratumumab
N=194
Active Monitoring
N=196
For up to 36 months

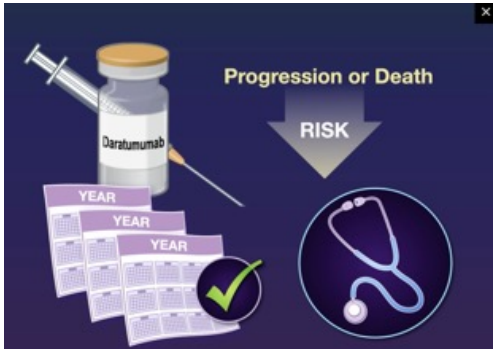
Daratumumab
Progression or Death
RISK
YEAR
YEAR
YEAR

The BCG vaccine, which stands for Bacillus Calmette-Guérin, is a live attenuated vaccine used to prevent tuberculosis (TB) and other mycobacterial infections. It is currently the only vaccine available against TB and is primarily given to infants in countries where TB is prevalent.

Purpose:

TB Prevention:

The BCG vaccine is primarily used to prevent severe forms of TB, particularly in children, such as TB meningitis (inflammation of the lining of the brain) and miliary TB (spread of TB infection to multiple organs).

Limited Protection:

While effective in preventing severe forms of TB in children, the BCG vaccine provides less protection against pulmonary TB in adults, according to the Centers for Disease Control and Prevention (CDC).

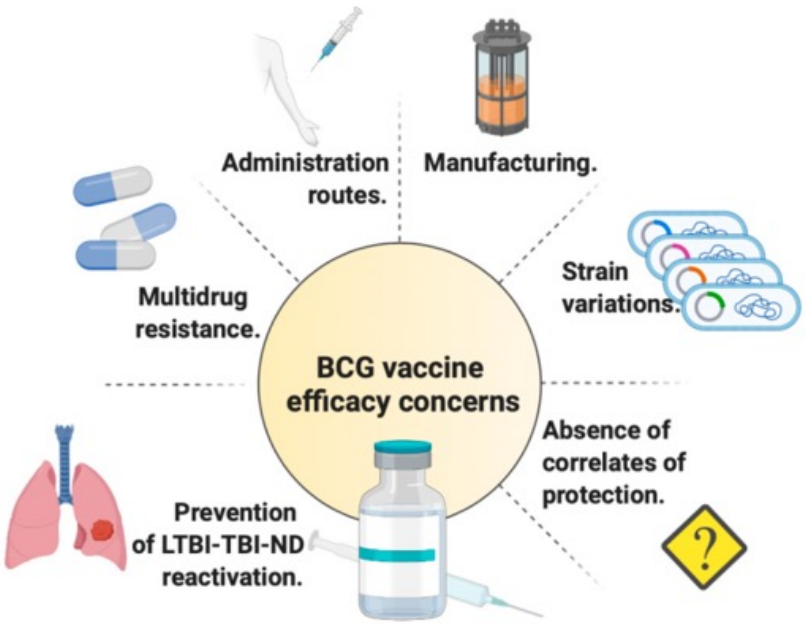

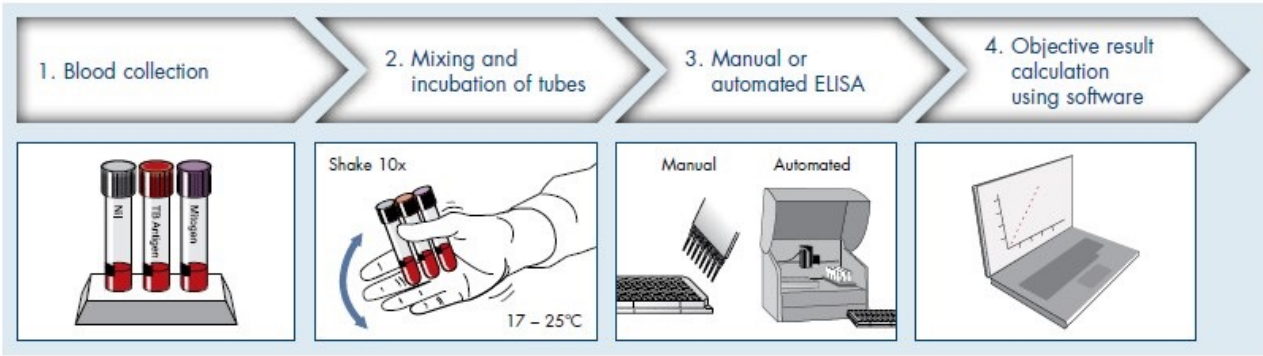

Der QFT (QuantiFERON®-TB Gold Test) ist ein in-vitro Test zur Diagnose einer Tuberkuloseinfektion. Er misst die zellvermittelte Immunantwort des Körpers auf Antigene von Mycobacterium tuberculosis. Ein positives Ergebnis deutet auf eine latente oder aktive Tuberkuloseinfektion hin.
Mehr Details:
Funktionsweise:
Der QFT verwendet eine Blutprobe und misst die Freisetzung von Interferon-Gamma (IFN-γ) durch T-Zellen, die durch die Antigene von M. tuberculosis stimuliert werden.
Anwendung:
Der QFT wird häufig als Alternative zum Tuberkulin-Hauttest eingesetzt, insbesondere bei Verdacht auf eine Tuberkuloseinfektion oder bei Kontakt zu erkrankten Personen.
Interpretation:
Ein positives Ergebnis weist auf eine latente oder aktive Tuberkuloseinfektion hin.
Vorteile:
Im Gegensatz zum Tuberkulin-Hauttest ist der QFT nicht durch die BCG-Impfung beeinflusst.

BCG Revaccination for the Prevention of *Mycobacterium tuberculosis* Infection

In a previous phase 2 trial, bacille Calmette–Guérin (BCG) revaccination was not shown to provide protection from primary *Mycobacterium tuberculosis* infection but prevented sustained *M. tuberculosis* infection, defined by an initial conversion on a QuantiFERON-TB (QFT) test (an interferon-γ release assay) from negative to positive, followed by two additional positive QFT tests at 3 and 6 months after the initial conversion (a secondary end point). A vaccine efficacy of 45% (95% confidence interval [CI], 6 to 68) was observed.

We performed a phase 2b, double-blind, randomized, placebo-controlled trial to evaluate the efficacy of BCG revaccination, as compared with placebo, for the prevention of sustained QFT test conversion (primary end point) in QFT test–negative, human immunodeficiency virus (HIV)–negative adolescents. Adverse events were assessed in a secondary analysis, and immunogenicity was assessed in an exploratory analysis. Vaccine efficacy was evaluated in the modified intention-to-treat population, which included all the participants who had undergone randomization, received the BCG vaccine or placebo, and had a negative QFT test 10 weeks after receipt of BCG vaccine or placebo; the last criterion was added to exclude participants with *M. tuberculosis* infection around the time that the vaccine or placebo was administered. Hazard ratios and 95% confidence intervals were estimated from a stratified Cox proportional-hazards model.

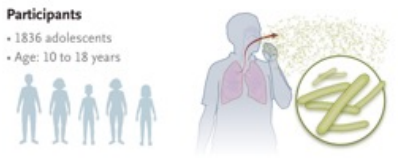

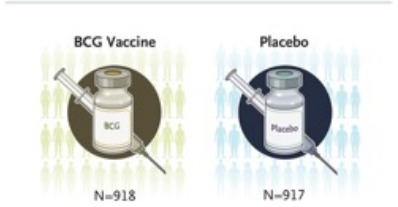

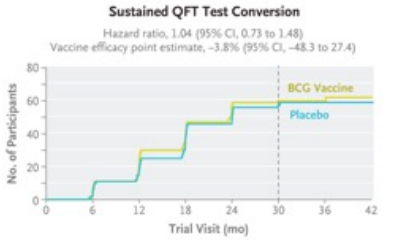

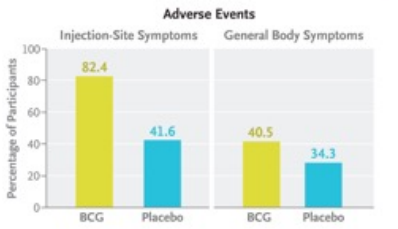

Approximately 1.7 billion people are estimated to be infected with *Mycobacterium tuberculosis* worldwide, of whom approximately 56 million are newly infected and at high risk for progression to tuberculosis disease. In 2022, an estimated 10.6 million new cases of tuberculosis disease were reported worldwide, which included 1.3 million cases in children younger than 15 years of age. Tuberculosis disease was responsible for 1.3 million deaths worldwide in 2022, which included 167,000 deaths in persons living with human immunodeficiency virus (HIV) infection. The incidence of tuberculosis disease in South Africa is among the highest in the world, with an estimated 468 cases per 100,000 persons in 2022. Cohort studies in the Western Cape province showed that the prevalence of *M. tuberculosis* infection, as assessed by means of an *M. tuberculosis*–specific interferon-*γ* release assay (IGRA) such as QuantiFERON-TB (QFT) tests, increases quickly among adolescents, with an incidence of QFT test conversion (from negative to positive) as high as 10% per year.

In the absence of a licensed vaccine for the prevention of tuberculosis disease in adolescents and adults, we aimed to confirm that BCG revaccination confers protection against sustained *M. tuberculosis* infection in a larger population with an expanded age range and geographic area and to identify candidate correlates of protection for this trial end point. We assumed that a confirmatory trial could potentially support a policy change for BCG revaccination in South Africa or motivate funders to invest in a large phase 3 trial of BCG revaccination for the prevention of disease in support of the global effort to accelerate the end of the tuberculosis disease epidemic. Here we report the results of a phase 2b trial to assess the efficacy of BCG revaccination for the prevention of sustained *M. tuberculosis* infection in South Africa.

Participant eligibility criteria

Participants were included in the trial if they met all the following criteria:

1. ≥ 10 years and ≤ 18 years on trial Day 1
2. General good health, confirmed by medical history and physical examination
3. Vaccinated with BCG at least 5 years ago, documented through medical history or by presence of healed BCG scar
4. Tested QFT negative at screening
5. For female participants: not pregnant and agreed to avoid pregnancy throughout the first 12 months of the trial. Women physically capable of pregnancy must agree to use an acceptable method of avoiding pregnancy during this period. Acceptable methods of avoiding pregnancy included sexual abstinence (not engaging in sexual intercourse), a confirmed sterile partner, or at least 2 contraception methods from the following list: male or female condom, diaphragm, intrauterine devices (IUDs), hormonal contraceptive (oral, injection, transdermal patch, or implant)
6. Agreed to stay in contact with the trial site for the duration of the trial, provided updated contact information as necessary, and had no current plans to move from the trial area for the duration of the trial
7. Capable of giving signed informed consent/assent and completed the written informed consent/assent process

Participants were excluded if they had one of the following:

1. Acute illness or body temperature ≥37.5°C on trial Day 1. This was a temporary exclusion for which the subject may be re-evaluated.
2. History or evidence of any clinically significant disease, including severe eczema and severe asthma, or any acute or chronic illness that might affect the safety, immunogenicity, or efficacy of trial vaccine in the opinion of the investigator
3. Any current medical, psychiatric, occupational, or substance abuse problems that, in the opinion of the investigator, will make it unlikely that the participant will comply with the protocol
4. History of autoimmune disease or allergic disease that is likely to be exacerbated by any component of the trial vaccine, or latent *Mtb* infection
5. History or evidence of active TB disease, or of any past or present possible immunodeficiency state including, but not limited to, any laboratory indication of HIV-1 infection
6. History of treatment for active TB disease or received investigational TB vaccine at any time prior to trial Day 1
7. Received a tuberculin skin test within 6 months prior to Day 1
8. Received immunosuppressive treatment, e.g., chemotherapy, biologics or radiation therapy, or used immunosuppressive medication (daily steroid equivalent of ≥5mg prednisone) within 42 days before trial Day 1.
9. Received immunoglobulin or blood products within 42 days before trial Day 1
10. Planned administration/administration of a licensed vaccine in the period starting 28 days before and ending 28 days after trial Day 1
11. Received any investigational drug therapy or investigational vaccine within 180 days before Day 1, or planned participation in any other clinical trial using investigational product during the trial period
12. Laboratory values from the most recent blood collected prior to randomization outside the normal range that are suggestive of a disease state

Methods

Trial Design and Objectives

In this double-blind, phase 2b, randomized, placebo-controlled trial, participants were enrolled at five sites in South Africa: Worcester, Cape Town, and Mbekweni in Western Cape province; Durban in KwaZulu-Natal province; and Johannesburg in Gauteng province. The primary objective was to show the efficacy of BCG revaccination, as compared with placebo, against sustained *M. tuberculosis* infection in QFT test–negative, healthy adolescents. The QFT Gold-Plus test was used for the assessment of *M. tuberculosis* infection.

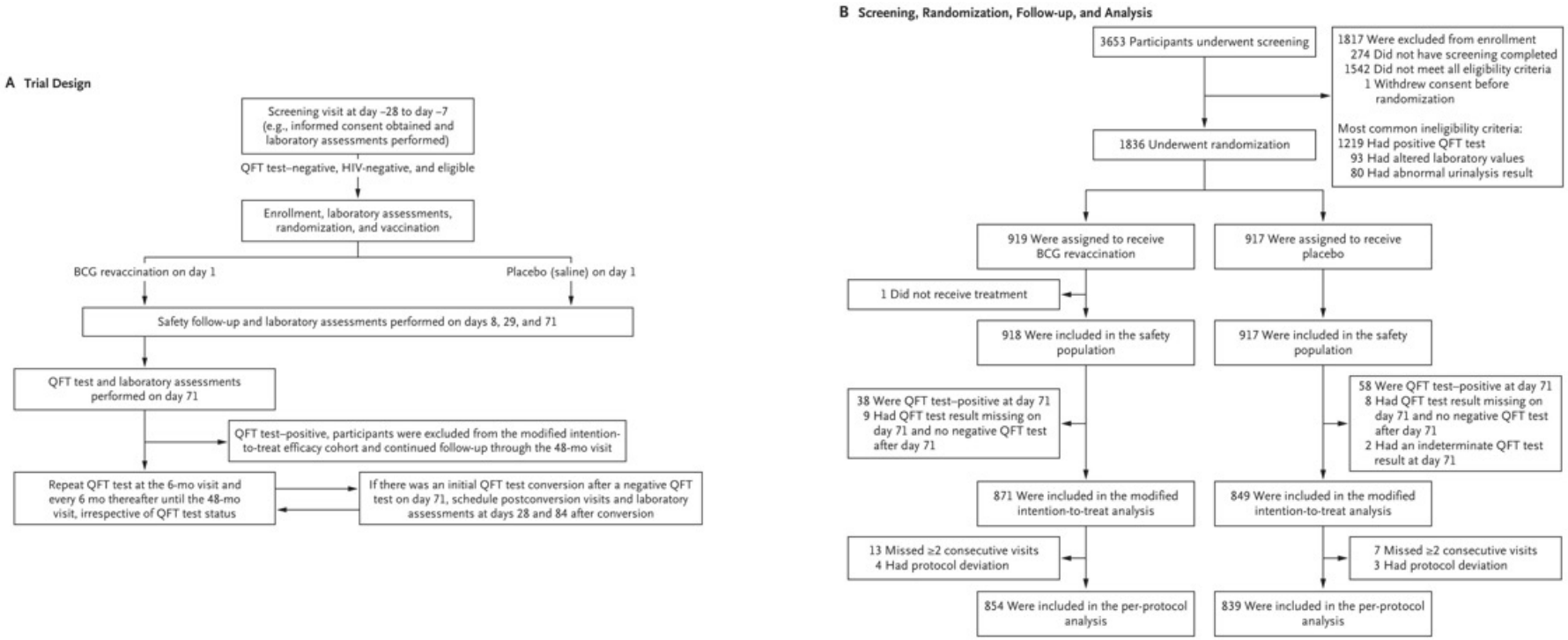

Sustained and Initial QFT Test Conversions.

Variable	BCG Vaccine (N=871)	Placebo (N=849)
Initial QFT test conversion on or after day 71 — no. (%)†	135 (15.5)	125 (14.7)
Not evaluable for QFT test reversion because of missing or indeterminate QFT results — no.	24	24
QFT test reversion at day 84 or 6 mo after conversion — no.	49	42
Sustained QFT test conversion‡		
No. with event	62	59
Proportion (95% CI)§	0.0712 (0.0541 to 0.0883)	0.0695 (0.0524 to 0.0866)
Person-time accrued — mo¶	19,719	19,383
Overall incidence — no. of events per person-mo (95% CI)‖	0.0031 (0.0024 to 0.0040)	0.0030 (0.0023 to 0.0039)
Hazard ratio (95% CI)**	1.04 (0.73 to 1.48)††	—
Vaccine efficacy — % (95% CI)‡‡	−3.8 (−48.3 to 27.4)	—
Initial QFT test conversion — proportion (95% CI)§	0.16 (0.13 to 0.18)	0.15 (0.12 to 0.17)
Person-time accrued — mo¶	19,695	19,371
Overall incidence — no. of events per person-mo (95% CI)‖	0.0069 (0.0057 to 0.0081)	0.0065 (0.0054 to 0.0077)

Incidence of Adverse Events and Medication Use.

Adverse Event or Medication Use	BCG Vaccine (N=918)	Placebo (N=917)
Solicited adverse events and medication use		
Any injection-site symptom		
No. with event/total no.	754/915	381/915
Percent (95% CI)	82.4 (79.8 to 84.8)	41.6 (38.5 to 44.9)
Any general body symptom		
No. with event/total no.	371/916	314/915
Percent (95% CI)	40.5 (37.4 to 43.7)	34.3 (31.3 to 37.4)
Use of medication 1 to 7 days after vaccination		
No. with event/total no.	30/903	27/899
Percent (95% CI)	3.3 (2.3 to 4.6)	3.0 (2.0 to 4.3)
Injection-site symptoms according to severity†		
Swelling — no./total no. (%)		
Any severity	657/912 (72.0)	248/910 (27.3)
Severe or life-threatening	2/912 (0.2)	1/910 (0.1)
Pain — no./total no. (%)		
Any severity	381/914 (41.7)	148/915 (16.2)
Severe or life-threatening	17/914 (1.9)	6/915 (0.7)
Redness — no./total no. (%)		
Any severity	349/912 (38.3)	111/911 (12.2)
Severe or life-threatening	0	0
Solicited systemic adverse events according to severity†		
Tiredness — no./total no. (%)		
Any severity	229/913 (25.1)	184/913 (20.2)
Severe or life-threatening	8/913 (0.9)	6/913 (0.7)
Headache — no./total no. (%)		
Any severity	195/913 (21.4)	164/913 (18.0)
Severe or life-threatening	7/913 (0.8)	9/913 (1.0)
Stomach problems — no./total no. (%)		
Any severity	136/913 (14.9)	140/913 (15.3)
Severe or life-threatening	8/913 (0.9)	8/913 (0.9)
Fever — no./total no. (%)‡		
Any severity	24/911 (2.6)	27/907 (3.0)
Severe or life-threatening	5/911 (0.5)	5/907 (0.6)
Adverse-event categories§		
Mild adverse events		
Any mild event — no.	315	90
Percent (95% CI)	34.3 (31.3 to 37.4)	9.8 (8.0 to 11.9)
Moderate adverse events		
Any moderate event — no.	47	28
Percent (95% CI)	5.1 (3.8 to 6.7)	3.1 (2.1 to 4.3)
Severe adverse events		
Any severe event — no.	5	3
Percent (95% CI)	0.5 (0.2 to 1.2)	0.3 (0.1 to 0.9)
Related adverse events¶		
Any related event — no.	273	9
Percent (95% CI)	29.7 (26.8 to 32.8)	1.0 (0.5 to 1.8)
Related severe adverse events¶		
Any related severe event — no.	1	0
Percent (95% CI)	0.1 (0 to 0.5)	—
Unsolicited nonserious adverse events		
Any unsolicited nonserious event — no.	185	117
Percent (95% CI)	20.2 (17.7 to 22.8)	12.8 (10.7 to 15.0)
Serious adverse events		
Any serious event — no.	3	3
Percent (95% CI)	0.3 (0.1 to 0.9)	0.3 (0.1 to 0.9)
Serious adverse event with outcome of death — no.	0	0
Serious adverse drug reaction — no.‖	0	0
Adverse events leading to premature trial discontinuation — no.	0	0
Adverse events of special interest		
Any event of special interest — no.	5	0
Percent (95% CI)	0.5 (0.2 to 1.2)	—
Most common nonserious adverse events**		
Headache — no. (%)	36 (3.9)	27 (2.9)
Injection-site pain — no. (%)	21 (2.3)	0
Injection-site ulceration — no. (%)	20 (2.2)	0
Pyrexia — no. (%)	12 (1.3)	3 (0.3)
Oropharyngeal pain — no. (%)	9 (1.0)	4 (0.4)
Upper respiratory tract infection — no. (%)	8 (0.9)	15 (1.6)

Of about 900 in each group

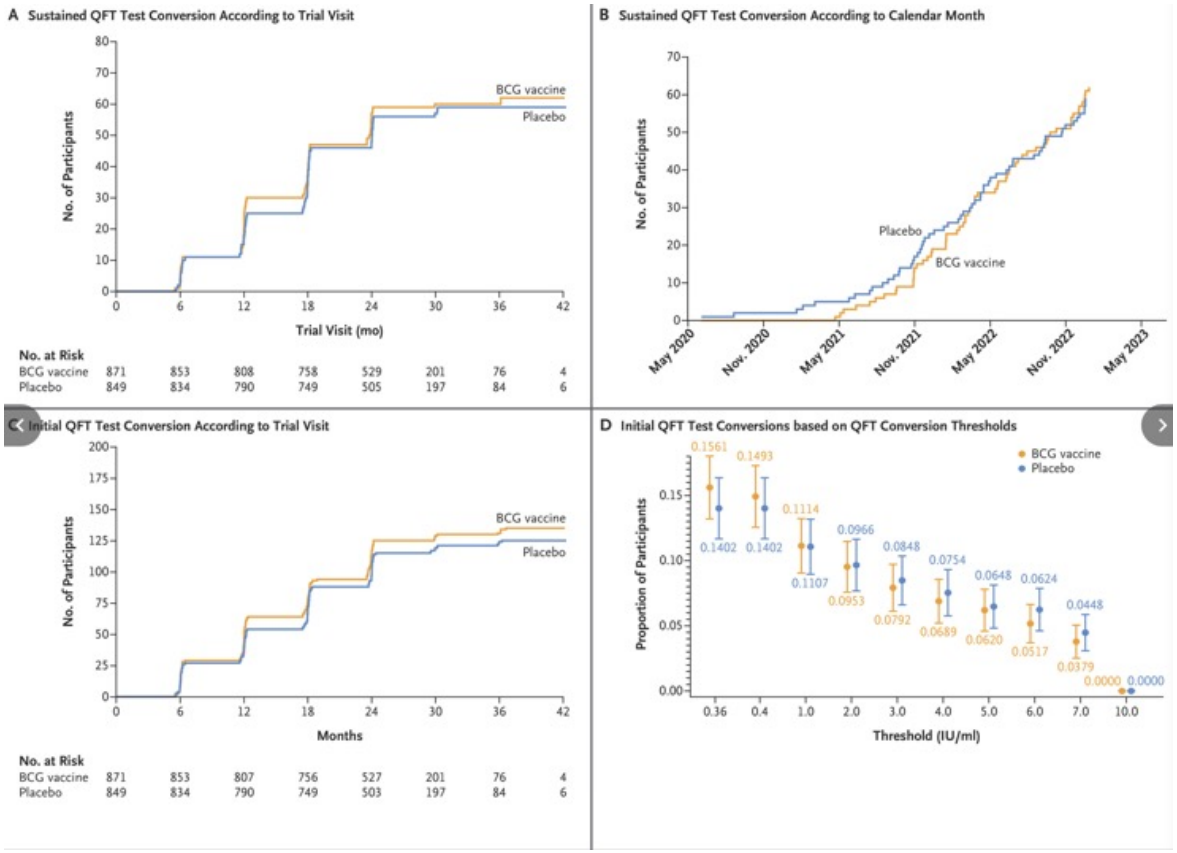

Vaccine Efficacy in the Modified Intention-to-Treat Population.

Panel A shows the cumulative event curves for a sustained QFT test conversion (primary efficacy end point) according to trial visit. Panel B shows the cumulative event curves for a sustained QFT test conversion according to calendar month. Panel C shows the cumulative event curves for an initial QFT test conversion according to trial visit. Panel D shows the proportion of participants with an initial QFT test conversion based on a range of increasingly stringent QFT test conversion thresholds higher than 0.35 IU per milliliter. I bars represent 95% confidence intervals.

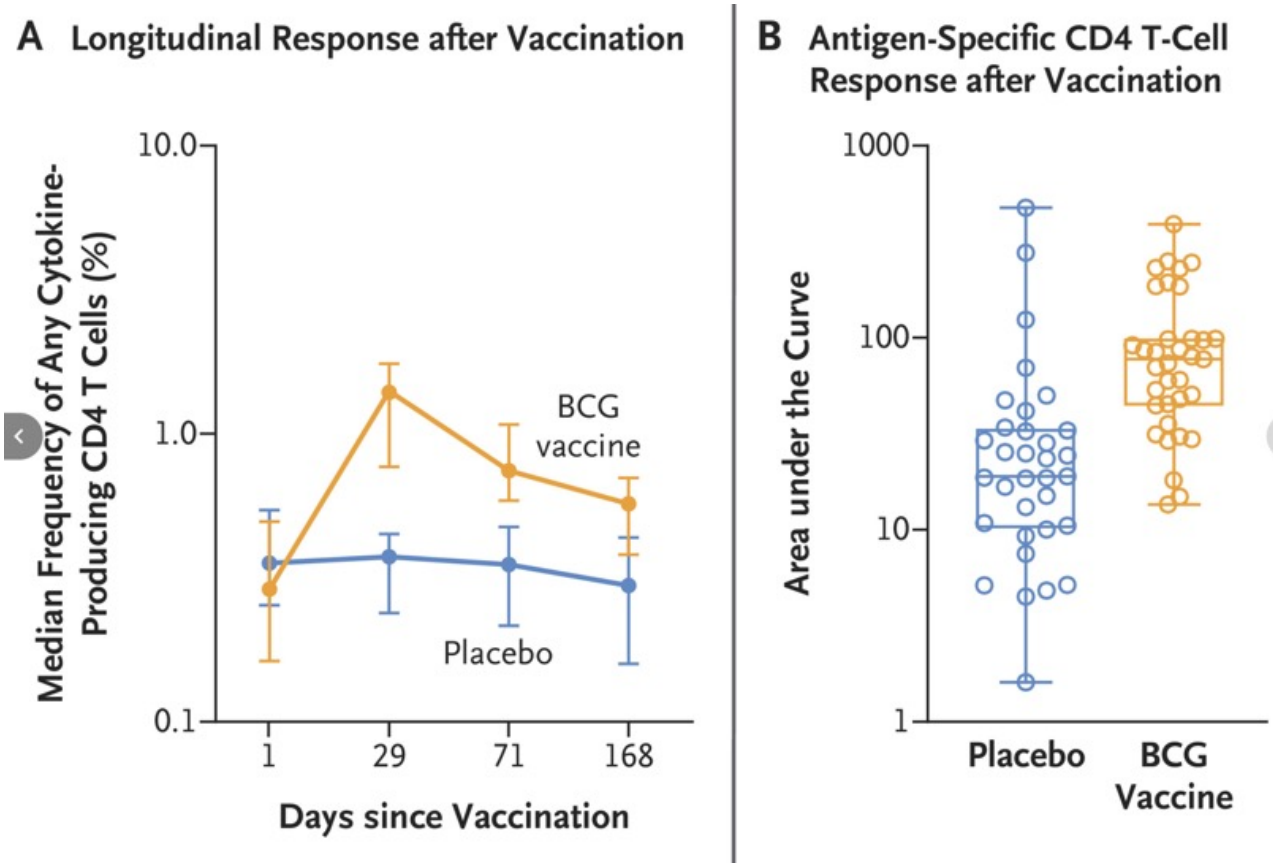

Immunogenicity of BCG Revaccination.

Shown are the frequencies of antigen-specific CD4 T cells expressing any combination of interferon-γ, tumor necrosis factor, interleukin-2, interleukin-17, or interleukin-22 after stimulation with BCG vaccine, as measured with the use of whole-blood intracellular cytokine staining assay in participants who received BCG revaccination (orange) or placebo (blue). Panel A shows longitudinal responses (plotted on a logarithmic scale) during the first 168 days after vaccination. I bars indicated 95% confidence intervals. Panel B shows the area under the curve (plotted on a logarithmic scale) for BCG-specific CD4 T-cell frequencies per participant during the first 168 days after vaccination. Each circle represents an individual participant. The horizontal line within each box indicates the median, the box indicates the interquartile range (quartile 1 to quartile 3), and the whiskers indicate the minimum and maximum values.

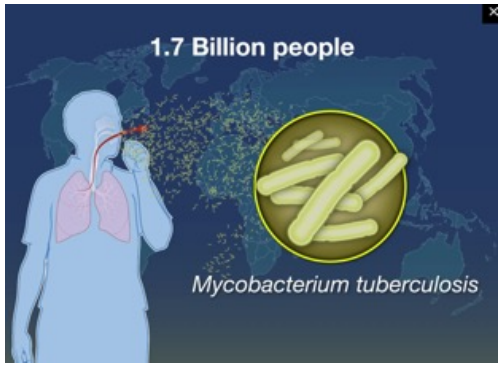
1.7 Billion people
Mycobacterium tuberculosis

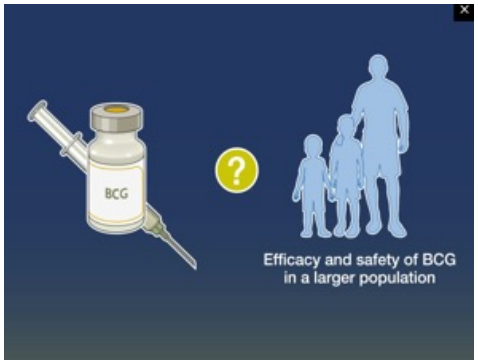
BCG
Efficacy and safety of BCG in a larger population

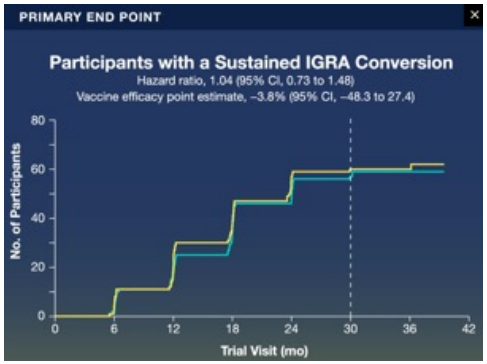
PRIMARY END POINT
Participants with a Sustained IGRA Conversion
Hazard ratio, 1.04 (95% CI, 0.73 to 1.48)
Vaccine efficacy point estimate, −3.8% (95% CI, −48.3 to 27.4)
No. of Participants
0
20
40
60
80
0
6
12
18
24
30
36
42
Trial Visit (mo)

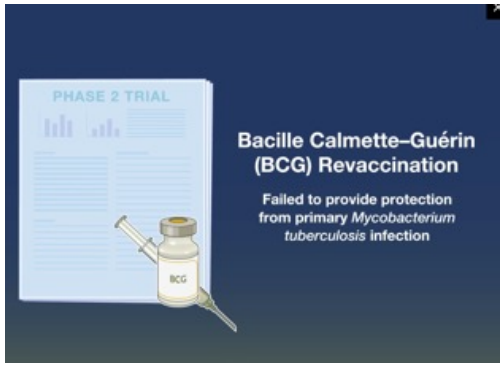
PHASE 2 TRIAL
BCG
Bacille Calmette–Guérin (BCG) Revaccination
Failed to provide protection from primary Mycobacterium tuberculosis infection


TRIAL DESIGN
• Phase 2b
• Randomized
• Controlled
• Double-blind
1836 Adolescents
• Interferon-γ release assay (IGRA)–negative
• HIV-negative

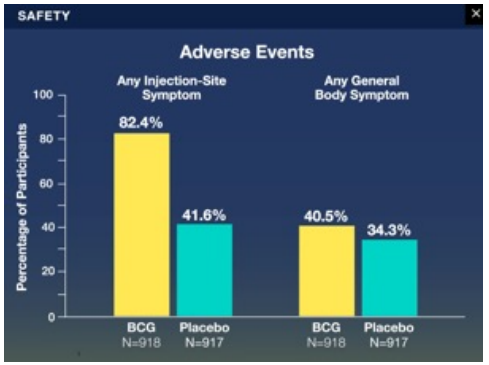
SAFETY
Adverse Events
Any Injection-Site Symptom
Any General Body Symptom
Percentage of Participants
0
20
40
60
80
100
82.4%
41.6%
40.5%
34.3%
BCG N=918
Placebo N=917
BCG N=918
Placebo N=917

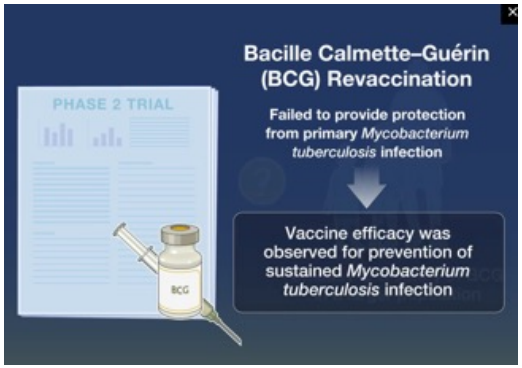
PHASE 2 TRIAL
BCG
Bacille Calmette–Guérin (BCG) Revaccination
Failed to provide protection from primary Mycobacterium tuberculosis infection
Vaccine efficacy was observed for prevention of sustained Mycobacterium tuberculosis infection

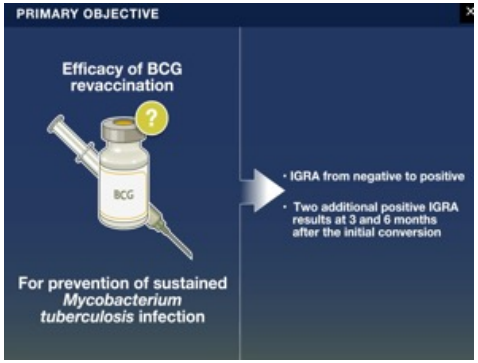
PRIMARY OBJECTIVE
Efficacy of BCG revaccination
BCG
For prevention of sustained Mycobacterium tuberculosis infection
• IGRA from negative to positive
• Two additional positive IGRA results at 3 and 6 months after the initial conversion


BCG revaccination of IGRA-negative adolescents
BCG
Does not provide protection from sustained Mycobacterium tuberculosis infection

Automated insulin delivery (AID) systems, also known as closed-loop systems or artificial pancreas, combine an insulin pump, a continuous glucose monitor (CGM), and an algorithm to automatically adjust insulin delivery based on real-time glucose levels. This technology aims to improve glycemic control, reduce the burden of diabetes, and enhance the quality of life for individuals with diabetes.

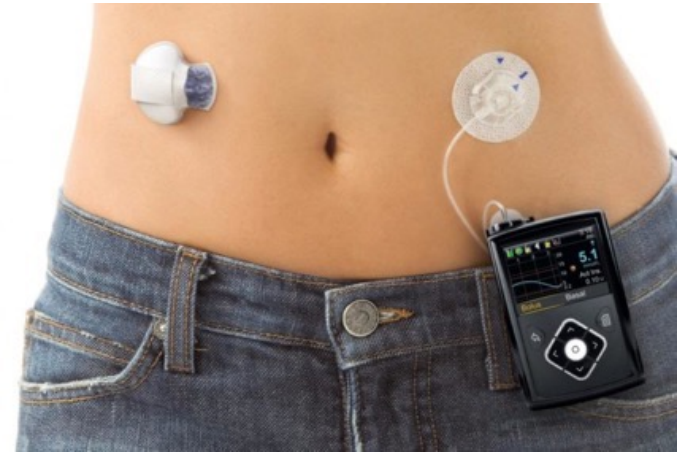

A Randomized Trial of Automated Insulin Delivery in Type 2 Diabetes

Automated insulin delivery (AID) systems have been shown to be beneficial for patients with type 1 diabetes, but data are needed from randomized, controlled trials regarding their role in the management of insulin-treated type 2 diabetes. In this 13-week, multicenter trial, adults with insulin-treated type 2 diabetes were randomly assigned in a 2:1 ratio to receive AID or to continue their pretrial insulin-delivery method (control group); both groups received continuous glucose monitoring (CGM). The primary outcome was the glycated hemoglobin level at 13 weeks.

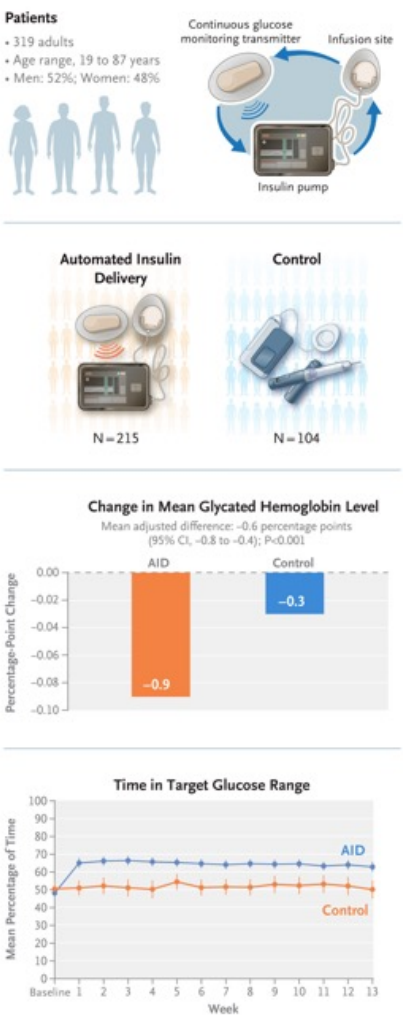

The benefits of automated insulin delivery (AID) systems are well established in patients with type 1 diabetes. However, the efficacy and safety of this technology in those with type 2 diabetes has not been established. Although promising results of AID in type 2 diabetes have been reported, patients have been evaluated either in uncontrolled trials or in short crossover trials with small sample sizes.

We conducted the Randomized Trial Evaluating the Efficacy and Safety of Control-IQ+ Technology in Adults with Type 2 Diabetes Using Basal-Bolus Insulin Therapy (2IQP) to evaluate the efficacy and safety of AID in adults with type 2 diabetes who were receiving multiple daily injections of insulin or using an insulin pump.

Trial Design and Patients

Trial patients were at least 18 years old and had had type 2 diabetes for at least 6 months, according to clinical history and available laboratory data. All the patients were receiving multiple daily injections of insulin with at least one injection containing rapid-acting insulin per day or were using an insulin pump for at least 3 months before enrollment. Mixed insulin use with a rapid-acting component was allowed. Concurrent treatment with noninsulin glucose-lowering medications or weight-reduction medications was permitted, provided the dose had been stable for the previous 3 months; during the trial, these medications were continued in both treatment groups.

Characteristics of the Patients at Baseline.

Characteristic	AID Group (N=215)	Control Group (N=104)
Age — yr		
Mean	59±12	57±12
Range	19–87	23–80
Female sex — no. (%)	105 (49)	49 (47)
Race or ethnic group — no. (%)†		
White	148 (69)	74 (71)
Black	45 (21)	24 (23)
Asian	10 (5)	3 (3)
Native Hawaiian or other Pacific Islander	2 (1)	0
American Indian or Alaska Native	1 (<1)	1 (1)
More than one race or ethnic group	6 (3)	2 (2)
Unknown or not reported	3 (1)	0
Hispanic or Latino — no. (%)†		
Yes	23 (11)	11 (11)
No	190 (88)	93 (89)
Unknown or not reported	2 (1)	0
Education level — no. (%)		
Less than bachelor's degree	123 (57)	52 (50)
Bachelor's degree	49 (23)	32 (31)
More than bachelor's degree	33 (15)	16 (15)
Unknown or did not wish to provide	10 (5)	4 (4)
Annual household income in U.S. dollars — no. (%)		
<$50,000	60 (28)	26 (25)
$50,000 to $100,000	52 (24)	21 (20)
>$100,000	53 (25)	36 (35)
Unknown or did not wish to provide	50 (23)	21 (20)
Health insurance — no. (%)		
Private	116 (54)	65 (62)
Medicare	57 (27)	15 (14)
Medicaid	10 (5)	13 (12)
Other government insurance	23 (11)	8 (8)
No coverage	2 (1)	2 (2)
Unknown	7 (3)	1 (1)
Diabetes duration — yr		
Median (IQR)	18 (11–26)	18 (11–24)
Range	1–59	2–45
Body-mass index‡		
Median (IQR)	33 (29–40)	35 (29–40)
Range	19–56	20–57
Glycated hemoglobin level§		
Distribution — no. (%)		
<7.0%	28 (13)	15 (14)
7.0 to <8.0%	73 (34)	40 (38)
8.0 to <9.0%	66 (31)	24 (23)
≥9.0%	47 (22)	25 (24)
Mean value — %	8.2±1.4	8.1±1.2
Range in values — %	5.7–14.1	5.2–12.4
Insulin delivery method — no. (%)		
Multiple daily injections	206 (96)	100 (96)
Insulin pump	9 (4)	4 (4)
Noninsulin glucose-lowering medication — no. (%)¶		
Metformin	109 (51)	61 (59)
SGLT2 inhibitor	76 (35)	41 (39)
GLP-1 receptor agonist	87 (40)	54 (52)
SGLT2 inhibitor and GLP-1 receptor agonist	44 (20)	24 (23)
Other	9 (4)	10 (10)
Use of CGM — no. (%)		
Current	147 (68)	78 (75)
In past, but not current	40 (19)	16 (15)
Never	28 (13)	10 (10)

Primary and Secondary Hierarchical Efficacy Outcomes.

Outcome	At Baseline		At 13 Weeks		Adjusted Difference between Groups (95% CI)	P Value
	AID Group	Control Group	AID Group	Control Group		
Primary outcome						
No. of patients evaluated	214†	104	209‡	102§		
Glycated hemoglobin level — %	8.2±1.4	8.1±1.2	7.3 ±0.9	7.7 ±1.1	−0.6 (−0.8 to −0.4)	<0.001
Secondary hierarchical outcomes						
No. of patients evaluated	215	104	214¶	104		
Percentage of time with glucose level in range of 70 to 180 mg/dl	48±24	51±21	64±16	52±21	14 (11 to 17)	<0.001
Mean glucose level — mg/dl	194±43	190±35	170±23	188±34	−21 (−26 to −15)	<0.001
Percentage of time with glucose level of >180 mg/dl	51±25	49±21	35±16	48±21	−14 (−17 to −11)	<0.001
Percentage of time with glucose level of >250 mg/dl‖	19.5±17.3	15.8±13.6	9.7±7.8	16.7±14.1	−9.1 (−11.7 to −6.6)	<0.001
No. of prolonged hyperglycemia events per wk‖**	1.7±1.7	1.6±1.7	0.9±0.9	1.6±1.5	−0.7 (−1.0 to −0.4)	<0.001
Percentage of time with glucose level of <70 mg/dl‖	0.7±0.8	0.3±0.3	0.4±0.4	0.4±0.4	−0.1 (−0.4 to 0.1)	NS††
Percentage of time with glucose level of <54 mg/dl‖	0.16±0.16	0.05±0.05	0.09±0.09	0.09±0.10	−0.02 (−0.09 to 0.04)	NA
No. of CGM-measured hypoglycemia events per wk‖‡‡	0.2±0.3	0.1±0.0	0.1±0.2	0.1±0.2	0.0 (−0.1 to 0.0)	NA
Coefficient of variation in glucose levels — %	28±6	27±5	30±5	29±5	0.3 (−0.5 to 1.2)	NA

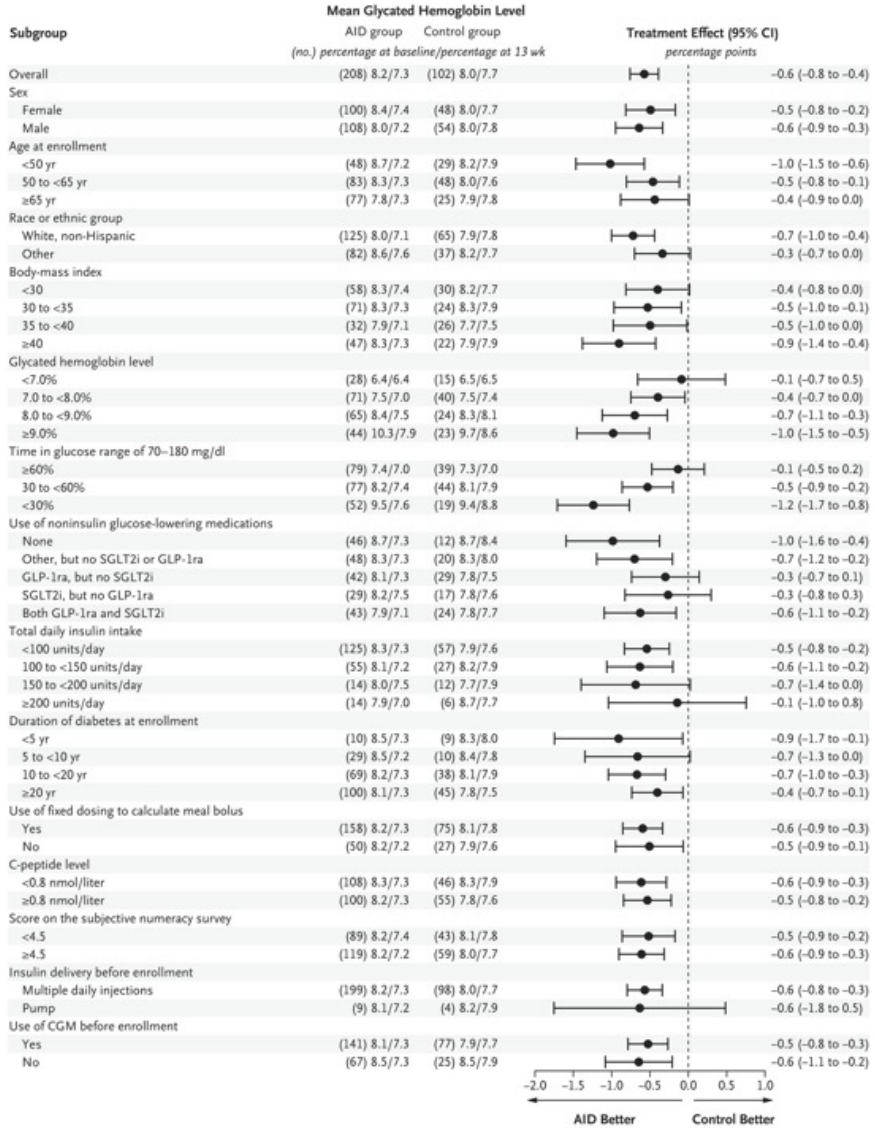

Glycated Hemoglobin Level, According to Baseline Subgroup.

The forest plot shows the treatment effect on the glycated hemoglobin level in the automated insulin delivery (AID) group and in the control group that continued their pretrial insulin-delivery method, according to subgroup variable. Both groups received continuous glucose monitoring (CGM). The overall treatment effect is the between-group difference at 13 weeks, as measured in percentage points (the overall primary outcome). Point estimates to the left of the vertical dashed line indicate a lower glycated hemoglobin level in the AID group than in the control group. The numeracy survey assessed the patients' beliefs about their ability to perform mathematical tasks and preference for numerical data as compared with prose information; the results were scored from 1 to 6, with higher scores indicating greater belief in ability. Race or ethnic group was reported by the patients. The body-mass index is the weight in kilograms divided by the square of the height in meters. To convert the values for glucose to millimoles per liter, multiply by 0.05551. GLP-1ra denotes glucagon-like peptide 1 receptor agonist, and SGLT2i sodium–glucose cotransporter 2 inhibitor.

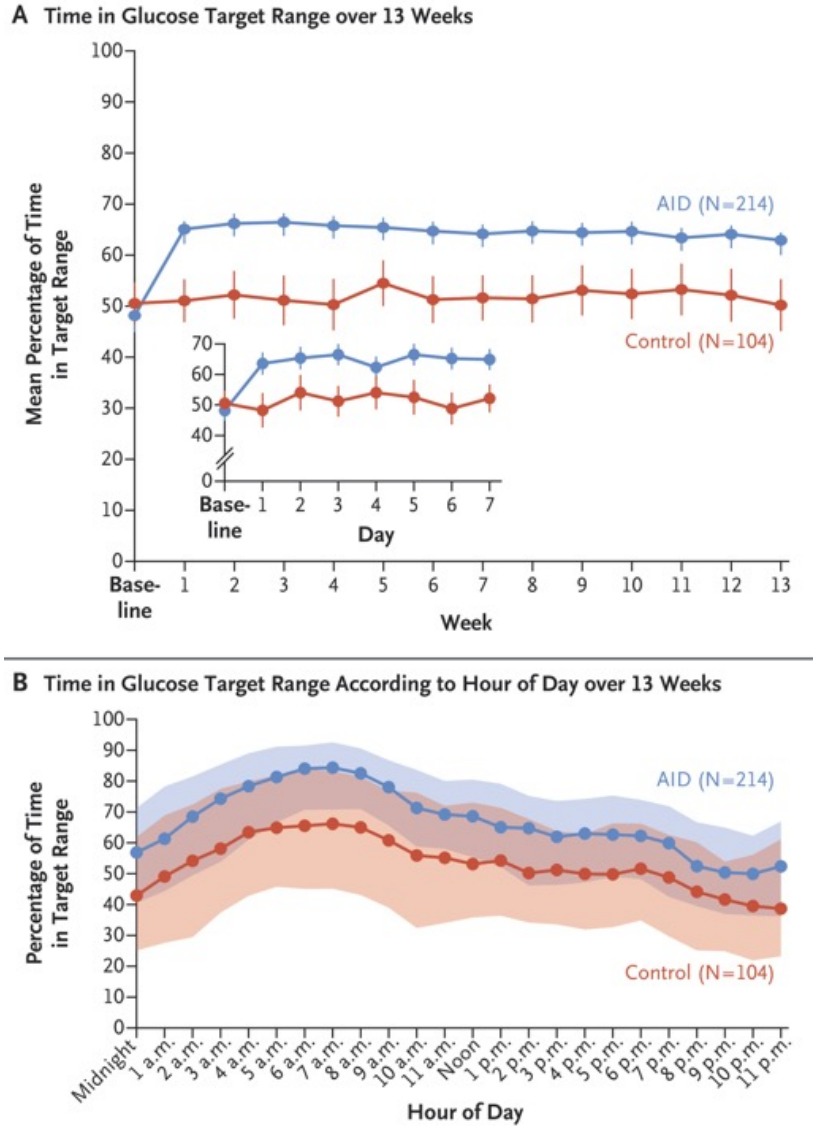

Mean Percentage of Time in the Glucose Target Range during the 13-Week Trial and According to the Time of Day.

Panel A shows the mean percentage of time that patients' glucose levels were in the target range of 70 to 180 mg per deciliter each week during the 13 weeks of the trial in each treatment group. The inset shows the mean time that the patients were in the target range each day for the first 7 days. The vertical lines denote 95% confidence intervals. Panel B shows an envelope plot of the percentage of time that patients were in the glucose target range according to the time of day, as measured by CGM during the 13-week period. Solid circles denote the hourly median values, and the shaded regions represent the interquartile ranges. To convert the values for glucose to millimoles per liter, multiply by 0.05551.


Patients with Insulin-Treated Type 2 Diabetes
Automated Insulin Delivery (AID) System

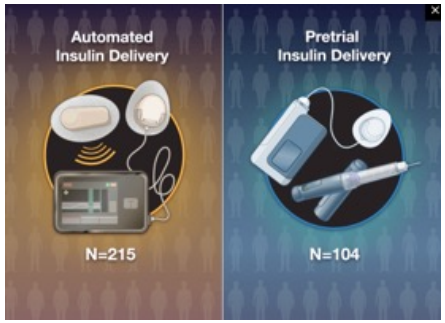
Automated Insulin Delivery
Pretrial Insulin Delivery
N=215
N=104

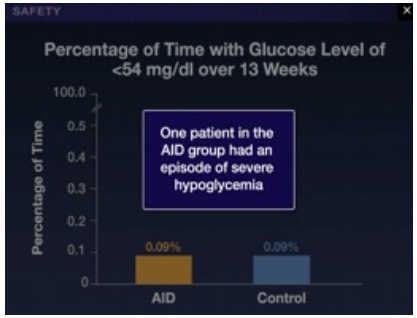
SAFETY
Percentage of Time with Glucose Level of <54 mg/dl over 13 Weeks
Percentage of Time
100.0
0.5
0.4
0.3
0.2
0.1
0
One patient in the AID group had an episode of severe hypoglycemia
0.09%
0.09%
AID
Control

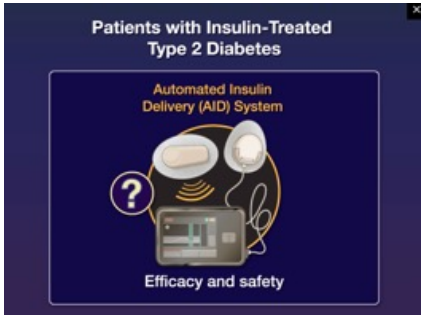
Patients with Insulin-Treated Type 2 Diabetes
Automated Insulin Delivery (AID) System
?
Efficacy and safety

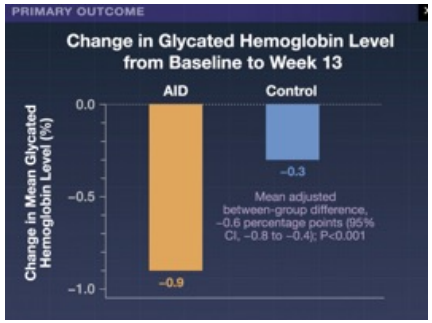
PRIMARY OUTCOME
Change in Glycated Hemoglobin Level from Baseline to Week 13
AID
Control
Change in Mean Glycated Hemoglobin Level (%)
0.0
−0.5
−1.0
−0.3
−0.9
Mean adjusted between-group difference, −0.6 percentage points (95% CI, −0.8 to −0.4); P<0.001

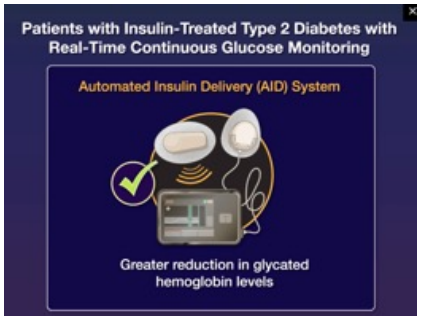
Patients with Insulin-Treated Type 2 Diabetes with Real-Time Continuous Glucose Monitoring
Automated Insulin Delivery (AID) System
Greater reduction in glycated hemoglobin levels

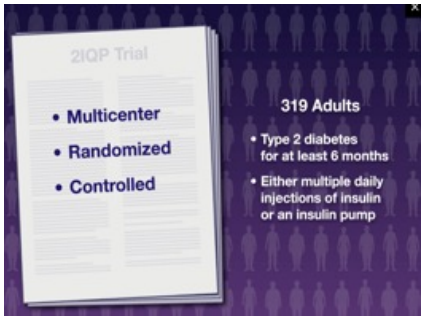
2IQP Trial
• Multicenter
• Randomized
• Controlled
319 Adults
• Type 2 diabetes for at least 6 months
• Either multiple daily injections of insulin or an insulin pump

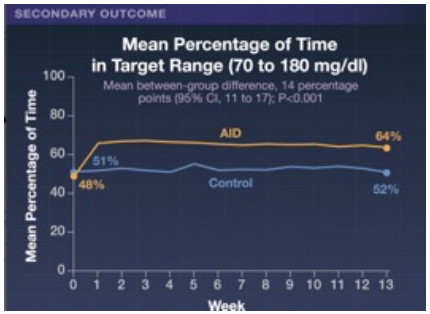
SECONDARY OUTCOME
Mean Percentage of Time in Target Range (70 to 180 mg/dl)
Mean between-group difference, 14 percentage points (95% CI, 11 to 17); P<0.001
Mean Percentage of Time
100
80
60
40
20
0
AID
64%
51%
48%
Control
52%
0 1 2 3 4 5 6 7 8 9 10 11 12 13
Week

Die CAR-T-Zelltherapie ist eine innovative Krebsbehandlung, bei der T-Zellen aus dem Blut des Patienten entnommen und im Labor gentechnisch so verändert werden, dass sie Krebszellen gezielt erkennen und zerstören können. Diese modifizierten T-Zellen, die CAR-T-Zellen genannt werden, werden dann wieder in den Körper des Patienten gegeben, wo sie die Krebszellen angreifen.

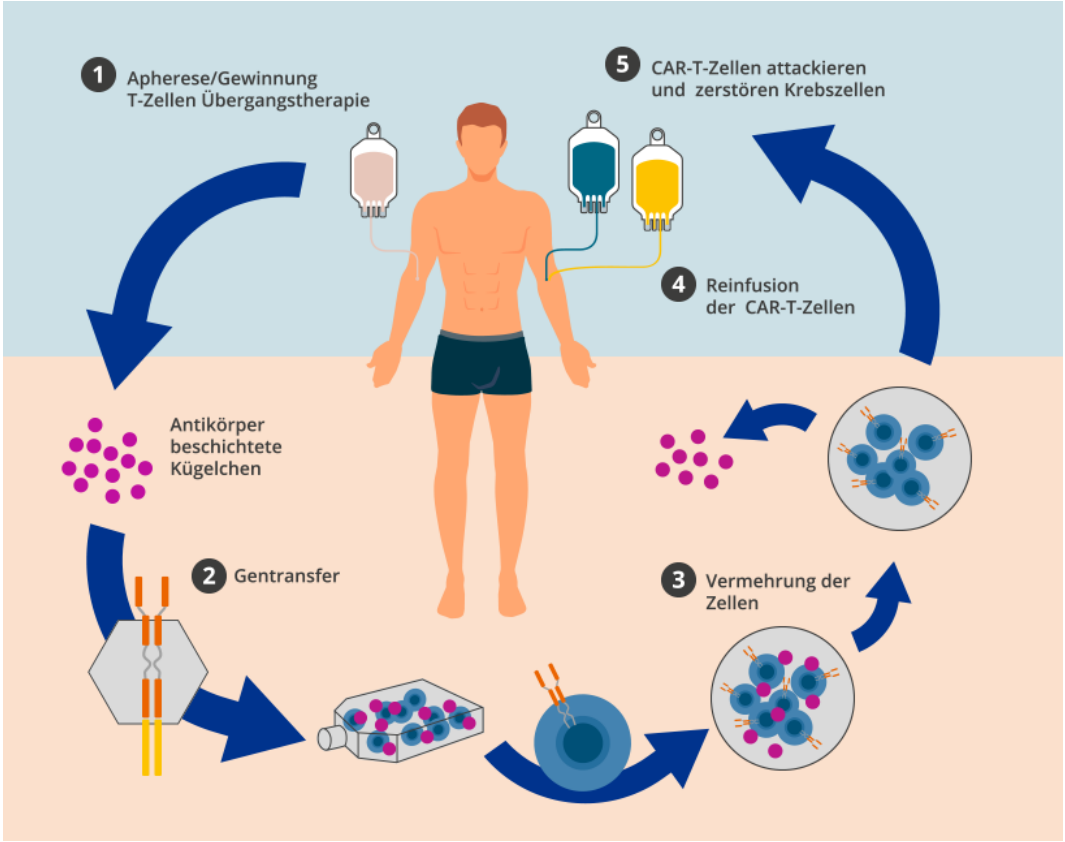

DIE VIERTE GENERATION MACHT'S BESSER

IL-18 boostet CAR-T-Zell-Funktion

HuCART19-IL-18, ein CAR-T-Zell-Konstrukt der vierten Generation, erzielte bei 88 Prozent von nach einer CAR-T-Zell-Therapie rezidivierten oder refraktären Patienten mit Non-Hodgkin-Lymphomen zumindest ein partielles Ansprechen. Die zusätzliche Expression von Interleukin 18 zu CD19 CAR scheint die Wirksamkeit eines CAR-T-Zell-Produktes also zu unterstützen.

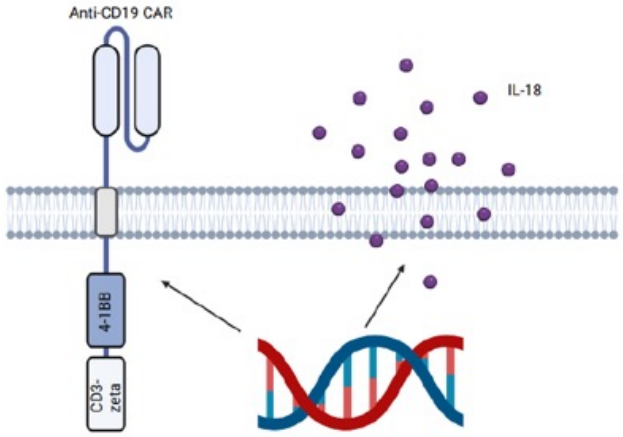

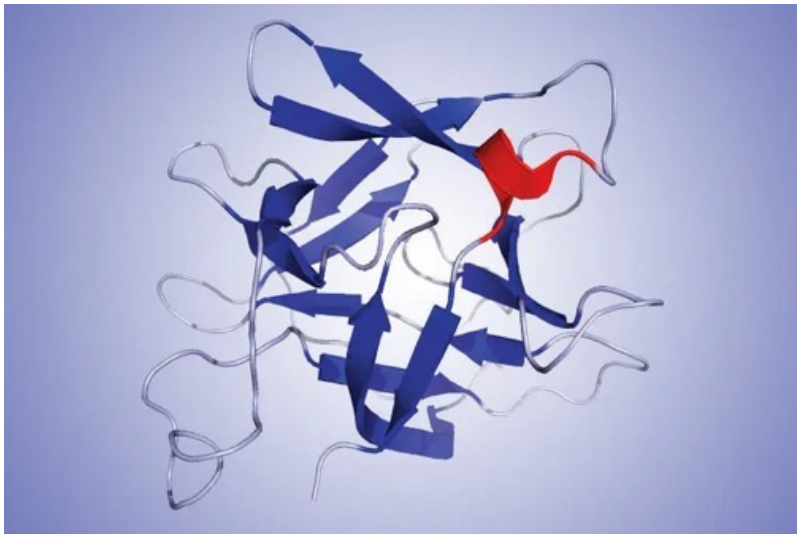

Ein zusätzliches Interleukin-18-Transkript ist das Schlüsselrezept des neuen huCART19-IL18-Konstruktes.

Interleukin-18, kurz IL-18, ist ein proinflammatorisches Zytokin, das zur IL-1-Superfamilie gehört. Es wird von Makrophagen und anderen Zelltypen (u.a. dendritische Zellen, Kupffer-Zellen, Keratinozyten, Osteoblasten, Mikroglia und Fibroblasten) produziert. Interleukin-18 entsteht aus einem Vorläuferpeptid (Pro-IL-18) mit 24 kDa, das durch die Caspase 1 in seine bioaktive 18-kDa-Form aufgespalten wird. In dieser Form bindet es an den Interleukin-18-Rezeptor (IL-18R). Zusammen mit Interleukin-12 induziert es nach einer Konfrontation mit mikrobiellen Lipopolysacchariden (LPS) die zellvermittelte Immunabwehr. Wenn sie mit IL-18 stimuliert werden, sezernieren natürliche Killerzellen und bestimmte T-Zellen Interferon-γ (IFN-γ) oder Typ-II-Interferon, das eine wichtige Rolle bei der Stimulation von Makrophagen spielt.

Enhanced CAR T-Cell Therapy for Lymphoma after Previous Failure

BACKGROUND

Chimeric antigen receptor (CAR) T cells targeting CD19 have transformed the treatment of B-cell cancers, but many patients do not have long-term remission. We designed an anti-CD19 enhanced (armored) CAR T-cell product (huCART19-IL18) that secretes interleukin-18 to enhance antitumor activity.

METHODS

In this study, we assessed the safety, feasibility, and preliminary efficacy of huCART19-IL18 in patients with relapsed or refractory lymphoma after previous anti-CD19 CAR T-cell therapy. Using a 3-day manufacturing process, we administered huCART19-IL18–positive cells in doses ranging from 3×10^6 to 3×10^8.

RESULTS

A total of 21 patients received huCART19-IL18. Cytokine release syndrome occurred in 62% of the patients (47% with grade 1 or 2), and immune effector-cell–associated neurotoxicity syndrome occurred in 14% (all grade 1 or 2). No unexpected adverse events were observed. Robust CAR T-cell expansion was detected across all dose levels. At 3 months after infusion, a complete or partial response was seen in 81% of the patients (90% confidence interval [CI], 62 to 93) and a complete response in 52% (90% CI, 33 to 71). With a median follow-up of 17.5 months (range, 3 to 34), the median duration of response was 9.6 months (90% CI, 5.5 to not reached).

CONCLUSIONS

In this small study, huCART19-IL18 had a safety profile consistent with other CAR T-cell treatments and showed promising efficacy at low cell doses in patients with lymphoma after the failure of previous anti-CD19 CAR T-cell therapy. (ClinicalTrials.gov number, NCT04684563.)

A promising strategy to improve CAR T-cell efficacy involves developing fourth-generation armored CAR T cells that secrete proinflammatory cytokines to bolster antitumor activity. This approach is currently being explored in solid tumors according to the hypothesis that cytokine secretion enhances the cytotoxicity of CAR and tumor-infiltrating T cells while modifying the immunosuppressive tumor microenvironment. One such cytokine, interleukin-18, is a proinflammatory molecule that is primarily produced by macrophages and dendritic cells. Interleukin-18 enhances the activation of T cells and natural killer cells, promotes the production of interferon-γ, and has potential therapeutic applications. Preclinical studies conducted by our group and others have shown that interleukin-18–armored CAR T cells have superior antitumor efficacy and result in prolonged survival in mouse models.
Building on this concept, we developed huCART19-IL18, an autologous anti-CD19 CAR T-cell product that constitutively secretes interleukin-18. In addition, huCART19-IL18 is manufactured in a rapid, 3-day process that is designed to preserve stem-cell–like characteristics and reduce exhaustion in T cells. To mitigate immunogenicity and improve CAR T-cell persistence, we incorporated a humanized anti-CD19 single-chain variable fragment.

Treatment

Autologous T cells were obtained from the patients by means of leukapheresis. Bridging therapy was optional. Manufacturing and cryopreservation of huCART19-IL18 was performed by the Clinical Cell and Vaccine Production Facility at the University of Pennsylvania. Dose levels of huCART19-IL18 between 3×10^6 and 3×10^8 cells were administered as a single intravenous infusion 2 to 5 days after lymphodepleting chemotherapy. Lymphodeletion was performed with either bendamustine (at a dose of 90 mg per square meter of body-surface area) for 2 days or a combination of cyclophosphamide (at a dose of 250 mg per square meter) and fludarabine (at a dose of 25 mg per square meter) for 3 days at the discretion of the investigator. Patients who had a clinical benefit after the huCART19-IL18 infusion but who had residual or relapsing disease could receive retreatment with huCART19-IL18.

Efficacy and Safety Measures

The initial response assessment was performed 3 months after the huCART19-IL18 infusion according to the Lugano 2014 response criteria. Patients were then transitioned to long-term follow-up. The grading of cytokine release syndrome and immune effector cell–associated neurotoxicity syndrome (ICANS) was performed according to consensus criteria.

Correlative Studies

We determined the degree of huCART19-IL18 expansion and persistence by measuring the number of copies of huCART19 transgene per microgram of genomic DNA using real-time quantitative polymerase-chain-reaction (qPCR) assays.

Characteristic	Patients (N=21)
Median age (range) — yr	64 (47–74)
Male sex — no. (%)	16 (76)
ECOG performance-status score — no. (%)†	
0	2 (10)
1	19 (90)
Lymphoma subtype — no. (%)	
Large B-cell lymphoma	12 (57)
Diffuse large B-cell lymphoma, not otherwise specified	8 (38)
Transformed follicular lymphoma	2 (10)
High-grade B-cell lymphoma	1 (5)
T-cell histiocyte-rich large B-cell lymphoma	1 (5)
Follicular lymphoma	6 (29)
Mantle-cell lymphoma	3 (14)
Median no. of previous medications (range)	7 (4–14)
Previous therapy or procedure — no. (%)	
Autologous stem-cell transplantation	7 (33)
Allogeneic stem-cell transplantation	1 (5)
Bispecific antibody therapy	7 (33)
Previous CAR therapy — no./total no. (%)	
CD28-based product	10/20 (50)
Axicabtagene ciloleucel	8/20 (40)
Brexucabtagene autoleucel	2/20 (10)
4-1BB–based product	10/20 (50)
Tisagenlecleucel	8/20 (40)
Lisocabtagene maraleucel	2/20 (10)
Response to previous therapy	
Progressive disease — no./total no. (%)	7/20 (35)
Median progression-free survival — mo (90% CI)	6.7 (3.1–10.2)

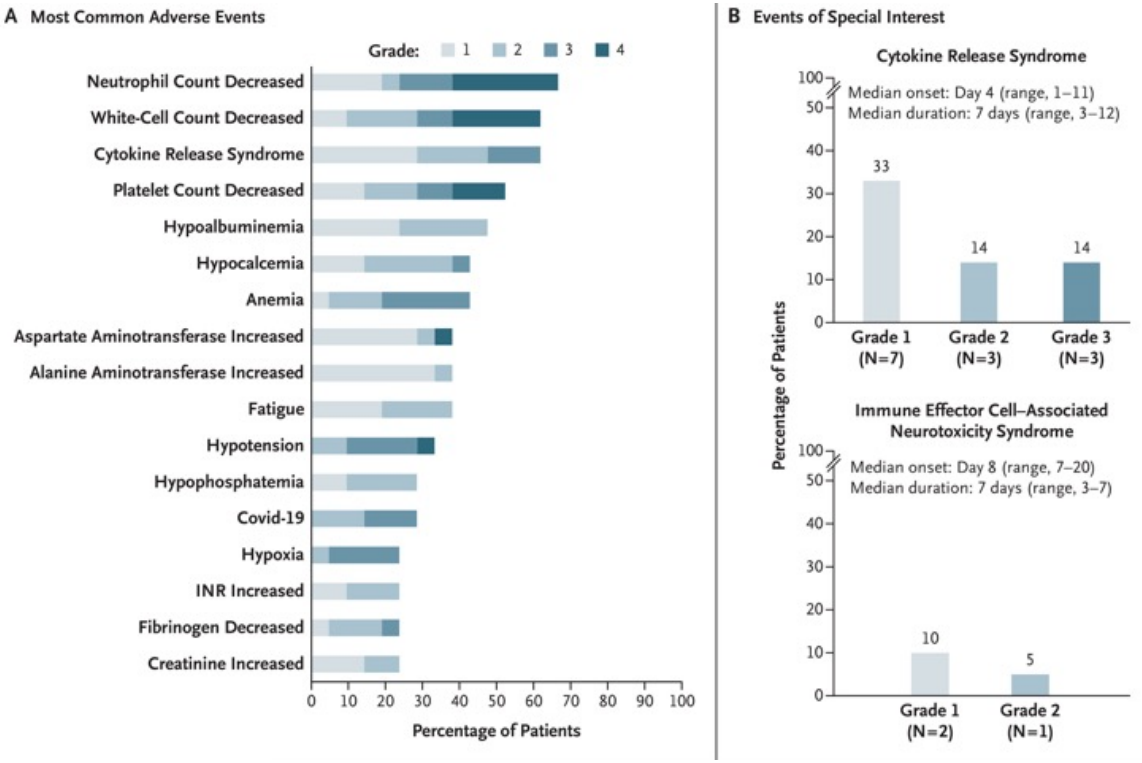

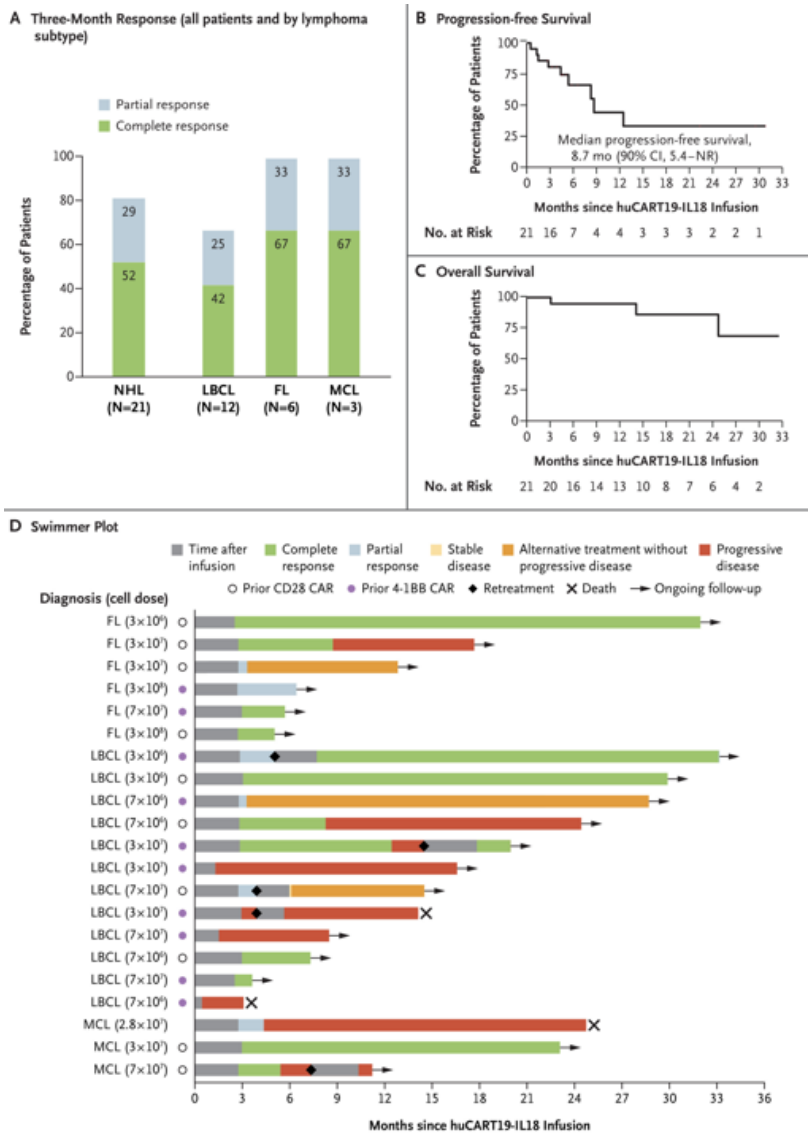

Clinical Response and Survival.

Shown are the responses at 3 months in all patients (left) and according to lymphoma subtype (right) (Panel A), Kaplan–Meier estimates of progression-free survival (Panel B) and overall survival (Panel C), and a swimmer plot indicating the response to treatment according to lymphoma subtype, huCART19-IL18 cell dose, previous second-generation CD19-directed chimeric antigen receptor (CAR) T-cell therapy, response to initial huCART19-IL18 therapy and retreatment (when applicable), and any alternative therapy that was used in patients without disease progression (Panel D). FL denotes follicular lymphoma, LBCL large B-cell lymphoma, MCL mantle-cell lymphoma, NHL non-Hodgkin's lymphoma, and NR not reached.

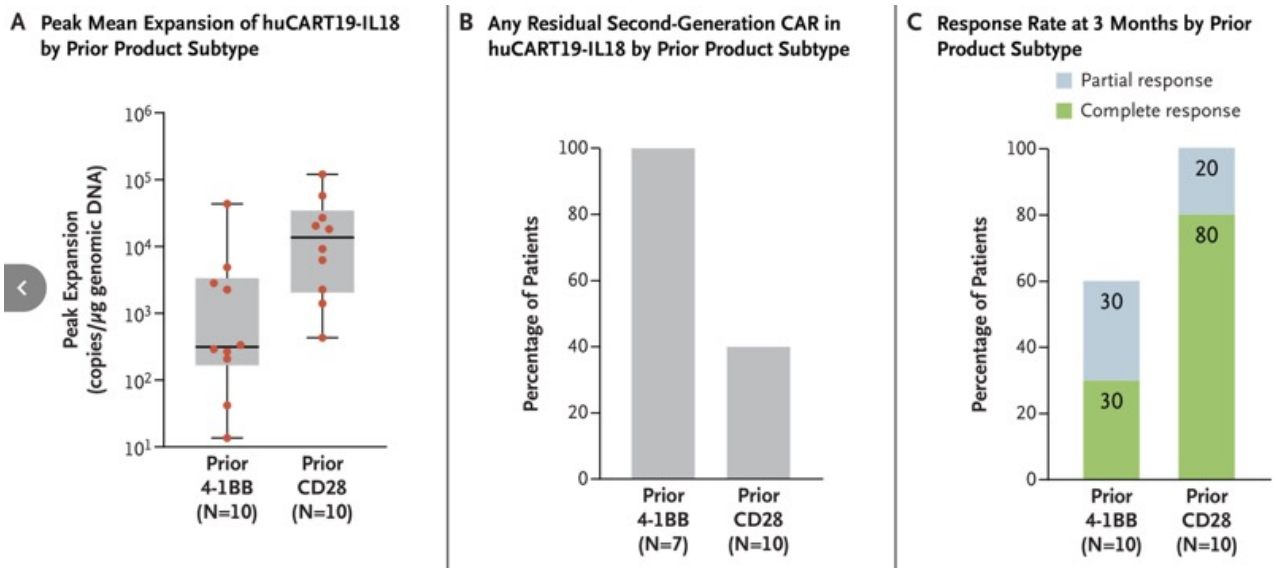

Effect of Previous CD19-Directed CAR T-Cell Therapy on Expansion and Efficacy of huCART19-IL18.

Panel A shows a comparison of values for the peak mean expansion of huCART19-IL18 according to the product subtype that the patient had previously received. The ratio of geometric means for peak expansion of huCART19-IL18 with prior CD28, as compared with prior 4-1BB product, was 16.3 (90% confidence interval [CI], 3.2 to 81.9). The huCART19-IL18 levels were assessed by means of quantitative real-time polymerase chain reaction (qPCR) and reported in copies per microgram of genomic DNA. Panel B shows the assessment of huCART19-IL18 products for the presence of previous second-generation CD19-directed CAR T cells in 17 patients. The assessment was performed with the use of Applied Biosystems TaqMan PCR to detect the sequences of integrated commercial CD19 CAR transgenes. Only 40% of the patients who had received previous treatment with a CD28-based product had detection of residual CAR, as compared with 100% of the patients who had previous treatment with a 4-1BB–based product. The odds ratio for residual CAR detection with prior CD28, as compared with prior 4-1BB product, was 0.1 (90% CI, 0 to 0.42). Panel C shows the differences in response distribution at 3 months according to previous CD19-directed CAR T-cell therapy. The odds ratio for a complete response with prior CD28, as compared with prior 4-1BB product, was 9.3 (90% CI, 1.2 to 84.0).

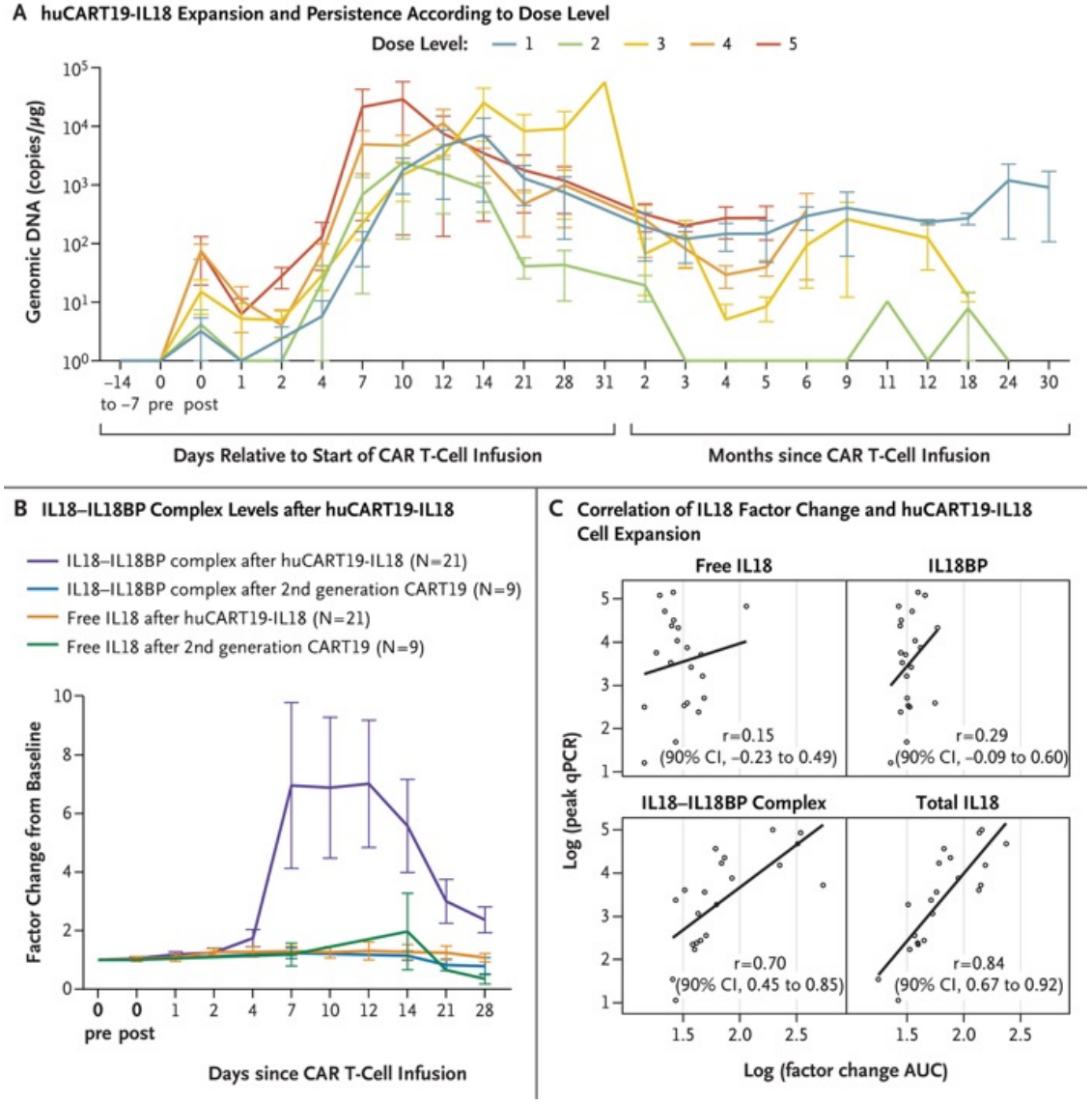

Correlative Studies.

Panel A shows the expansion of huCART19-IL18 T cells in peripheral blood as assessed by qPCR assay and measured as copies per microgram of genomic DNA, separated according to dose level 1 (DL1) through dose level 5 (DL5). Panel B shows the levels of free interleukin-18 (IL18) and interleukin-18 binding protein (IL18BP) complex, as measured by enzyme-linked immunosorbent assay. The amount of free interleukin-18 and interleukin-18 bound to IL18BP is plotted. Although serum levels of free interleukin-18 remained low (probably owing to rapid binding by IL18BP), the substantial increases in total levels of interleukin-18–IL18BP complex may serve as surrogate markers for interleukin-18 production by huCART19-IL18. The elevations in interleukin-18–IL18BP were not seen in historical blood samples after the infusion of second-generation anti-CD19 CAR T cells from the same patients. Panel C shows a scatter plot that illustrates the relationship between the log factor change in interleukin-18 forms (on the x axis) and huCART19-IL18 expansion in blood (on the y axis). Calculations of the Pearson correlation coefficient (r) and corresponding 90% confidence intervals are indicated for each plot. The increases in levels of total interleukin-18 and interleukin-18–IL18BP complex correlate with the expansion of huCART19-IL18 T cells, but no correlation is seen with levels of either free interleukin-18 or free IL18BP. AUC denotes area under the curve.

Discussion

In our trial, we found that autologous interleukin-18–armored CAR T cells had promising clinical activity in patients with relapsed or refractory CD19+ lymphomas after the failure of previous anti-CD19 CAR T-cell therapy. The treatment was associated mainly with toxic effects of grade 1 or 2, with no unexpected or delayed effects observed. Our findings indicate that 3-day manufacturing of huCART19-IL18 from autologous T cells is feasible, with 21 of 22 eligible patients receiving the product.

Our goal of using an expedited 3-day manufacturing process was to enrich the product with less differentiated naive-like CAR T cells, which could enhance in vivo expansion and activity. We observed the expansion of huCART19-IL18 with persistence for more than 2 years in some patients. Such persistence occurred even in patients who had received the lowest dose of huCART19-IL18 (3×10^6), which is lower than the dose used for treatment of lymphomas with currently available second-generation CAR T products by a factor of approximately 20 to 100. Although the median vein-to-vein time was more than 2 months in this trial because of the protocol-mandated safety stagger design, a shorter manufacturing process may have the additional benefit of reducing the time required to produce and administer the CAR T-cell therapy.

Der Begriff "dunkle Materie der Ernährung" bezieht sich auf die große Anzahl an unbekannten oder nicht vollständig verstandenen Verbindungen in Lebensmitteln, die möglicherweise eine Rolle für die menschliche Gesundheit spielen. Diese "dunkle Materie" kann durch innovative Technologien wie AI und Netzwerkforschung identifiziert und erforscht werden, um die Auswirkungen von Lebensmitteln auf die Gesundheit besser zu verstehen.

•Unbekannte Verbindungen:

•In Lebensmitteln gibt es eine Vielzahl von Molekülen und Verbindungen, die noch nicht vollständig identifiziert oder verstanden sind. Diese Verbindungen könnten wichtige Auswirkungen auf unsere Gesundheit haben, aber ihre Rolle bleibt oft unklar.

•Potenzielle Auswirkungen:

•Diese "dunkle Materie" könnte für die Erklärung der positiven Auswirkungen bestimmter Lebensmittel auf die Gesundheit entscheidend sein, wie z.B. die gesundheitsfördernden Eigenschaften von Tee oder Knoblauch.

•AI und Netzwerkforschung:

•Künstliche Intelligenz und Netzwerkforschung werden eingesetzt, um diese unbekannten Verbindungen zu identifizieren und ihre Auswirkungen auf die Gesundheit zu verstehen.

•**Beispiel: Polyphenole:** Nature food nennt Polyphenole als ein Beispiel für eine Verbindung, die in Lebensmitteln wie Kakao, Früchten, Nüssen und Samen vorkommt und möglicherweise für viele der gesundheitlichen Vorteile dieser Lebensmittel verantwortlich ist.

MHP Dark Matter, 1560g Dose, Fruit Punch

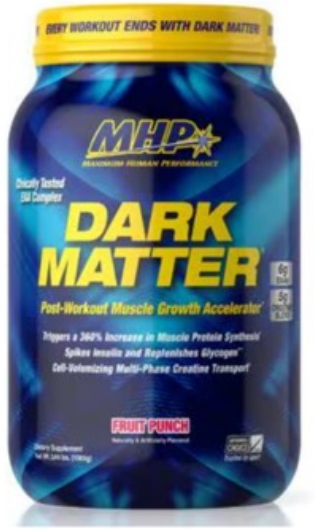

METASPORT

Chemical Complexity of Food and Implications for Therapeutics

Poor nutrition is a leading cause of illness in the United States, contributes to more than half a million deaths each year and affects half of all American adults who have one or more preventable noncommunicable diseases, such as cardiovascular disease, hypertension, type 2 diabetes mellitus, cancer, and poor bone health. Beyond increasing the risk of disease, poor nutrition has broad societal effects, driving up health care costs and decreasing productivity, with expenditures for obesity alone reaching $173 billion annually. By contrast, adopting a healthy diet and lifestyle can significantly counteract even a strong genetic predisposition to coronary heart disease and reduce the relative risk by nearly 50%.

Growing evidence further highlights the importance of dietary quality in disease prevention, particularly amid a global surge in early-onset cancers — an emerging research priority identified by the National Cancer Institute. Indeed, since the 1990s, the incidence of cancer among adults under the age of 50 years has risen worldwide, despite unchanged hereditary cancer rates, a finding that underscores the influence of environmental and lifestyle factors. Early-life exposures have shifted markedly over the past several decades and reflect trends toward overweight, obesity, and Western-style diets, even among children and adolescents.

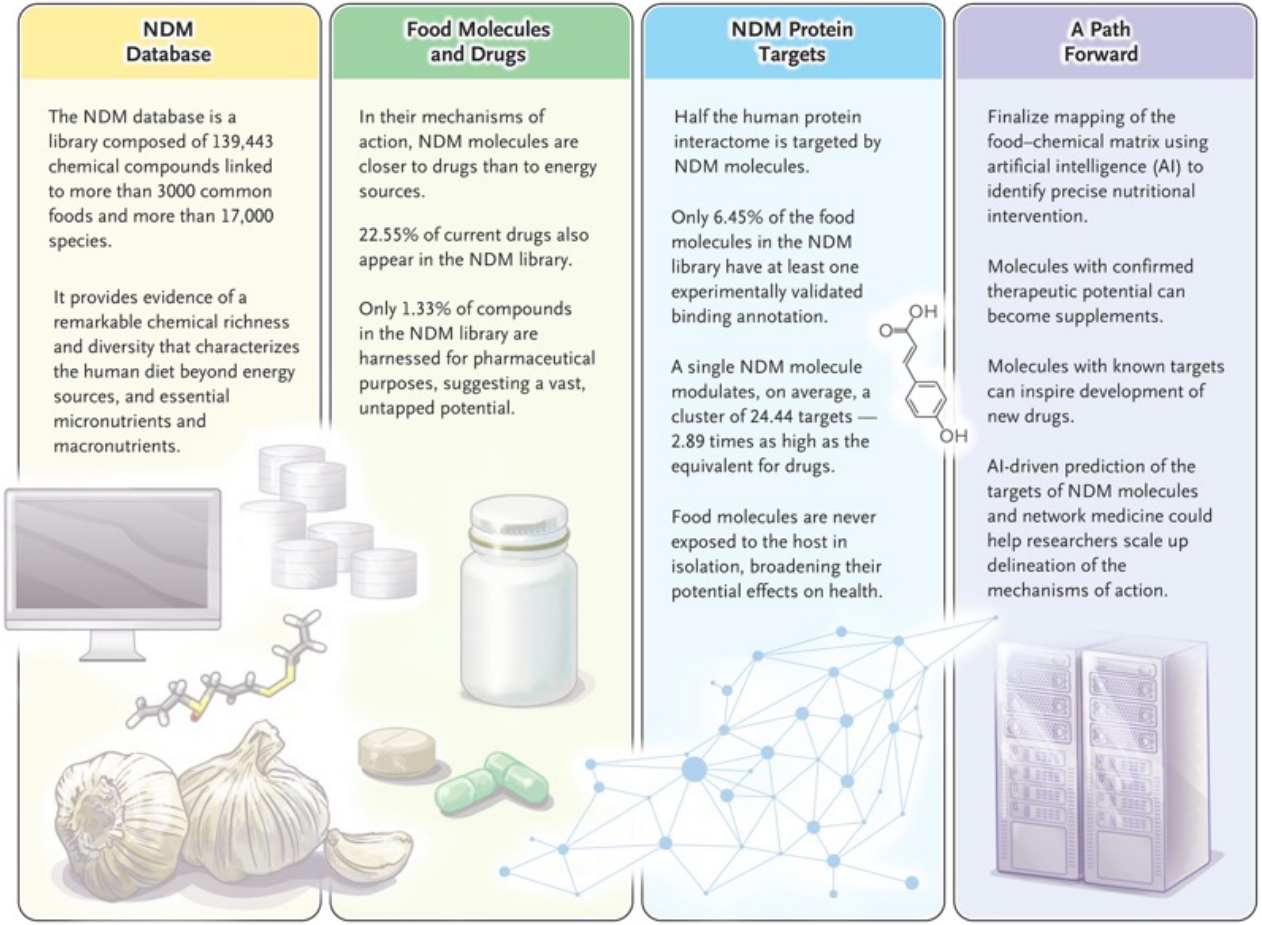

Overall Approach to Food Molecule Research, from Nutrition Dark Matter (NDM) to Food as Medicine.

As the Food Is Medicine initiative progresses, promising better health through nutritious food, it becomes essential to go beyond standard nutritional components and map the full spectrum of food molecules in order to identify the mechanisms that support well-being. By characterizing the bioactivity of food compounds as compared with that of drugs and exploring the broader therapeutic potential of NDM, we can deepen our understanding of the effect of diet on health and contribute to the progress of systems pharmacology.

KEY POINTS

Chemical Complexity of Food

- More than 139,000 molecules in food, termed “nutrition dark matter” (NDM), hold immense, largely untapped therapeutic potential.
- Food molecules affect nearly half the human proteome and play a role as broad modulators of biologic processes.
- Approximately 2000 food molecules are already used as drugs, which highlights the pharmaceutical relevance of food chemicals.
- Advanced artificial intelligence (AI) tools and network medicine frameworks could help researchers decode the health relevance of NDM and enable predictions of molecular targets and biologic mechanisms.
- The lack of systematic food–chemical mapping limits progress; strategic funding and scalable AI-based approaches are urgently needed.
- Mapping NDM could revolutionize dietary science and accelerate drug discovery, which would complement the achievements of the Human Genome Project.

Conclusions

The sequencing of the human genome has revolutionized biology by offering a platform to explore genomic variations, as well as to understand how these variations lead to disease. This information is essential but not sufficient to understand human disease, as illustrated by the fact that genetic effects account for only 10% of disease occurrences; the bulk of the remaining occurrences can be linked to environmental and dietary factors. To harness fully the potential for the role of diet in improving health and longevity, we must characterize the vast molecular repertoire of foods. The approach we describe — systematically identifying, cataloguing, and analyzing tens of thousands of food molecules — represents a critical step forward. By unveiling the molecular mechanisms through which these compounds interact with human biologic pathways, this strategy not only refines our definition of dietary quality but also opens new avenues for targeted therapies and precision nutrition. We are only at the beginning of this journey. Although we have thus far documented more than 139,000 molecules in food, for the vast majority of them, we do not yet know if they are absorbed after ingestion, how they are metabolized (by the gut microbiome, the host, or both), to which proteins they bind, and what cellular processes they affect. Unlocking this knowledge could revolutionize the way we think about the role of food in health.

Zusammenfassend: Die "dunkle Materie der Ernährung" ist ein Bereich, der sich auf die Identifizierung und Untersuchung von unbekannten oder wenig verstandenen Verbindungen in Lebensmitteln konzentriert, um ein besseres Verständnis ihrer Auswirkungen auf die menschliche Gesundheit zu erlangen.

Sea Anemone Sting

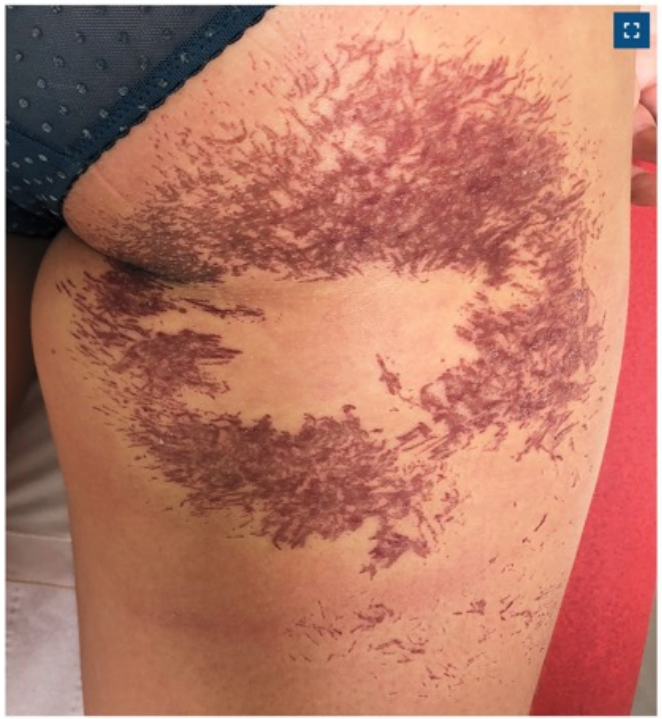

A previously healthy 28-year-old woman presented to the outpatient clinic with a painful rash on her right thigh. Five days before presentation, she had been walking on sea rocks on an island in the Cyclades region of Greece — an area of the Mediterranean known to have a large population of sea anemones — when she fell, landing on her buttocks. She immediately felt a severe pain in her right thigh, and an itchy, red lesion developed. She did not see what had stung her. She cleaned the skin with seawater and applied an emollient cream. On physical examination at the current presentation, innumerable fine, erythematous, linear lesions in a stellate distribution with central clearing on the posterior right thigh were seen. A diagnosis of sea anemone sting was made. Skin exposure to sea anemone venom leads to local inflammation at the site of the wound. Treatment with a topical glucocorticoid and emollient cream was provided. At a follow-up visit at 3 months, the skin showed only mild residual hyperpigmentation.

Central Nervous System Tuberculomas

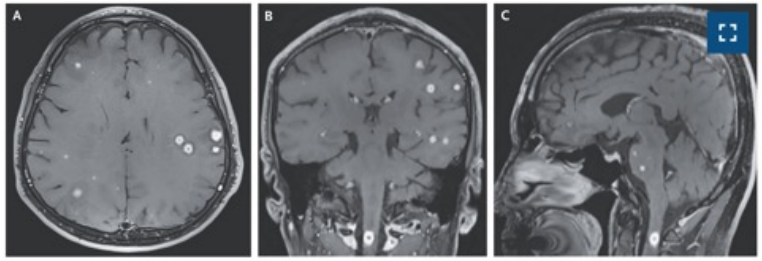

A 57-year-old man with previously treated pulmonary tuberculosis presented to the emergency department with a 2-week history of neck pain, headache, and tingling in his right hand. Physical examination was notable for decreased grip strength in the right hand. Computed tomography of the chest revealed a miliary pattern of nodules in both lungs. Magnetic resonance imaging (MRI) of the head with gadolinium enhancement revealed numerous small, spherical, peripherally enhancing nodules in the cerebral hemispheres (Panels A and B), basal ganglia, cerebellum, and brain stem, as well as in the upper spinal cord with surrounding edema (Panel C). No leptomeningeal enhancement was noted. Results of cerebrospinal fluid analysis were normal, and cerebrospinal fluid cultures showed no growth. A sputum culture grew *Mycobacterium tuberculosis*. A diagnosis of central nervous system (CNS) tuberculomas in the context of miliary tuberculosis was made. Tuberculomas are granulomatous lesions that result from the hematogenous spread of tuberculosis. When many such lesions are present in the brain, a "starry sky" pattern may be seen on imaging. CNS tuberculomas may or may not (as in this case) be associated with tuberculous meningitis. Treatment with antituberculous agents and dexamethasone was initiated. Approximately 1 month later, the patient's symptoms began to abate. At an 18-month follow-up visit, his symptoms had resolved completely, and repeat MRI of the head was normal.

Case 13-2025: A 70-Year-Old Man with Weight Loss, Weakness, and Anorexia

A 70-year-old man presented to the emergency department of this hospital because of a 6-week history of anorexia, weakness, and weight loss.

Six weeks before this presentation, the patient's psychiatrist, who had been treating him for depression, increased his dose of bupropion because of progressive fatigue. The fatigue continued to worsen, and the patient had a loss of appetite; the dose of bupropion was decreased and then discontinued 2 weeks later.

The patient first presented to the emergency department of this hospital 8 days before the current presentation because of muscle weakness, headache, and ongoing anorexia. Imaging studies were obtained.

Computed tomography (CT) of the abdomen and pelvis, performed after the administration of intravenous contrast material, revealed a left adrenal nodule that measured 1.9 cm in diameter. This lesion was indeterminate for adenoma on the basis of the attenuation level, which was greater than 10 Hounsfield units. No splenomegaly, lymphadenopathy, or evidence of other inflammatory or infectious process was present in the abdomen. CT angiography of the head and neck, performed before and after the administration of intravenous contrast material, was unremarkable.

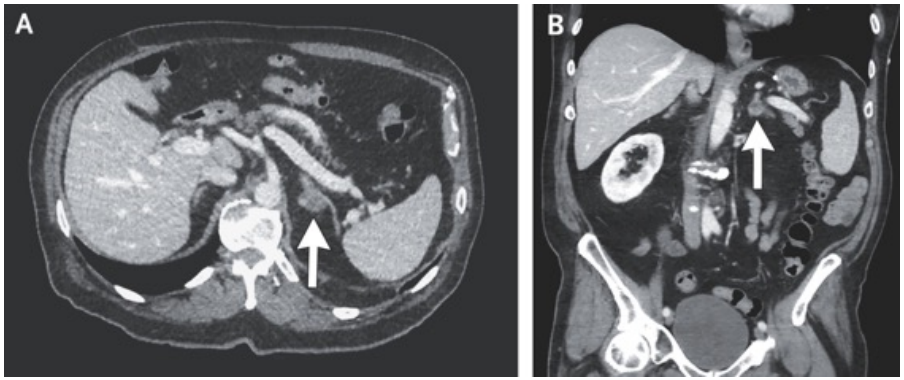

CT of the abdomen and pelvis and CT angiography of the head and neck were performed on the day of admission. An axial image of the abdomen (Panel A) and a coronal image of the abdomen and pelvis (Panel B), obtained after the administration of contrast material, show an indeterminate adrenal lesion (arrows), measuring 1.9 cm in diameter.

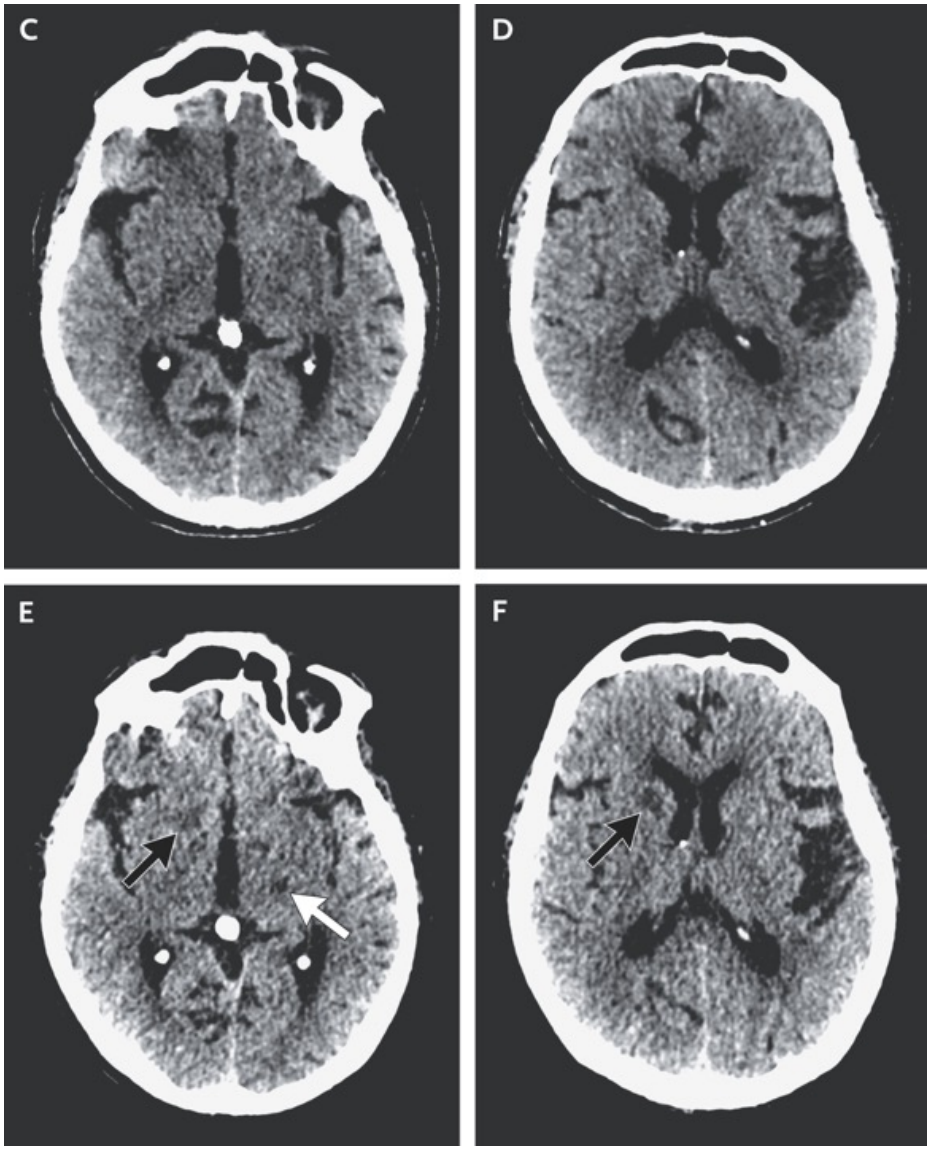

Axial images of the head (Panels C and D), obtained before the administration of contrast material, show no acute intracranial pathologic features.

CT of the head was performed without the administration of intravenous contrast material on hospital day 5 after the patient was transferred to the intensive care unit.

Second CT of the head done on next admission.
Axial images (Panels E and F) at the same levels as those of the previous images (Panels C and D) show new areas of parenchymal hypoattenuation involving the right caudate and anterior limb of the internal capsule (black arrows) and the left lateral thalamus (white arrow).

Owing to progressive fatigue and anorexia, the patient returned to the emergency department of this hospital 7 days after his initial presentation. On evaluation, he noted marked anorexia, dysgeusia, and severe fatigue, despite discontinuation of bupropion. Progressive generalized muscle weakness persisted, and the patient reported a weight loss of 13.6 kg that had occurred during the previous 6 weeks. A review of systems was notable for intermittent headache without photophobia, phonophobia, or neck stiffness; skin thinning, worsening mood, and anhedonia were also noted. There was no abnormal bleeding, proximal muscle weakness, fever, rigors, night sweats, cough, diarrhea, abdominal pain, rash, or dyspnea.

The patient's medical history was notable for hairy-cell leukemia, which had been treated and was in remission for 7 years; major depressive disorder, for which he had had multiple psychiatric admissions and had been treated with electroconvulsive therapy and implantation of a vagus-nerve stimulator; obesity, for which he had undergone Roux-en-Y gastric bypass; primary hypertension; and benign prostatic hyperplasia. Medications included bupropion, escitalopram, gabapentin, risperidone, tamsulosin, and lisinopril. His family history included bipolar disorder in his mother. He lived alone in an urban area of New England and was homebound most of the time owing to debility; a caretaker was needed to perform many household activities. He did not smoke, drink alcohol, or use recreational drugs. He had no known adverse reactions to medications. There had been no recent travel or exposure to sick contacts.

On examination, the oral temperature was 36.3°C, the blood pressure 136/81 mm Hg, the pulse 100 beats per minute, the respiratory rate 24 breaths per minute, and the oxygen saturation 99% while the patient was breathing ambient air. Tachypnea was noted, without increased work of breathing. The jugular venous pulsation was seen under the clavicle with the patient lying flat. Cardiac examination was normal. Scattered bruises and thinning of the skin were present, but he had no rash or petechiae. No proximal muscle weakness was observed on strength testing. The patient was alert and able to recite the days of the week backward without difficulty.

Laboratory test results were notable for hypokalemia, with a potassium level of 3.1 mmol per liter (reference range, 3.4 to 5.0), and a blood glucose level of 225 mg per deciliter (12.5 mmol per liter; reference range, 70 to 110 mg per deciliter [3.9 to 6.1 mmol per liter]). A complete blood count showed thrombocytopenia (platelet count, 91,000 per microliter; reference range, 150,000 to 400,000), a chronic condition that the patient had had since undergoing cancer treatment, as well as lymphopenia (absolute lymphocyte count, 570 per microliter; reference range, 1000 to 4800). Testing was negative for human immunodeficiency virus (HIV) types 1 and 2, syphilis, hepatitis C virus, and hepatitis B virus. Blood levels of vitamin B_{12}, copper, and thyrotropin were normal. The glycated hemoglobin level was 7.2%; 1 year earlier, the level had been 6.2%. Measurement of venous blood gases revealed respiratory alkalosis, with a pH of 7.48 (reference range, 7.35 to 7.45) and a partial pressure of carbon dioxide of 22 mm Hg (reference range, 38 to 50).

Variable	Reference Range, Adults, This Hospital†	On Admission, This Hospital
Blood		
Hemoglobin (g/dl)	13.5–17.5	16.7
Hematocrit (%)	41–53	48
White-cell count (per μl)	4500–11,000	7.17
Differential count (per μl)		
Neutrophils	1800–7700	5930
Lymphocytes	1000–4800	570
Monocytes	200–1200	540
Eosinophils	0–900	70
Basophils	0–300	50
Immature granulocytes	0–100	0
Platelet count (per μl)	150,000–400,000	91,000
Sodium (mmol/liter)	135–145	137
Potassium (mmol/liter)	3.4–5.0	3.1
Chloride (mmol/liter)	98–108	100
Carbon dioxide (mmol/liter)	23–32	16
Urea nitrogen (mg/dl)	8–25	28
Creatinine (mg/dl)	0.60–1.50	1.15
Glucose (mg/dl)	70–110	225
Total protein (g/dl)	2.6–4.5	7.3
Albumin (g/dl)	8.5–10.5	4.3
Alanine aminotransferase (U/liter)	7.30–7.40	14
Aspartate aminotransferase (U/liter)	0.5–2.0	21
Alkaline phosphatase (U/liter)	2.3–6.6	66
Total bilirubin (mg/dl)	6.0–8.3	0.5
High-sensitivity troponin T (ng/liter)	3.3–5.0	14
N-terminal pro–B-type natriuretic peptide (pg/ml)	0–900	247
Erythrocyte sedimentation rate (mm/hr)	45–115	12
C-reactive protein (mg/liter)	0.0–1.0	7.7
Venous blood gases		
Fraction of inspired oxygen	13–60	21
pH	7.35–7.45	7.48
Partial pressure of carbon dioxide (mm Hg)	38–50	22
Cerebrospinal fluid		
Total protein (mg/dl)	5–55	92
Glucose (mg/dl)	50–75	2
Red-cell count (per μl)	0–5	500
Nucleated-cell count (per μl)	0–5	67
Differential count (%)		
Neutrophils	0	48
Lymphocytes	0–100	32
Monocytes	0	16

Rather severe chronic respiratory alkalosis that is appropriately compensated.
Cushing‘s syndrome would be expected to cause metabolic alkalosis.

CT of the chest, performed after the administration of intravenous contrast material in accordance with a pulmonary embolism protocol, did not show a pulmonary embolism or any other radiologically significant findings. The adrenal adenoma that had been observed on previous abdominopelvic imaging was stable in appearance.

Blood cultures were obtained, and treatment with high-dose intravenous thiamine and high-dose oral ascorbic acid was initiated. The patient was admitted to this hospital.

Over the course of the next 2 days, progressive confusion developed in the patient. Physical examination revealed intermittent episodes of unresponsiveness that later became sustained; there were no motor deficits or cranial nerve asymmetry. Continuous electroencephalography showed diffuse delta and theta slowing, without overt seizure activity. The patient had episodes of narrow-complex tachycardia with retrograde P waves and blood pressure that remained stable; these episodes did not reliably correlate with periods of obtundation. Treatment with metoprolol resulted in suppression of the tachycardia.

The patient underwent endotracheal intubation for airway protection on hospital day 5 because of progressive encephalopathy. He was subsequently transferred to the intensive care unit.

CT of the head was performed without the administration of intravenous contrast material on hospital day 5 and revealed small areas of hypoattenuation involving the right caudate and anterior limb of the internal capsule and the left lateral thalamus. Although incompletely characterized by CT, these lesions were most likely recent lacunar infarcts. Given the presence of systemic illness, the differential diagnosis for these findings also includes parenchymal edema and changes seen with infections of the central nervous system.

Owing to the persistent encephalopathy in this patient, a lumbar puncture was performed; findings were notable for an opening pressure of at least 58 cm of water (the meniscus surpassed the manometer). Cerebrospinal fluid (CSF) analysis revealed 67 total nucleated cells per microliter (reference range, 0 to 5), of which 48% were neutrophils and 32% were lymphocytes, with 500 red cells per microliter (reference value, <5), as well as a CSF total protein level of 92 mg per deciliter (reference range, 5 to 55) and a CSF glucose level of 2 mg per deciliter (0.1 mmol per liter; reference range, 50 to 75 mg per deciliter [2.8 to 4.2 mmol per liter]).

Before the development of altered mental status in this patient, initial investigations were targeted toward evaluating for nutritional and endocrinologic disorders, namely evaluation of hypercortisolism given the findings of skin thinning, hypokalemia, worsening hyperglycemia, and the adrenal nodule. A 24-hour urine collection for measurement of urinary cortisol excretion was completed.

Differential Diagnosis

This 70-year-old man presented with subacute progressive anorexia, weight loss, and headache. Shortly after admission to this hospital, fulminant encephalopathy developed in the patient. This case requires iterative clinical reasoning with synthesis of multiple pivot points to arrive at a diagnosis. The process of clinical reasoning often unfolds much like the way we approach a jigsaw puzzle. Thus, I will apply a framework I will call “jigsaw heuristics” to approach this complex case.

There are several stages of assembling a jigsaw puzzle, including unboxing the pieces, identifying the corners and edges, assembling landmarks, and bridging across the more homogeneous parts of the puzzle. I will use a similar strategy to develop a differential diagnosis for this patient.

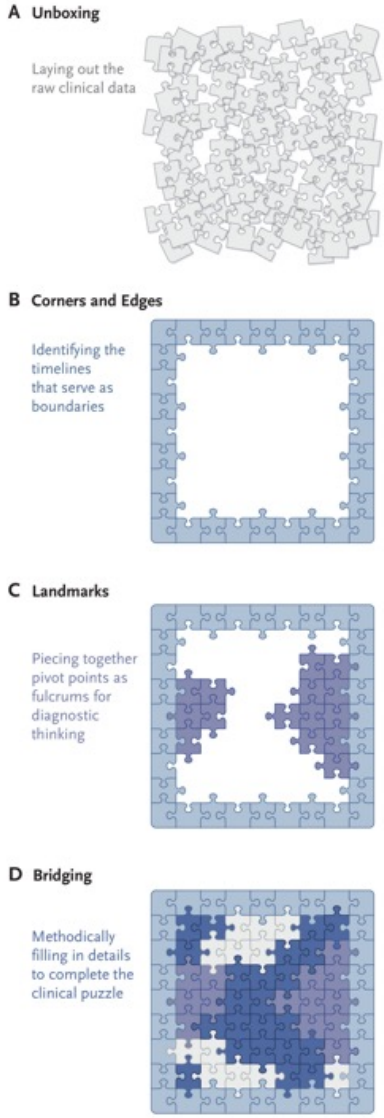

Jigsaw Heuristics.
Shown are the principles of assembling a jigsaw puzzle, including unboxing the pieces, identifying the corners and edges, assembling the landmarks, and bridging across the more homogeneous parts of the puzzle, as applied to clinical reasoning.

Cushing's Syndrome

This patient has numerous features that are consistent with a diagnosis of hypercortisolism, or Cushing's syndrome, including fatigue, hypertension, anhedonia, dysgeusia, skin changes, and laboratory abnormalities such as hypokalemia and hyperglycemia. Cushing's syndrome results from an excess of cortisol from endogenous production or from an exogenous source.

Glucocorticoid excess results in many pathophysiological changes, including catabolism of various tissues, insulin resistance, and neuropsychiatric consequences. It is important to note that characteristic features of hypercortisolism, including weight gain, central adiposity, and facial plethora, were all absent in this patient.

The admitting team astutely identified thinning skin in this patient. This finding results from catabolic effects on keratinocytes, fibroblasts, and epidermal lipids, and it can be identified by measuring skin thickness at the proximal metacarpal–phalangeal joint. Diagnostic testing for Cushing's syndrome includes confirming an excess level of cortisol, followed by localizing the source of cortisol production by measurement of the corticotropin level in the blood, dexamethasone suppression testing, and if needed, inferior petrosal sinus sampling. In the absence of definitive testing, the presence of an adrenal nodule is our only clue to the source.

Abnormal CSF

The striking constellation of CSF findings in this patient, including mild pleocytosis without neutrophilic predominance, a mildly elevated CSF protein level, an extremely low CSF glucose level (hypoglycorrhachia), and a very high opening pressure, are suggestive of meningoencephalitis. When we combine the patient's laboratory findings of meningoencephalitis with his acute-to-subacute course of illness, the absence of risk factors or exposures, and negative laboratory tests, we can narrow the differential diagnosis.

The CSF cell count and the timeline of this patient's presentation are not consistent with acute bacterial meningitis caused by a typical community-acquired organism such as *Neisseria meningitidis*, *Streptococcus pneumoniae*, or common gram-negative bacteria. Infections with viral pathogens such as herpes simplex virus and varicella–zoster virus typically occur suddenly and often in the context of noticeable skin lesions. This patient had a negative screening test for syphilis, and he has no epidemiologic risk factors for tuberculosis. Finally, he did not have symptoms or signs of vasculitis, rheumatologic disorders, or widespread cancer. He also had no pancytopenia, lymphadenopathy, or splenomegaly that would indicate recurrence of hairy-cell leukemia.

To establish the diagnosis of cryptococcal meningitis in the context of Cushing's syndrome, I would obtain specimens of blood and CSF to test for cryptococcal antigen, and if positive, I would confirm the diagnosis with fungal culture of the CSF.

Pathological Discussion

A specimen of peripheral blood was first submitted to the microbiology laboratory on the first hospital day for diagnostic studies, followed by CSF testing on hospital day 5. Blood culture showed a positive result on hospital day 5 with growth of gray-white, mucoid colonies observed on blood agar, findings suggestive of a yeast. India ink staining of the fungal isolate revealed encapsulated budding yeast forms, measuring 2 to 12 µm in diameter, that were consistent with cryptococcus species. Matrix-assisted laser desorption ionization–time-of-flight (MALDI-TOF) mass spectrometry was performed and established a definitive diagnosis of *C. neoformans* infection of the peripheral blood. Subsequent culture of the CSF also grew *C. neoformans*, confirming a diagnosis of cryptococcal meningitis. Latex agglutination antigen testing of both blood and CSF were positive for cryptococcal antigen, with a titer greater than 1:4096 (reference range, negative).

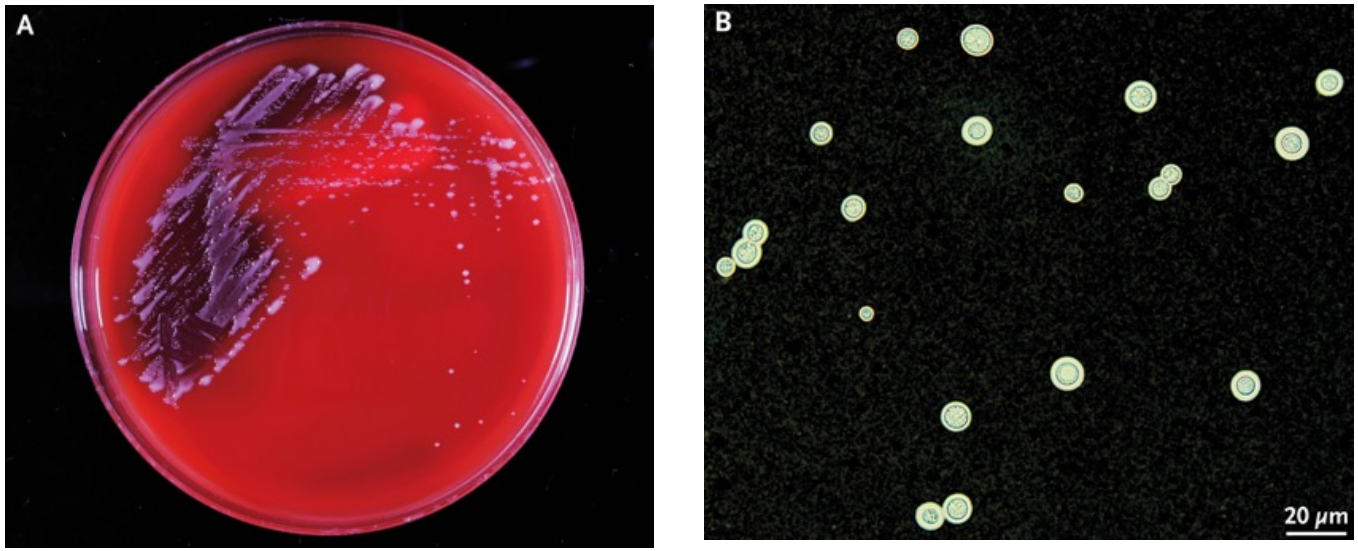

Microbiologic Studies of the Peripheral Blood.

Culture on a blood agar plate (Panel A) shows fungal colony growth with a gray-white, mucoid appearance. An India ink preparation of the fungal colony (Panel B) is morphologically consistent with cryptococcus.

"Zeichentusche"

Shortly after initiation of treatment with amphotericin, apneic episodes and circulatory collapse ensued. Additional neurologic imaging was obtained.
CT of the head, performed without the administration of intravenous contrast material 7 days after admission, revealed diffuse loss of differentiation of gray matter and white matter; marked cerebral edema with near-complete effacement of the ventricles, sulci, and basilar cisterns; and transtentorial herniation. These finding are compatible with severe hypoxic–ischemic injury.

After discussion with the patient's family, it was decided that ongoing invasive treatment would not be in keeping with his wishes after his prolonged illness. Extubation was performed, and the patient died peacefully. A diagnostic test had been ordered before death, with the results reported posthumously.

A 24-hour urinary free cortisol level was 400 µg (reference range, 3.5 to 45), which confirms an elevated level of circulating cortisol and makes Cushing's syndrome a likely diagnosis in this patient.

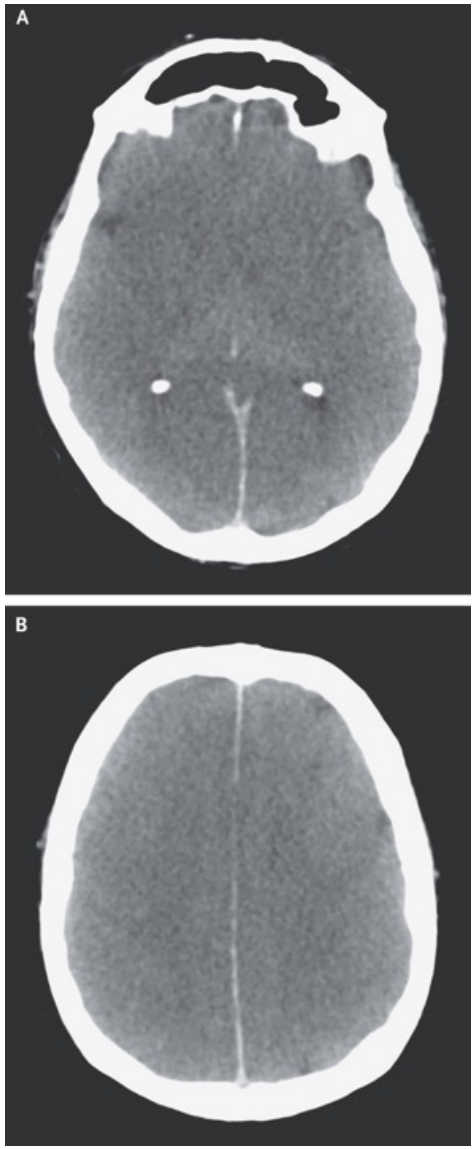

Sierra Leone treibt Mpox-Ausbruch in Afrika voran, meldet Gesundheitsbehörde

Mpox ist eine virale Infektion, die durch engen Kontakt übertragen wird und typischerweise grippeähnliche Symptome sowie mit Eiter gefüllte Hautläsionen verursacht. Die Erkrankung verläuft meist mild, kann jedoch tödlich enden.Nach Angaben der Weltgesundheitsorganisation (WHO), die den Notstand erstmals im August letzten Jahres ausrief, bleibt Mpox aufgrund der weiterhin steigenden Fallzahlen und der zunehmenden geografischen Ausbreitung ein öffentlicher Gesundheitsnotstand.

Die Africa Centres for Disease Control and Prevention (Africa CDC) teilten mit, dass Sierra Leone innerhalb einer Woche 384 bestätigte Fälle meldete, was 50,7 % aller Fälle auf dem Kontinent entspricht.
Sierra Leone, das Mpox bereits im Januar zum öffentlichen Gesundheitsnotstand erklärte, verzeichnete innerhalb nur einer Woche einen Anstieg der bestätigten Fälle um 63 %, erklärte Africa-CDC-Vertreter Ngashi Ngongo in einem Online-Briefing.
Ngongo betonte, dass die Finanzierung das Hauptproblem sei, fügte jedoch hinzu, dass auch die Kontaktverfolgung und die Laborkapazitäten verbessert werden müssten.
"Die Behandlungseinrichtungen für Mpox verfügen lediglich über 60 Betten, wir sprechen jedoch von 800 aktiven Fällen", sagte Ngongo und ergänzte, dass die meisten Infizierten daher zu Hause bleiben müssten.
Bereits im August des vergangenen Jahres hatten Beamte darauf hingewiesen, dass das Budget zur Bekämpfung von Mpox stark unterfinanziert sei. Im Februar warnten sie zudem, dass die von den Vereinigten Staaten zu Beginn des Jahres vorgeschlagenen Kürzungen die Bemühungen zur Eindämmung von Krankheitsausbrüchen gefährden würden.

Clinical presentation and epidemiological assessment of confirmed human mpox cases in DR Congo: a surveillance-based observational study

Summary

Background Mpox, caused by the monkeypox virus, is a serious public health threat in Africa, especially in DR Congo. Previously limited to endemic areas with clade 1a, monkeypox virus has recently spread to non-endemic regions, where clade 1b has emerged. This study provides a clinical comparison of mpox cases in DR Congo regions where clade 1a and clade 1b are prevalent.

Methods We conducted a retrospective observational study, analysing PCR-confirmed mpox cases reported from sentinel health zones in seven provinces between Oct 1, 2023, and Sept 31, 2024. Cases from the newly affected provinces (South-Kivu and Kinshasa) were described along with those from four endemic provinces (Mai-Ndombe, Tshuapa, Tshopo, South-Ubangi, and Équateur). Surveillance data, including type of exposure, demographic details, clinical presentation, complications, and outcomes were collected from national surveillance systems and local health facilities, with laboratory confirmation using quantitative PCR. All analyses were restricted to descriptive statistics.

Findings Of 17 927 suspected cases identified, 10 986 were investigated, 5948 were PCR-positive, and 4895 met the inclusion criteria based on data completeness: 4436 in newly affected and 459 in endemic regions. In newly affected provinces, median age was 20 years (IQR 8–28), 2119 (47·8%) participants were female, and 2310 (52·1%) were male. In endemic provinces, median age was 15 years (7–26), 179 (39·0%) participants were female, and 277 (60·3%) were male. Direct or intimate human contact was reported by 1951 (44·0%) individuals in newly affected provinces versus 25 (5·4%) in endemic provinces, and zoonotic exposure in 11 (0·2%) and 99 (21·6%), respectively. The proportions of partcipants with systemic symptoms (3828 [86·3%] in newly affected provinces and 427 [93·0%] in endemic provinces) and respiratory symptoms (2450 [55·2%] and 219 [47·7%]), and median skin lesion counts (91 [IQR 37–200] and 163 [95–345]) were similar between newly affected and endemic regions. Complications included skin infections (2041 [46·0%] in newly affected provinces and 201 [43·8%] in endemic provinces), respiratory distress (82 [1·8%] and 29 [6·3%]), vision impairment (7 [0·2%] and 28 [6·1%]), and prostration (695 [15·7%] and 51 [11·1%]). The case-fatality rate was 0·7% (95% CI 0·4–1·3; 14 of 1924) in children and 0·6% (0·3–1·0; 14 of 2483) in adults in newly affected areas, compared with 5·9% (3·4–10·0; 14 of 236) in children and 2·7% (1·1–6·1; six of 222) in adults in endemic regions. Content note: this Article and its appendix contain graphic images of mpox lesions affecting various sites including the face and genitals.

Interpretation Our study indicates concurrent mpox outbreaks in DR Congo, involving younger individuals, a higher proportion of women and girls, and distinct presentations with higher lesion counts and respiratory symptoms compared with clade 2b lineage B.1 outbreaks. The high proportion of infectious complications and case-fatality rates, especially in endemic regions, emphasise the need for timely antibiotic therapy and targeted vaccination to reduce morbidity and mortality.

Introduction

Mpox, caused by the monkeypox virus, has become a major public health concern in Africa, particularly in DR Congo.[1] In response to a surge in cases, WHO declared the mpox outbreak in DR Congo a public health emergency of international concern on Aug 14, 2024.[2] Monkeypox virus is divided into clade 1 and clade 2; only clade 1 is present in DR Congo. The situation is complex, with two distinct outbreaks occurring. In northern and western DR Congo, the transmission of clade 1a has increased since early 2023 in long-standing endemic provinces, including Mai-Ndombe, Tshuapa, Tshopo, South-Ubangi, and Équateur.[3] Meanwhile, a second outbreak due to the novel clade 1b lineage began in September, 2023, in previously unaffected regions of eastern DR Congo, particularly South-Kivu province, and has since spread to other cities and provinces, including Kinshasa.[4–7]

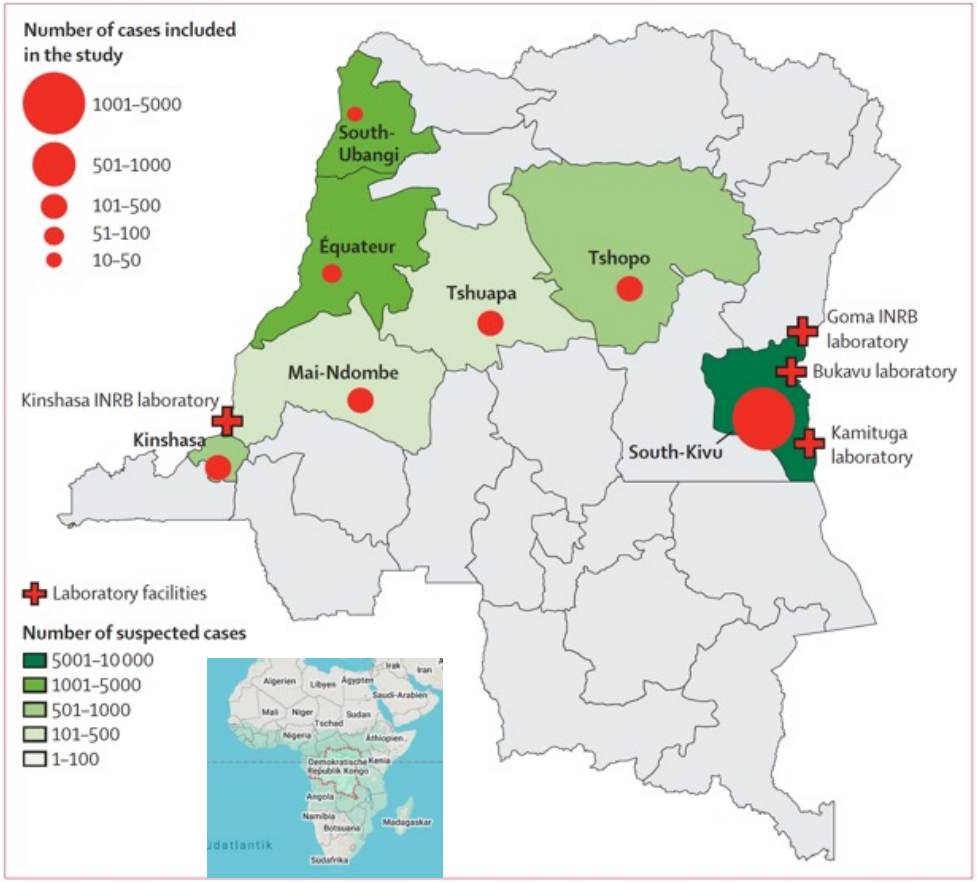

Figure 1: **Geographical distribution of suspected and PCR-confirmed mpox cases identified in DR Congo in this study**

The map shows the geographical distribution of suspected cases and PCR-confirmed cases included in the study across seven provinces: Équateur (4235 suspected, 54 included), Mai-Ndombe (348 suspected, 127 included), South-Ubangi (2368 suspected, 47 included), Tshuapa (365 suspected, 106 included), Tshopo (4317 suspected, 125 included), Kinshasa (502 suspected, 119 included), and South-Kivu (9804 suspected, 4317 included). Laboratories equipped to perform monkeypox virus PCR testing within the country are indicated on the map. INRB=National Institute for Biomedical Research.

	Newly affected provinces (n=4436)	Endemic provinces (n=459)
Age, years		
Median	20 (8–28)	15 (7–26)
0–4	991 (22·3%)	74 (16·1%)
5–14	876 (19·7%)	148 (32·2%)
15–24	1164 (26·2%)	113 (24·6%)
≥25	1375 (31·0%)	123 (26·8%)
Unknown	30 (0·7%)	1 (0·2%)
Sex		
Female	2119 (47·8%)	179 (39·0%)
Male	2310 (52·1%)	277 (60·3%)
Unknown	7 (0·2%)	3 (0·7%)
Pregnancy	18 (0·4%)	3 (0·7%)
Smallpox vaccination in childhood	129 (2·9%)	13 (2·8%)
Profession		
Child not in school	547 (12·3%)	90 (19·6%)
Student	828 (18·7%)	163 (35·5%)
Homemaker	247 (5·6%)	45 (9·8%)
Farmer	302 (6·8%)	28 (6·1%)
Hunter	2 (<0·1%)	13 (2·8%)
Wild game merchant	0	15 (3·3%)
Shopkeeper	216 (4·9%)	0
Miner	139 (3·1%)	0
Health-care worker	14 (0·3%)	1 (0·2%)
Individual engaging in sex work	312 (7·0%)	2 (0·4%)
Police officer	33 (0·7%)	0
Driver	75 (1·7%)	17 (3·7)
Teacher	20 (0·5%)	2 (0·4%)
Unemployed	331 (7·5%)	8 (1·7%)
Other*	431 (9·7%)	9 (2·0%)
Not reported	939 (21·2%%)	66 (14·4%)
Type of exposure†		
Direct or intimate contact‡	1951 (44·0%)	25 (5·4%)
Household contact	918 (20·7%)	146 (31·8%)
Caregiving contact§	327 (7·4%)	30 (6·5%)
Interaction at school, market, or church¶	NA	61 (13·3%)
Animal contact	11 (0·2%)	99 (21·6%)
No documented exposure	1241 (28·0%)	239 (52·1%)

Data are median (IQR) or n (%). NA=not applicable. *Includes professions such as artisans, small business owners, civil servants, independent workers, construction workers, and fishers. †Types of exposure were not mutually exclusive. ‡Includes both "casual physical contact" and "sexual contact", and we could not differentiate between the two. §Defined as "contact with bodily secretions or excretions" during caregiving or health-care activities. ¶In endemic provinces, an additional category was included to capture "other human contact", such as interactions at school, market, or church.

Table 1: **Demographic and exposure characteristics of people with mpox in newly affected provinces and endemic provinces**

	Newly affected provinces (n=4436)	Endemic provinces (n=459)
Systemic symptoms		
Any systemic symptom	3828 (86·3%)	427 (93·0%)
Fever	3544 (79·9%)	403 (87·8%)
Adenopathy	1625 (36·6%)	206 (44·9%)
Headache	2067 (46·6%)	284 (61·9%)
Myalgia	1663 (37·5%)	220 (47·9%)
Nausea or vomiting	NR	85 (18·5%)
Conjunctivitis	460 (10·4%)	130 (28·3%)
Oral involvement	802 (18·1%)	161 (35·1%)
Respiratory symptoms		
Any respiratory symptom	2450 (55·2%)	219 (47·7%)
Cough	1991 (44·9%)	160 (34·9%)
Sore throat	1698 (38·3%)	103 (22·4%)
Rash severity		
Median lesion count	91 (37–200), n=701	163 (95–345), n=113
Mild (≤25 lesions)	131/701 (18·7%)	0/113
Moderate (26–100 lesions)	253/701 (36·1%)	32/113 (28·3%)
Severe (101–249 lesions)	212/701 (30·2%)	49/113 (43·4%)
Critical (≥250 lesions)	105/701 (15·0%)	32/113 (28·3%)
Rash location		
Face	559/701 (79·7%)	113/113 (100·0%)
Thorax	571/701 (81·5%)	113/113 (100·0%)
Arms	560/701 (79·9%)	94/113 (83·2%)
Hand palms	414/701 (59·1%)	90/113 (79·6%)
Foot soles	332/701 (47·4%)	89/113 (78·8%)
Genitals	536/701 (76·5%)	32/113 (28·3%)
Complications		
Any complication	2202 (49·6%)	210 (45·8%)
Skin infection	2041 (46·0%)	201 (43·8%)
Respiratory distress	82 (1·8%)	29 (6·3%)
Sepsis	82 (1·8%)	4 (0·9%)
Impaired vision	7 (0·2%)	28 (6·1%)
Prostration	695 (15·7%)	51 (11·1%)
Pregnancy loss	2 (<0·1%)	0
Treatment		
Paracetamol or ibuprofen	1981 (44·7%)	NR
Ceftriaxone (intravenous or intramuscular)	1796 (40·5%)	NR
Cloxacillin (intravenous)	412 (9·3%)	NR
Amoxicillin (oral)	523 (11·8%)	NR
Topical treatments*	1099 (24·8%)	NR
Antihistamine	483 (10·9%)	NR
Debridement	10 (0·2%)	NR
Dexamethasone	40 (0·9%)	NR
Outcomes		
Hospitalisation	2387 (53·8%)	233 (50·8%)
Death	28 (0·6%)	20 (4·4%)
Monkeypox virus PCR positivity by type of sample		
Vesicles or crust	4415/4416 (100·0%)	370/371 (99·7%)
Blood	61/68 (89·7%)	130/139 (93·5%)
Oropharyngeal	80/94 (85·1%)	1/1 (100·0%)

Data are median (IQR), n (%), or n/N (%). Treatment data were unavailable for endemic provinces. NR=not reported. *Topical treatment included baths (soap or potassium permanganate) or bandages (povidone, chlorhexidine, zinc oxide, or silver sulfadiazine).

Table 2: **Clinical and laboratory characteristics of mpox cases**

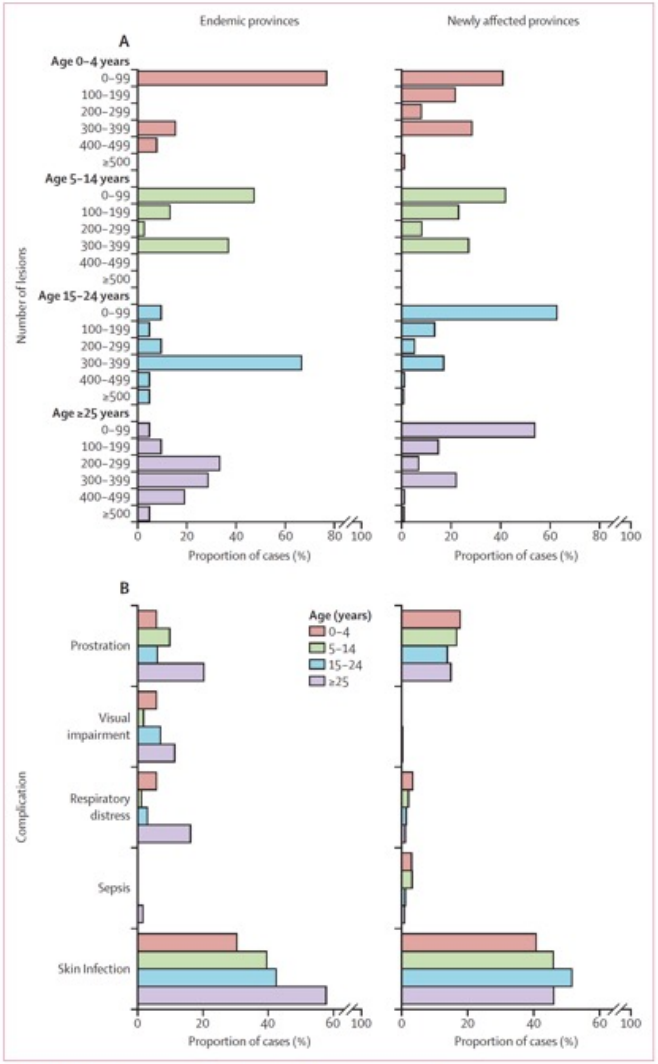

Figure 2: **Number of lesions and complications stratified by age and region**
(A) Distribution of lesion counts by age group in endemic and newly affected provinces. (B) Frequency of complications by age group in endemic and newly affected provinces.

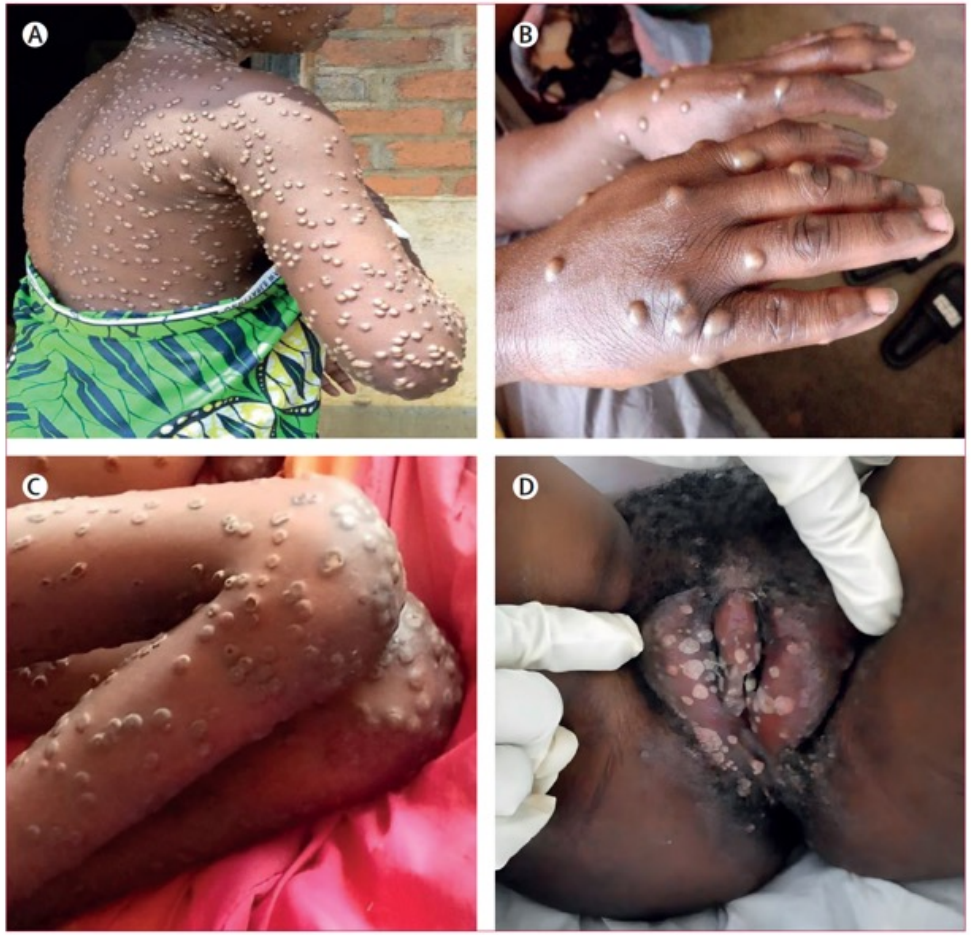

Figure 3: **Distinct dermatological lesions of mpox in DR Congo across multiple anatomical sites**
(A) Vesicles distributed densely across the face, neck, upper extremities, and trunk; central umbilication is noticeable in many (South-Kivu). (B) Dorsum of the hand with multiple non-follicular vesicles (Équateur). (C) Legs with centrifugally distributed vesicles showing umbilication (Équateur). (D) Perineum, inner labia majora, labia minora, and clitoral area exhibit circular ulcerations of varying diameters, covered with white fibrin, with surrounding erythema and oedema (South-Kivu).

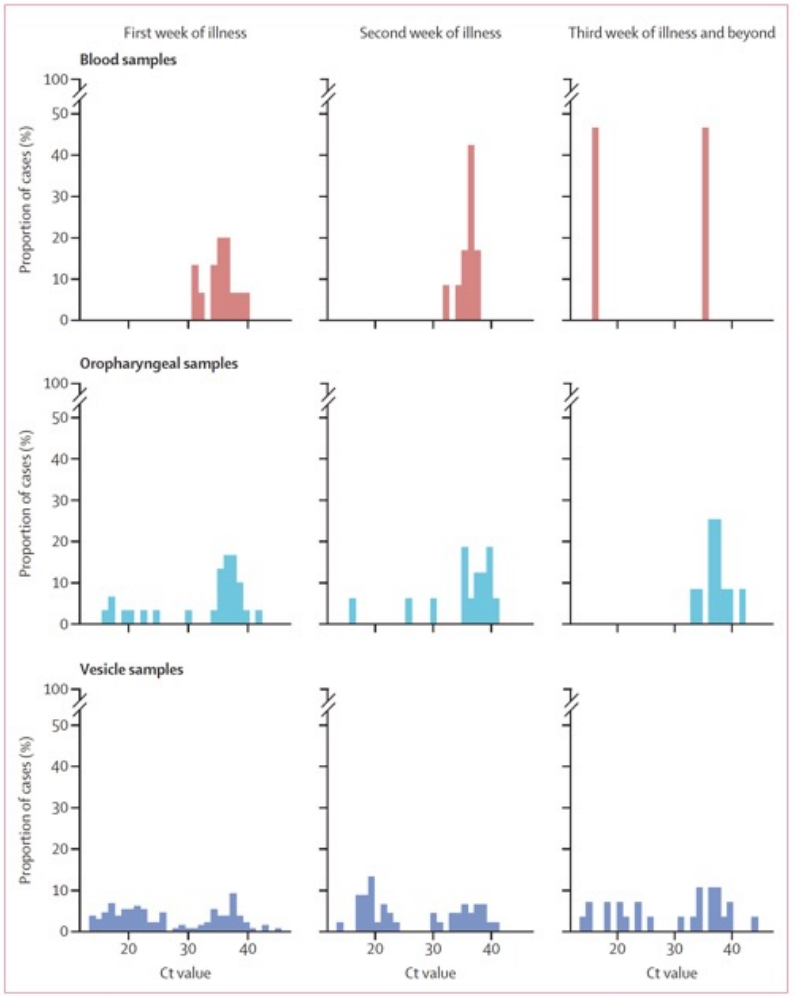

Figure 4: **Ct values of monkeypox virus PCR stratified by sample type and week of illness**
Data are derived from 271 individuals from South-Kivu for whom comprehensive data were available on the timing of sample collection, specimen type, and raw Ct value from the PCR run. Samples included 190 vesicle swabs, 54 oropharyngeal swabs, and 27 blood samples. Ct=cycle threshold.

Research in context

Evidence before this study

We searched PubMed and Google Scholar from database inception to Oct 29, 2024, to identify studies on the clinical presentation of mpox in DR Congo, including the newly identified clade 1b variant in South-Kivu and Kinshasa provinces, which were previously non-endemic for mpox. The search terms used were "clinical" AND ("Zaire" OR "Congo") AND ("monkeypox" OR "mpox" OR "MPXV"). The search retrieved 131 articles reporting clinical information on mpox. Of these, only three observational studies focused on clinical presentation. These studies highlighted generalised centrifugal rashes and systemic complications associated with the disease. However, each study had at least a major limitation: they were restricted to one province, had small sample sizes, or lacked PCR confirmation. Additionally, all reported cases occurred between 1981 and 2015 and lacked information on the newly identified 2023 clade 1b variant circulating in South-Kivu and Kinshasa.

Added value of this study

This study is the first to comprehensively describe the clinical presentation of individuals from regions affected by the monkeypox virus clade 1b outbreak. It provides a large-scale, multiprovince, detailed clinical characterisation of PCR-confirmed mpox cases in DR Congo, including 4436 cases from provinces affected by clade 1b and 459 cases from provinces where clade 1a is endemic. All cases were confirmed by PCR testing, ensuring diagnostic accuracy. By using standardised case investigation forms, the study maintains a sufficient level of consistency of data across diverse settings. Photographs were collected to ascertain dermatological features and illustrate various dermatological lesions. The inclusion of multiple provinces enhances the generalisability of the findings and allows for regional comparison of cases occurring in the same period. Importantly, the study reports a high number of patients with critical disease and deaths and investigates their causes, offering insights into disease severity and outcomes.

Implications of all the available evidence

The clinical presentation of mpox in the current DR Congo outbreak is notably severe, with higher case-fatality rates than the 2022 clade 2b lineage B.1 multicountry outbreak. Both newly affected (clade 1b) and endemic (clade 1a) regions in DR Congo reported elevated complication rates and extensive viraemia, confirmed by PCR positivity in blood tests; however, case-fatality rates were higher in endemic provinces. This suggests that factors such as differences in monkeypox virus strains, case ascertainment, or access to supportive care might differentially influence outcomes in these regions. Transmission varies regionally, with intimate human-to-human contact as the primary route in South-Kivu and Kinshasa, while endemic regions see more animal exposure. The types and frequency of complications observed should inform updates to clinical guidelines, particularly regarding early antibiotic intervention to mitigate bacterial infection risks. Regional case-fatality rates (higher in endemic regions) should guide targeted vaccination, while specific transmission patterns should inform containment strategies. Finally, our findings emphasise the importance of global pandemic preparedness, given the risk of monkeypox virus clade 1 spreading further.

Handdermatitis, auch Handekzem genannt, ist eine nicht ansteckende, entzündliche Hauterkrankung, die an den Händen auftritt. Sie kann in verschiedenen Formen auftreten, von mild bis schwerwiegend. Zu den häufigsten Symptomen gehören Rötungen, Juckreiz, Trockenheit, Bläschenbildung und Schuppenbildung.

Ursachen:

Handdermatitis kann durch verschiedene Faktoren ausgelöst werden, darunter:

•**Allergische Reaktionen:**

•Kontakt mit bestimmten Stoffen wie Seifen, Reinigungsmitteln, Kosmetika oder Metalle können allergische Reaktionen auslösen.

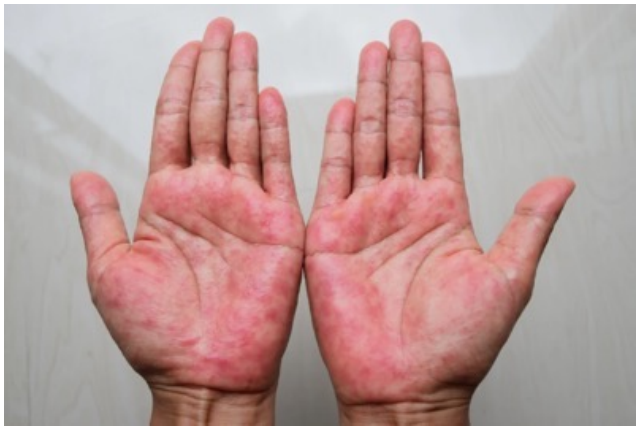

Irritative Reaktionen:

Häufiges Händewaschen mit warmem Wasser, Kontakt mit Chemikalien oder bestimmte Produkte können die Haut reizen.

Atopische Dermatitis (Neurodermitis):

Eine genetisch bedingte Erkrankung, die die Hautbarriere schwächt und sie anfälliger für Entzündungen macht.

Delgocitinib

Delgocitinib ist ein Pan-Januskinase-(JAK)-Inhibitor, der durch Hemmung des JAK-STAT-Signalwegs die Signalgebung proinflammatorischer Zytokine blockiert. Es wird zur topischen Behandlung von mittelschwerem bis schwerem chronischem Handekzem bei Erwachsenen eingesetzt, bei denen Glukokortikoide nicht ausreichen oder ungeeignet sind.

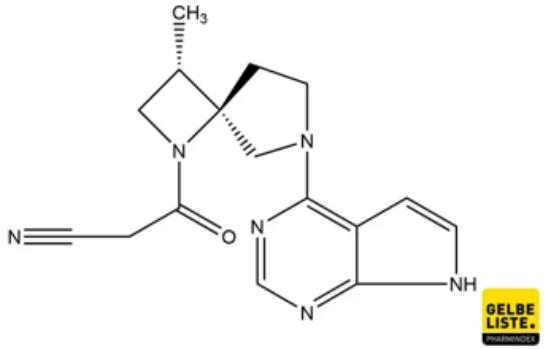

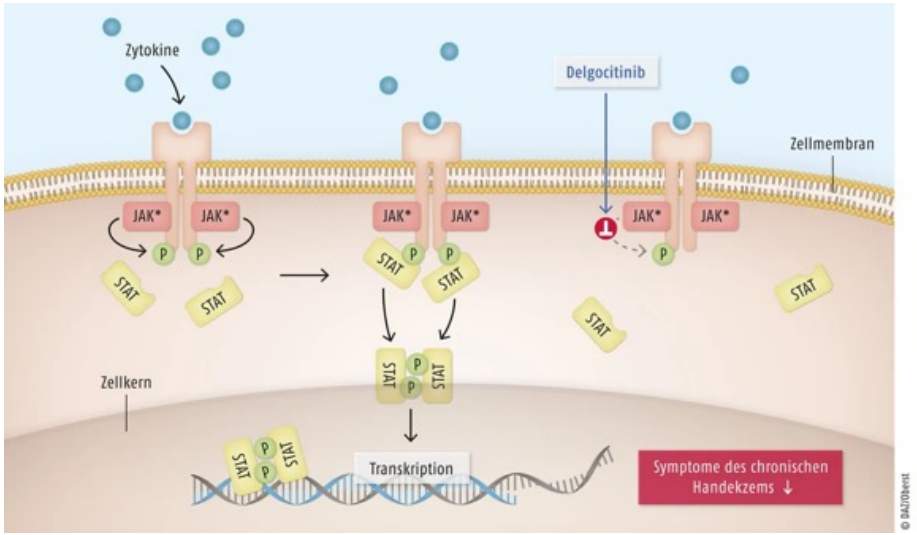

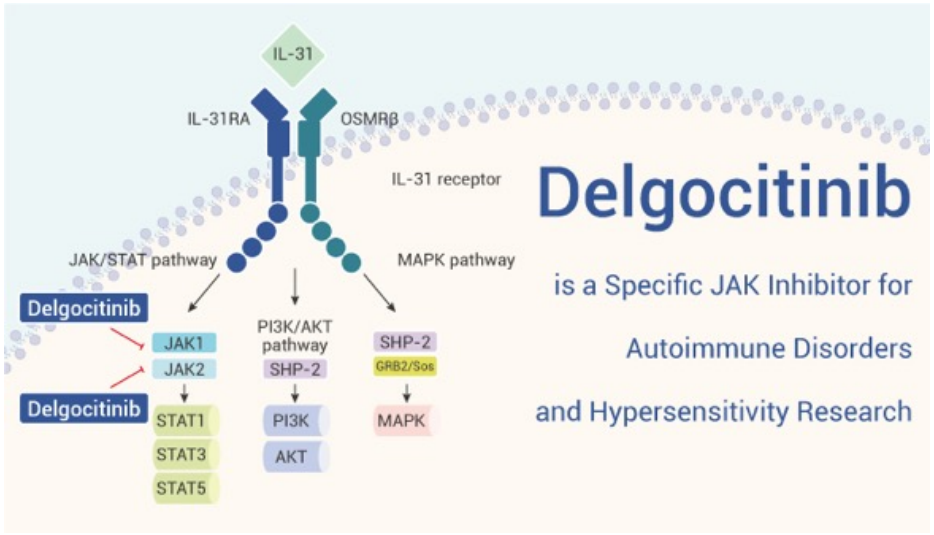

Efficacy and safety of topical delgocitinib cream versus oral alitretinoin capsules in adults with severe chronic hand eczema (DELTA FORCE): a 24-week, randomised, head-to-head, phase 3 trial

Summary

Background Chronic hand eczema is a heterogeneous, fluctuating, and long-lasting disease affecting the hands and wrists that substantially affects quality of life. For severe chronic hand eczema, topical corticosteroids are often unsatisfactory and systemic treatment can be required. The aim of the head-to-head, phase 3 DELTA FORCE trial was to evaluate the efficacy and safety of topical delgocitinib cream versus oral alitretinoin, the only currently approved systemic drug for severe chronic hand eczema.

Methods This randomised, assessor-masked, trial was conducted at 102 trial centres in Austria, Canada, France, Germany, Italy, Norway, Poland, Slovakia, Spain, and the UK. Adults (aged ≥18 years) with severe chronic hand eczema were randomly assigned (1:1) via an interactive response technology system to delgocitinib cream 20 mg/g (twice daily) or alitretinoin 30 mg (once daily) for up to 24 weeks. The primary endpoint was change in Hand Eczema Severity Index (HECSI) score from baseline to week 12. Efficacy of delgocitinib cream versus alitretinoin was assessed in all eligible randomly assigned patients who had available data at baseline, and safety was assessed in all patients exposed to trial treatment. The trial is registered with ClinicalTrials.gov (NCT05259722) and is complete.

Findings Between June 15, 2022, and Dec 5, 2023, 513 (334 [65%] female and 179 [35%] male) patients were randomly assigned to receive delgocitinib cream (n=254) or alitretinoin (n=259). Ten patients were excluded after randomisation due to not meeting eligibility criteria, so the full analysis set consisted of 250 patients in the delgocitinib group and 253 in the alitretinoin group. One patient in the delgocitinib group and three in the alitretinoin group were excluded from the primary analysis as they had missing HECSI data at baseline. A significantly greater least squares mean change in HECSI score from baseline to week 12 was observed with delgocitinib cream (–67·6 [SE 3·4]; n=249) versus alitretinoin (–51·5 [3·4]; n=250; difference –16·1 [95% CI –23·3 to –8·9], p<0·0001). Fewer patients reported adverse events in the delgocitinib group (125 [49%] of 253 patients) than in the alitretinoin group (188 [76%] of 247). The most frequent adverse events were headache (ten [4%] in the delgocitinib group *vs* 80 [32%] in the alitretinoin group), nasopharyngitis (30 [12%] *vs* 34 [14%]), and nausea (one [<1%] *vs* 14 [6%]).

Interpretation Delgocitinib cream showed superior efficacy and a more favourable safety profile versus oral alitretinoin over 24 weeks. These results support the benefit of delgocitinib cream in patients with severe chronic hand eczema.

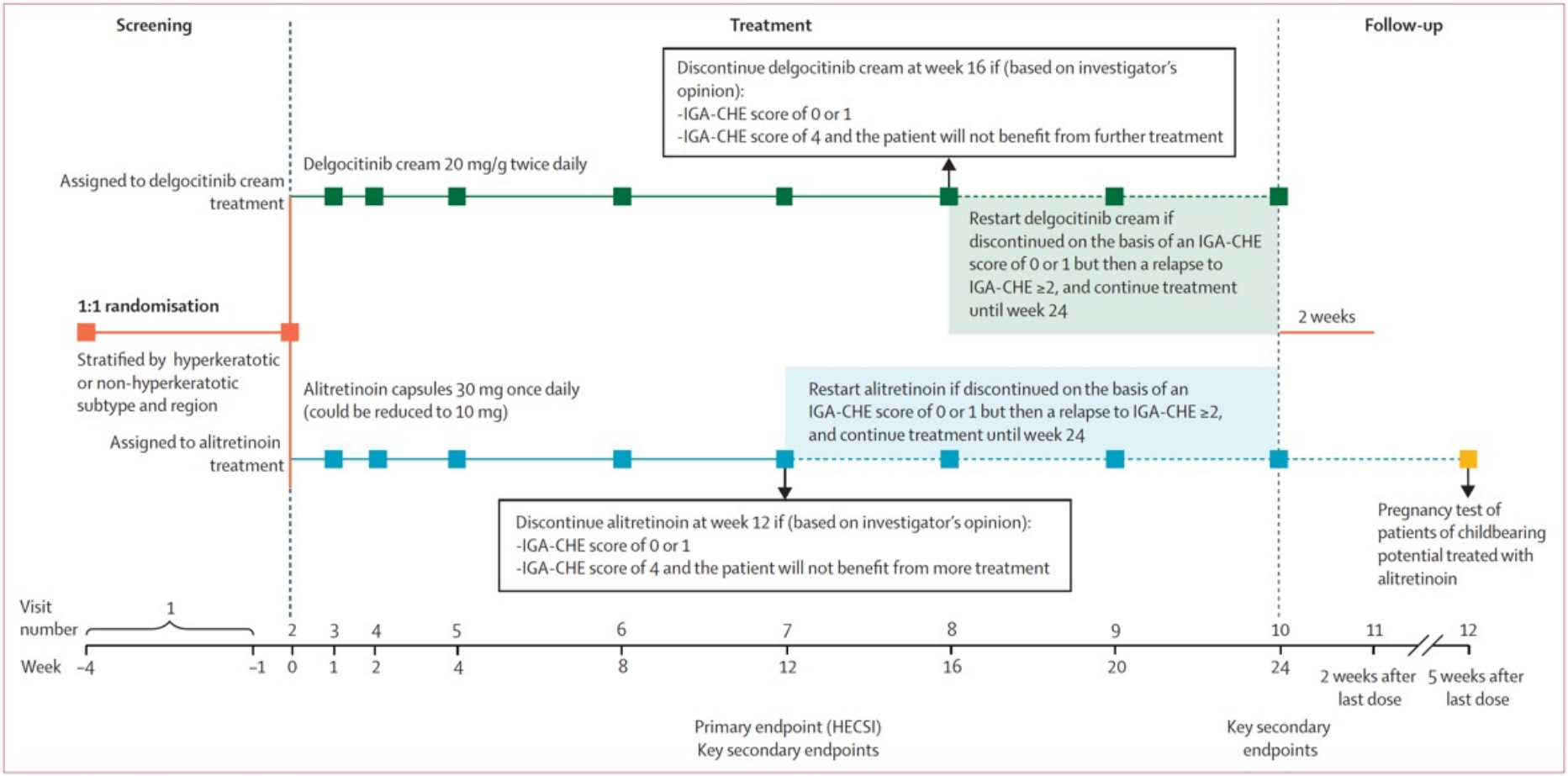

Figure 1: **Trial design for DELTA FORCE**

For patients treated with medications requiring a 28-day washout period before baseline, the duration of the screening period was extended to up to 31 days to ensure appropriate washout. For patients of childbearing potential, the duration of the screening period was extended to up to 42 days to ensure compliance with contraceptive and pregnancy prevention programme requirements. IGA-CHE scores relate to severity, with a score of 0 indicating clear, 1 indicating almost clear, 2 indicating mild, 3 indicating moderate, and 4 indicating severe. HECSI=Hand Eczema Severity Index. IGA-CHE=Investigator's Global Assessment for Chronic Hand Eczema.

	Total (n=513)	Delgocitinib cream (n=254)	Alitretinoin (n=259)
Age, years	45·0 (33·0–56·0)	46·0 (34·0–56·0)	44·0 (31·0–56·0)
Sex*			
Male	179 (35%)	87 (34%)	92 (36%)
Female	334 (65%)	167 (66%)	167 (64%)
Race			
White	477 (93%)	237 (93%)	240 (93%)
Asian	14 (3%)	9 (4%)	5 (2%)
Black or African American	4 (1%)	1 (<1%)	3 (1%)
Multiple	2 (<1%)	2 (1%)	0
Other or not reported	16 (3%)	5 (2%)	11 (4%)
Region†			
Europe	459 (89%)	229 (90%)	230 (89%)
North America	54 (11%)	25 (10%)	29 (11%)
Country†			
Austria	5 (1%)	2 (1%)	3 (1%)
Canada	54 (11%)	25 (10%)	29 (11%)
France	30 (6%)	14 (6%)	16 (6%)
Germany	136 (27%)	63 (25%)	73 (28%)
Italy	22 (4%)	13 (5%)	9 (3%)
Norway	2 (<1%)	1 (<1%)	1 (<1%)
Poland	180 (35%)	89 (35%)	91 (35%)
Slovakia	14 (3%)	9 (4%)	5 (2%)
Spain	64 (12%)	36 (14%)	28 (11%)
UK	6 (1%)	2 (1%)	4 (2%)
Age at onset of chronic hand eczema, years	37·0 (22·0–50·0)	37·5 (22·0–51·0)	36·0 (22·0–49·0)
Duration of chronic hand eczema, years	4·0 (2·0–10·0)	4·0 (2·0–13·0)	4·0 (2·0–10·0)
Chronic hand eczema subtype‡			
Irritant contact dermatitis	151 (29%)	75 (30%)	76 (29%)
Atopic hand eczema	123 (24%)	66 (26%)	57 (22%)
Allergic contact dermatitis	112 (22%)	58 (23%)	54 (21%)
Hyperkeratotic eczema	63 (12%)	31 (12%)	32 (12%)
Vesicular hand eczema (pompholyx)	58 (11%)	22 (9%)	36 (14%)
Not reported	6 (1%)	2 (1%)	4 (2%)
IGA-CHE			
Severe	512 (100%)	254 (100%)	258 (>99%)
Mild	1 (<1%)§	0	1 (<1%)§
HECSI			
n	508	252	256
Mean (SD)	91·8 (54·7)	90·9 (54·7)	92·7 (54·9)
Median (IQR)	80·0 (52·0–117·0)	79·5 (52·5–114·5)	80·0 (52·0–119·0)
DLQI			
n	475	233	242
Mean (SD)	12·8 (6·2)	12·7 (6·3)	13·0 (6·1)
Median (IQR)	12·0 (8·0–17·0)	12·0 (8·0–17·0)	12·0 (8·0–17·0)
≥4	457/475 (96%)	222/233 (95%)	235/242 (97%)
HESD itch (weekly average)¶			
n	484	240	244
Mean (SD)	5·9 (2·7)	5·8 (2·8)	6·0 (2·7)
Median (IQR)	6·2 (3·9–8·0)	6·1 (3·8–8·0)	6·4 (4·1–8·0)
≥4	362/484 (75%)	177/240 (74%)	185/244 (76%)

(Table 1 continues on next page)

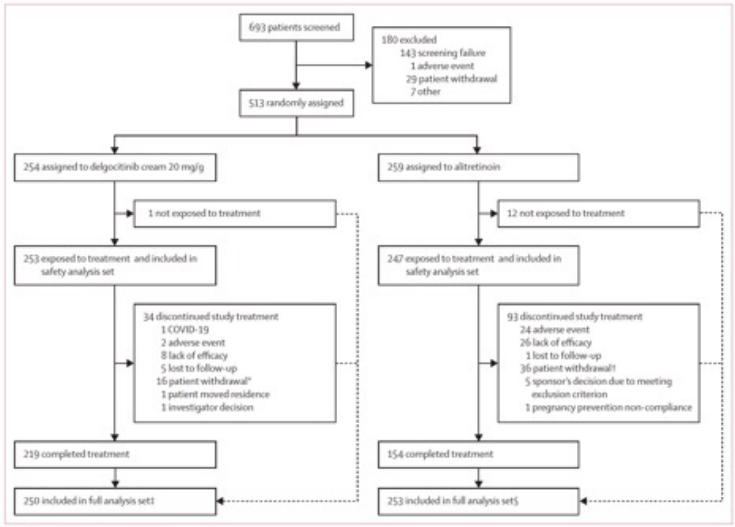

Figure 2: **DELTA FORCE trial profile**
*Including 1 patient whose primary reason was recorded as Other: patient decision. †Including 2 patients whose primary reasons were recorded as Other: patient decision, and 1 patient whose primary reason was recorded as Other: personal issues. ‡Four patients were excluded from the full analysis set due to inclusion criteria not being met (n=1) or exclusion criteria being met (n=3). §Six patients were excluded from the full analysis set due to inclusion criteria not being met (n=1) or exclusion criteria being met (n=5).

	Total (n=513)	Delgocitinib cream (n=254)	Alitretinoin (n=259)
(Continued from previous page)			
HESD pain (weekly average)¶			
n	484	240	244
Mean (SD)	5·5 (2·9)	5·2 (2·9)	5·8 (2·8)
Median (IQR)	6·0 (3·3–7·9)	5·6 (3·1–7·6)	6·1 (3·6–8·0)
≥4	339/484 (70%)	163/240 (68%)	176/244 (72%)

Data are n, n (%), median (IQR), or mean (SD). IGA-CHE scores range from 0, meaning clear, to 4, meaning severe. HECSI scores range from 0–360. DLQI scores range from 0–30. HESD itch and HESD pain scores range from 0–10. DLQI=Dermatological Life Quality Index. HECSI=Hand Eczema Severity Index. HESD=Hand Eczema Symptom Diary. IGA-CHE=Investigator's Global Assessment for Chronic Hand Eczema. *As determined by the unmasked investigator. †Trial centres are listed in the appendix (pp 2–6). ‡Chronic hand eczema subtypes were assessed by the investigator on the basis of medical history, morphology of the present lesions at baseline, and a mandatory diagnostic patch test completed so results were available before baseline assessments on day 1. For patients who had a diagnostic patch test performed within 3 years before screening, the results from the most recent patch test were used for the chronic hand eczema subtype classification. §One patient with a baseline IGA-CHE score of 2 was excluded from the full analysis set due to inclusion criteria not being met. ¶Baseline weekly average was defined as the average of the daily observations during the 7 days preceding the randomisation date.

Table 1: **Patient demographics and baseline characteristics in DELTA FORCE (randomised population)**

	Delgocitinib cream (n=250)	Alitretinoin (n=253)	Difference (95% CI)	p value
Primary endpoint				
Change in HECSI score*, week 12	−67·6 (3·4; n=249)	−51·5 (3·4; n=250)	−16·1 (−23·3 to −8·9)	<0·0001
Key secondary endpoints				
HECSI-90,† week 12	96/249 (39%)	65/250 (26%)	12·6% (4·3 to 20·8)	0·0027
IGA-CHE treatment success†, week 12	68/250 (27%)	42/253 (17%)	10·6% (3·3 to 17·9)	0·0041
Change in HESD itch*, week 12	−3·0 (0·2; n=238)	−2·4 (0·2; n=238)	−0·7 (−1·1 to −0·2)	0·0051
Change in HESD pain*, week 12	−2·9 (0·2; n=238)	−2·3 (0·2; n=238)	−0·6 (−1·1 to −0·1)	0·018
AUC of HECSI-90‡, week 24	49·2 (4·0; n=249)	34·9 (4·0; n=250)	14·3 (5·8 to 22·9)	0·0010
AUC of reduction in DLQI score‡§, week 24	1124·7 (61·4; n=230)	790·7 (62·7; n=236)	334·0 (195·7 to 472·3)	<0·0001
Change in HECSI score*, week 24	−69·6 (3·8; n=249)	−45·1 (3·8; n=250)	−24·5 (−32·6 to −16·4)	<0·0001

Data are n (%) or least squares mean (SE) unless otherwise specified. Missing data were imputed with worst observation carried forward (WOCF; continuous endpoints) or non-response (binary endpoints). Data after initiation of rescue treatments or permanent discontinuation of trial drug were treated as missing. The numbers of missing values imputed with WOCF or non-response for each outcome and treatment group are shown in the appendix (pp 22–23). Two-sided p values are reported. The order of endpoints in this table reflects the order of the testing hierarchy. IGA-CHE treatment success was defined as an IGA-CHE score of 0 or 1 with at least a two-step improvement from baseline. AUC=area under the curve. DLQI=Dermatology Life Quality Index. HECSI=Hand Eczema Severity Index. HECSI-90=at least 90% improvement in HECSI score from baseline. HESD=Hand Eczema Symptom Diary. IGA-CHE=Investigator's Global Assessment for Chronic Hand Eczema. *ANCOVA, adjusted for hyperkeratotic or non-hyperkeratotic subtype and baseline value of the score. †Cochran–Mantel–Haenszel test stratified for hyperkeratotic or non-hyperkeratotic subtype. ‡Robust ANCOVA, adjusted for hyperkeratotic or non-hyperkeratotic subtype, and baseline value of the score. §The AUC of reduction from baseline in DLQI score up to week 24 was based on all changes of DLQI score values until week 24.

Table 2: **Summary of efficacy results for the primary and all key secondary endpoints in DELTA FORCE (full analysis set)**

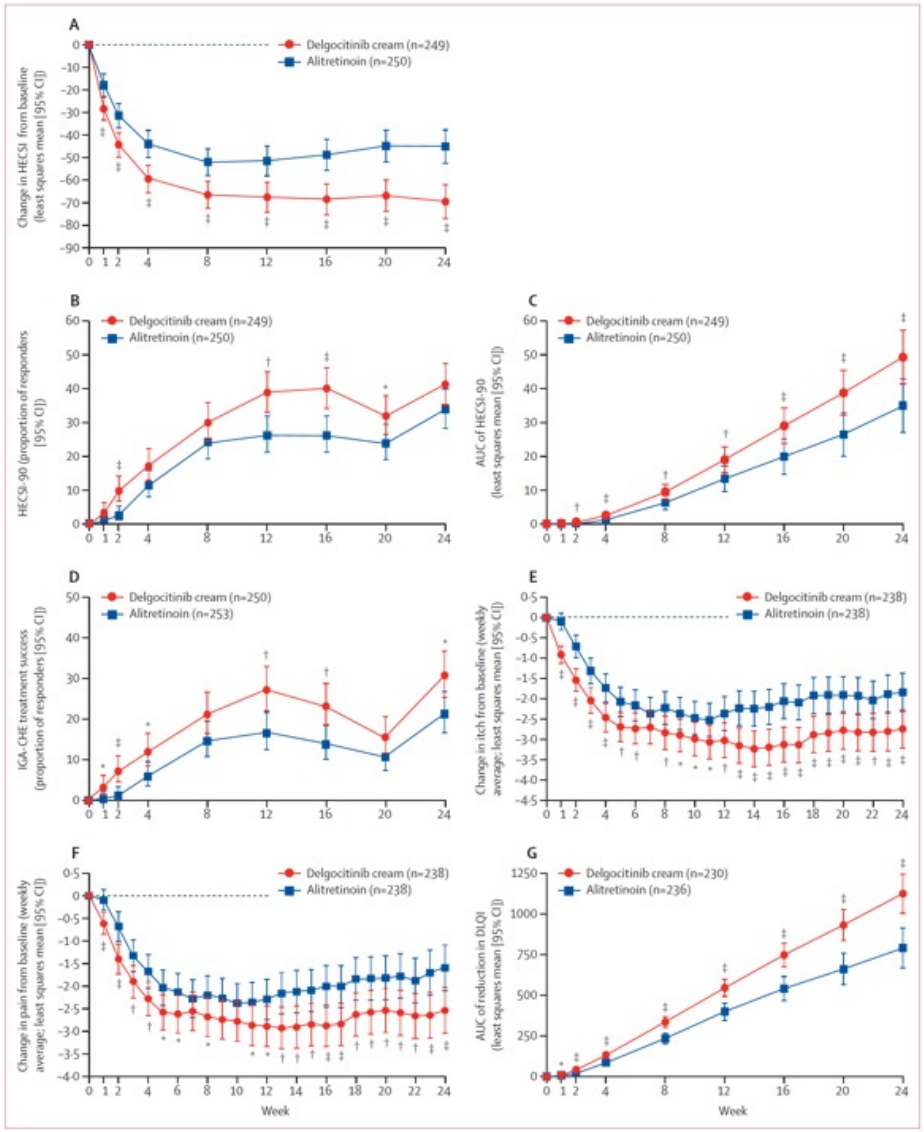

***Figure 3*: Key efficacy results of the DELTA FORCE trial**
(A) Change in HECSI score. (B) Proportion of patients who reached HECSI-90. (C) AUC of HECSI-90. (D) Proportion of patients who reached IGA-CHE treatment success (defined as an IGA-CHE score of 0 or 1 with at least a two-step improvement from baseline). (E) Change in HESD itch score. (F) Change in HESD pain score. (G) AUC of reduction from baseline in DLQI score. Data collected after initiation of rescue treatments or permanent discontinuation of trial drug were treated as missing. The ANCOVA model in graphs A, E, and F was change in score from baseline=treatment + hyperkeratotic or non-hyperkeratotic subtype + baseline score; missing data were imputed with WOCF. For graphs B and D, missing data were imputed with non-response. The ANCOVA model in graph C is AUC of HECSI-90=treatment + hyperkeratotic or non-hyperkeratotic + baseline HECSI score; missing data were imputed with non-response. The ANCOVA model in graph G is AUC of reduction from baseline in DLQI score=treatment + hyperkeratotic or non-hyperkeratotic + baseline DLQI score; missing data were imputed with WOCF. The numbers of missing values imputed with worst observation carried forward (WOCF) or non-response for each outcome and treatment group are shown in the appendix (p 22). AUC=area under the curve. DLQI=Dermatology Life Quality Index. HECSI=Hand Eczema Severity Index. HECSI-90=at least 90% improvement in HECSI score from baseline. HESD=Hand Eczema Symptom Diary. IGA-CHE=Investigator's Global Assessment for Chronic Hand Eczema. *p<0·05. †p<0·01. ‡ps0·001. Exact p values can be found in the appendix (pp 20–21).

	Delgocitinib cream (n=253, PYO 120·9)			Alitretinoin (n=247, PYO 104·0)			Rate ratio (95% CI)	Risk difference (95% CI)
	N	Event	Rate*	N	Event	Rate*		
All adverse events	125 (49%)	280	231·5	188 (76%)	620	596·1	0·39 (0·34 to 0·45)	−26·7% (−34·5 to −18·3)
Serious adverse events	5 (2%)	5	4·1	12 (5%)	12	11·5	0·36 (0·13 to 1·02)	−2·9% (−6·5 to 0·4)
Deaths	0	0	0	0	0	0	NA	0·0% (−1·5 to 1·5)
Severity								
Mild	92 (36%)	168	138·9	151 (61%)	397	381·7	0·36 (0·30 to 0·44)	−24·8% (−32·9 to −16·1)
Moderate	68 (27%)	108	89·3	104 (42%)	198	190·4	0·47 (0·37 to 0·59)	−15·2% (−23·3 to −6·9)
Severe	4 (2%)	4	3·3	14 (6%)	25	24·0	0·14 (0·05 to 0·40)	−4·1% (−7·8 to −0·8)
Probably or possibly related to trial drug	24 (9%)	30	24·8	134 (54%)	311	299·0	0·08 (0·06 to 0·12)	−44·8% (−51·6 to −37·2)
Adverse events leading to permanent discontinuation of trial drug	3 (1%)	4	3·3	25 (10%)	44	42·3	0·08 (0·03 to 0·22)	−8·9% (−13·4 to −5·1)
Outcome								
Fatal	0	0	0	0	0	0	NA	0·0% (−1·5 to 1·5)
Not recovered or not resolved	26 (10%)	35	28·9	39 (16%)	66	63·5	0·46 (0·30 to 0·69)	−5·5% (−11·5 to 0·4)
Recovering or resolving	11 (4%)	13	10·7	29 (12%)	38	36·5	0·29 (0·16 to 0·55)	−7·4% (−12·4 to −2·6)
Recovered or resolved	111 (44%)	227	187·7	172 (70%)	513	493·2	0·38 (0·33 to 0·44)	−25·8% (−33·8 to −17·2)
Recovered or resolved with sequelae	0	0	0	1 (<1%)	1	1·0	NA	−0·4% (−2·3 to 1·1)
Unknown	2 (1%)	5	4·1	1 (<1%)	2	1·9	2·15 (0·42 to 11·1)	0·4% (−1·6 to 2·5)
Action taken with trial drug								
Dose not changed	110 (43%)	239	197·6	156 (63%)	466	448·1	0·44 (0·38 to 0·52)	−19·7% (−28·0 to −11·0)
Dose reduced	0	0	0	42 (17%)	67	64·4	NA	−17·0% (−22·2 to −12·6)
Drug withdrawn	3 (1%)	4	3·3	25 (10%)	44	42·3	0·08 (0·03 to 0·22)	−8·9% (−13·4 to −5·1)
Not applicable	28 (11%)	37	30·6	35 (14%)	43	41·3	0·74 (0·48 to 1·15)	−3·1% (−9·0 to 2·8)
Unknown	0	0	0	0	0	0	NA	0·0% (−1·5 to 1·5)
Adverse events of special interest								
Eczema herpeticum	0	0	0	0	0	0	NA	0·0% (−1·5 to 1·5)
Deep vein thrombosis	0	0	0	1 (<1%)	1	1·0	NA	−0·4% (−2·3 to 1·1)
Pulmonary embolism	0	0	0	0	0	0	NA	0·0% (−1·5 to 1·5)

(Table 3 continues on next page)

(Continued from previous page)

	Delgocitinib cream (n=253, PYO 120·9)			Alitretinoin (n=247, PYO 104·0)			Rate ratio (95% CI)	Risk difference (95% CI)
	N	Event	Rate*	N	Event	Rate*		
Frequent adverse events (≥2% in any treatment group) by preferred term								
Infections and infestations								
Nasopharyngitis	30 (12%)	38	31·4	34 (14%)	46	44·2	0·71 (0·46 to 1·09)	−1·9% (−7·8 to 4·0)
Upper respiratory tract infection	6 (2%)	8	6·6	8 (3%)	8	7·7	0·86 (0·32 to 2·29)	−0·9% (−4·1 to 2·3)
COVID-19	5 (2%)	5	4·1	9 (4%)	9	8·7	0·48 (0·16 to 1·43)	−1·7% (−5·0 to 1·4)
Urinary tract infection	1 (<1%)	1	0·8	10 (4%)	11	10·6	0·08 (0·01 to 0·61)	−3·7% (−6·9 to −1·1)
Skin and subcutaneous tissue disorders								
Dry skin	3 (1%)	3	2·5	9 (4%)	9	8·7	0·29 (0·08 to 1·06)	−2·5% (−5·7 to 0·4)
Eczema	2 (1%)	2	1·7	5 (2%)	6	5·8	0·29 (0·06 to 1·42)	−1·2% (−3·9 to 1·1)
Hand dermatitis	2 (1%)	3	2·5	5 (2%)	5	4·8	0·52 (0·12 to 2·16)	−1·2% (−3·9 to 1·1)
Atopic dermatitis	1 (<1%)	1	0·8	5 (2%)	5	4·8	0·17 (0·02 to 1·47)	−1·6% (−4·3 to 0·5)
Erythema	1 (<1%)	1	0·8	9 (4%)	10	9·6	0·09 (0·01 to 0·67)	−3·2% (−6·4 to −0·8)
Musculoskeletal and connective tissue disorders								
Back pain	2 (1%)	2	1·7	6 (2%)	6	5·8	0·29 (0·06 to 1·42)	−1·6% (−4·5 to 0·8)
Investigations								
Blood triglycerides increased	2 (1%)	2	1·7	7 (3%)	8	7·7	0·22 (0·05 to 1·01)	−2·0% (−5·0 to 0·5)
Nervous system disorder								
Headache	10 (4%)	19	15·7	80 (32%)	114	109·6	0·14 (0·09 to 0·23)	−28·4% (−34·8 to −22·1)
Migraine	2 (1%)	2	1·7	6 (2%)	7	6·7	0·25 (0·05 to 1·18)	−1·6% (−4·5 to 0·8)
Dizziness	1 (<1%)	1	0·8	6 (2%)	6	5·8	0·14 (0·02 to 1·19)	−2·0% (−4·8 to 0·2)
Gastrointestinal disorders								
Nausea	1 (<1%)	1	0·8	14 (6%)	15	14·4	0·06 (0·01 to 0·43)	−5·3% (−8·9 to −2·4)
Diarrhoea	0	0	0	5 (2%)	5	4·8	NA	−2·0% (−4·7 to −0·1)
Lip dry	0	0	0	8 (3%)	8	7·7	NA	−3·2% (−6·3 to −1·1)
Respiratory, thoracic and mediastinal disorders								
Epistaxis	1 (<1%)	1	0·8	5 (2%)	6	5·8	0·14 (0·02 to 1·19)	−1·6% (−4·3 to 0·5)
Metabolism and nutrition disorders								
Hypertriglyceridaemia	3 (1%)	3	2·5	6 (2%)	7	6·7	0·37 (0·10 to 1·43)	−1·2% (−4·1 to 1·4)
Hypercholesterolaemia	0	0	0	9 (4%)	10	9·6	NA	−3·6% (−6·8 to −1·4)
Vascular disorders								
Flushing	0	0	0	5 (2%)	6	5·8	NA	−2·0% (−4·7 to −0·1)
Eye disorders								
Dry eye	0	0	0	7 (3%)	7	6·7	NA	−2·8% (−5·7 to −0·7)

Adverse events that started or worsened in severity after first trial drug dose and were reported on or before week 26 are presented. Relation to trial drug was based on investigator's assessment. Adverse events were coded using the Medical Dictionary for Regulatory Activities version 24.0 dictionary. Rate ratios were estimated with CIs based on a Poisson regression model with treatment as fixed effect and natural logarithm of patient years of observation as offset. CIs for risk differences were Newcombe-Wilson CIs. NA=not applicable. PYO=patient years of observation. *Rate calculated as the number of events per PYO×100.

Table 3: **Summary of adverse events in the DELTA FORCE trial (safety analysis set)**

Research in context

Evidence before this study

A search of PubMed and ClinicalTrials.gov for comparative studies assessing the efficacy and safety of alitretinoin and other treatments in chronic hand eczema with the terms "chronic hand eczema" AND "alitretinoin" was done from database inception to July 17, 2024, with no language restrictions applied. The search identified one article of a discontinued randomised controlled trial of alitretinoin versus oral azathioprine as well as two articles of retrospective comparative studies and one terminated randomised controlled trial comparing alitretinoin versus oral ciclosporin. Alitretinoin is currently the only systemic drug specifically approved in a few countries worldwide for the treatment of severe chronic hand eczema. Delgocitinib cream is a topical pan-Janus kinase (JAK) inhibitor that affects the activation of multiple JAK-signal transducer and activator of transcription pathways involved in the skin barrier dysfunction and inflammation associated with chronic hand eczema pathogenesis. In patients with moderate to severe chronic hand eczema, delgocitinib cream showed significant improvement in all key efficacy endpoints and was well tolerated versus cream vehicle in the pivotal phase 3 DELTA 1 and DELTA 2 trials, as well as when used long-term as needed in the open-label DELTA 3 trial.

Added value of this study

To our knowledge, DELTA FORCE is the first clinical trial to assess, in a head-to-head comparison, the efficacy and safety of a topical treatment for chronic hand eczema against the only approved oral systemic therapy. The trial showed superior efficacy and a more favourable safety profile of topical delgocitinib cream compared with oral alitretinoin in patients with severe chronic hand eczema.

Implications of all the available evidence

The data from the DELTA FORCE trial support the benefits of delgocitinib cream as an efficacious and well tolerated topical treatment for this patient population with a high disease burden and unmet treatment needs. Delgocitinib cream has the potential to provide a non-steroidal topical treatment option that combines effective disease control without the safety concerns associated with long-term use of topical corticosteroids and systemic therapies.

Negative pressure wound therapy (NPWT), also known as vacuum-assisted closure (VAC), is a medical device that uses suction to promote healing in wounds. It works by applying negative pressure to a wound, which helps remove excess fluid, reduce inflammation, and stimulate the growth of new tissue. This process can accelerate healing and improve outcomes for various types of wounds, including chronic ulcers, surgical incisions, and skin grafts.

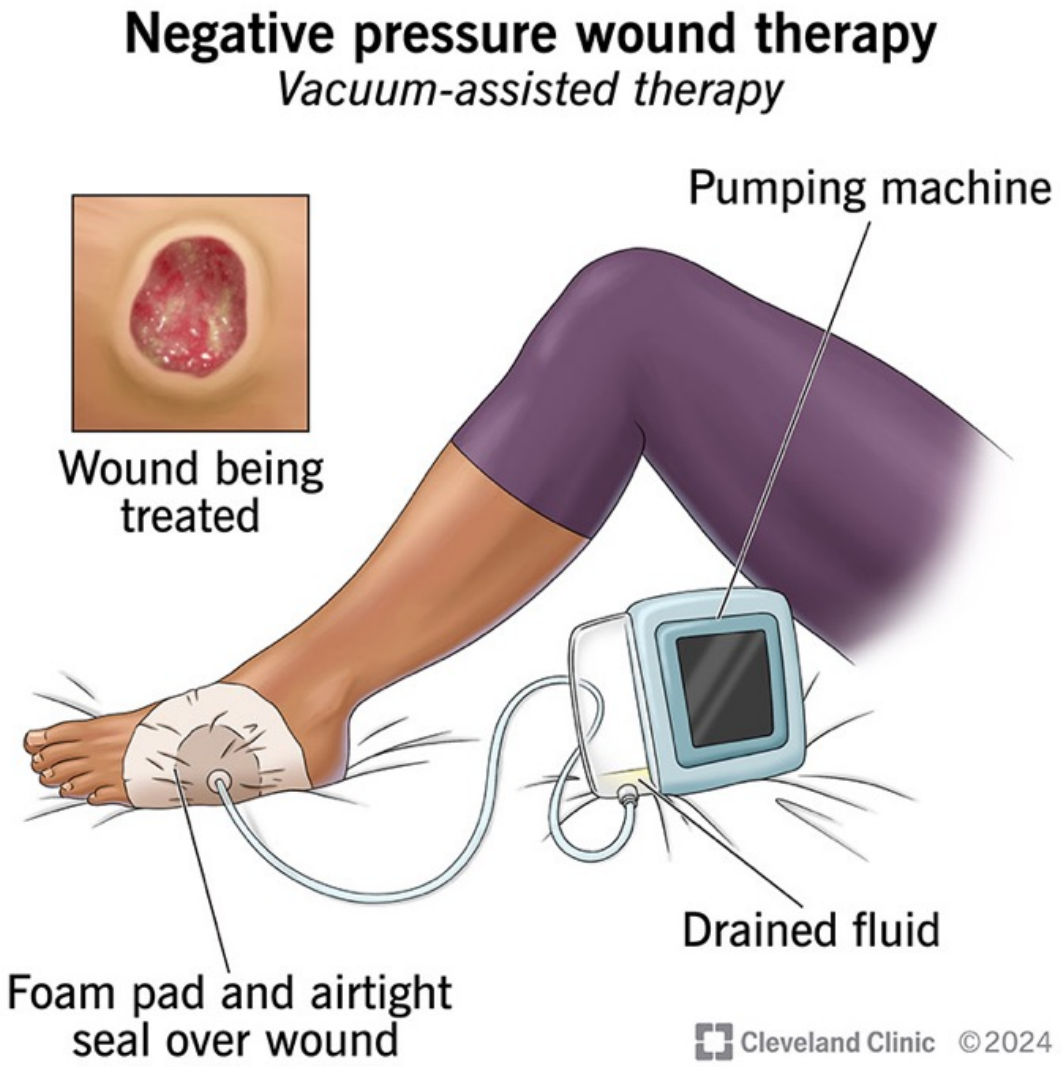

Negative pressure wound therapy versus usual care in patients with surgical wound healing by secondary intention in the UK (SWHSI-2): an open-label, multicentre, parallel-group, randomised controlled trial

Summary

Background Surgical wound healing by secondary intention (SWHSI) presents a substantial management and financial challenge. Negative pressure wound therapy (NPWT) has increasingly been used as a treatment despite an absence of comparative evidence of effectiveness. We evaluated the effectiveness of NPWT compared with usual care for improving time to wound healing in patients with an SWHSI.

Methods We did a pragmatic, open-label, multicentre, parallel-group, randomised controlled trial in 29 UK National Health Service Trusts. Participants aged 16 years or older with an SWHSI appropriate for both study treatments (NPWT or usual care) were randomly assigned (1:1) by a centralised web-based system. Randomisation was stratified by wound location, wound area, and study centre. Participants were followed up for 12 months. Participants and clinical and research teams could not be masked to treatment. Assessors masked to treatment reviewed wound photography to verify the outcome. The primary outcome was time to wound healing (days from randomisation to complete epithelial cover), analysed via intention to treat using Kaplan–Meier survival curves and a proportional hazards Cox regression model. The trial was registered with ISRCTN, ISRCTN26277546.

Findings Between May 15, 2019, and Jan 13, 2023, 686 participants with an SWHSI were randomly assigned to receive NPWT (n=349) or usual care (n=337). All participants were included in the primary analysis. Most participants were diabetic (n=549, 80·0%) and had a single SWHSI (n=622, 90·7%), located on the foot or leg (n=620, 90·4%), arising after vascular surgery (n=619, 90·2%). There was no clear evidence that NPWT reduced the time to wound healing compared with usual care (hazard ratio 1·08 [95% CI 0·88–1·32], p=0·47). There were 448 adverse events, of which 14 were serious (nine participants in the NPWT group and five participants in the usual care group); 124 were deemed potentially related to treatment. NPWT was found not to be cost-effective compared with usual care.

Interpretation In patients with a lower limb SWHSI, including those with complications of diabetes, there is no clear evidence that NPWT reduced the time to wound healing compared with standard dressings. These findings do not support the use of NPWT to augment SWHSI healing.

Funding National Institute for Health Research Health Technology Assessment Programme.

	NPWT (n=349)	Usual care (n=337)
Age, years	62·00 (54·00–71·0)	64·00 (55·0–72·0)
Gender		
Male	267 (76·5%)	246 (73·0%)
Female	79 (22·6%)	91 (27·0%)
Missing	3 (0·9%)	0
Ethnicity		
White	317 (90·8%)	313 (92·9%)
Asian or Asian British	14 (4·0%)	14 (4·2%)
Black or Black British	11 (3·2%)	9 (2·7%)
Other ethnicity	1 (0·3%)	0
Missing	6 (1·7%)	1 (0·3%)
Smoking status		
Never	121 (34·7%)	143 (42·4%)
Current	66 (18·9%)	53 (15·7%)
Previous	158 (45·3%)	140 (41·5%)
Missing	4 (1·1%)	1 (0·3%)
Routine alcohol consumption*		
Yes	125 (35·8%)	128 (38·0%)
No	219 (62·8%)	205 (60·8%)
Missing	6 (1·7%)	9 (2·7%)
Comorbidities		
Cardiovascular disease (hypertension, myocardial infarction, angina, or heart failure)		
Yes	218 (66·3%)	228 (71·9%)
No	111 (31·8%)	89 (26·4%)
Missing	20 (5·7%)	20 (5·9%)
Peripheral vascular disease		
Yes	181 (55·0%)	168 (53·0%)
No	148 (42·4%)	149 (44·2%)
Missing	21 (6·0%)	20 (5·9%)
Diabetes		
Yes	281 (85·4%)	268 (84·5%)
No	48 (13·8%)	49 (14·5%)
Missing	20 (5·7%)	20 (5·9%)
Surgery type		
Vascular	314 (90·0%)	305 (90·5%)
Colorectal	9 (2·6%)	14 (4·2%)
Plastics	2 (0·6%)	1 (0·3%)
Other	21 (6·0%)	17 (5·0%)
Missing	3 (0·9%)	0
Urgency of surgery		
Elective	141 (40·4%)	143 (42·4%)
Emergency	205 (58·7%)	194 (57·6%)
Missing	3 (0·9%)	0

(Table 1 continues on next page)

	NPWT (n=349)	Usual care (n=337)
(Continued from previous page)		
Contamination level of surgery		
Clean	94 (26·9%)	77 (22·8%)
Clean contaminated	36 (10·3%)	30 (8·9%)
Contaminated	26 (7·4%)	20 (5·9%)
Dirty	190 (54·4%)	210 (62·3%)
Missing	3 (0·9%)	0
Wound area, cm²	18·30 (8·10–35·00)	18·00 (7·26–33·75)
<28 cm²	243 (69·6%)	231 (68·5%)
≥28 cm²	106 (30·3%)	106 (31·5%)
Wound location		
Foot	279 (79·9%)	272 (80·7%)
Leg	40 (11·5%)	29 (8·6%)
Abdomen	11 (3·2%)	13 (3·9%)
Other	19 (5·4%)	23 (6·8%)
Number of SWHSIs		
1	318 (91·1%)	304 (90·2%)
2	21 (6·0%)	28 (8·3%)
≥3	7 (2·0%)	5 (1·5%)
Missing	3 (0·9%)	0
Previous history of SWHSI	57 (17·6%)	51 (16·0%)
SWHSI currently infected (based on clinical opinion)	54 (15·6%)	41 (12·2%)
WHQ score	7·77 (5·28)	8·08 (5·31)
Wound pain score	27·9 (29·8)	26·3 (28·9)

Data are n (%), mean (SD), or median (IQR). NPWT=negative pressure wound therapy. SWHSI=surgical wound healing by secondary intention. WHQ=Bluebelle Wound Healing Questionnaire. *Participants were asked if they consume alcohol (yes or no) and then subsequently asked their average number of units per week.

Table 1: **Baseline characteristics for the intention-to-treat population by treatment group**

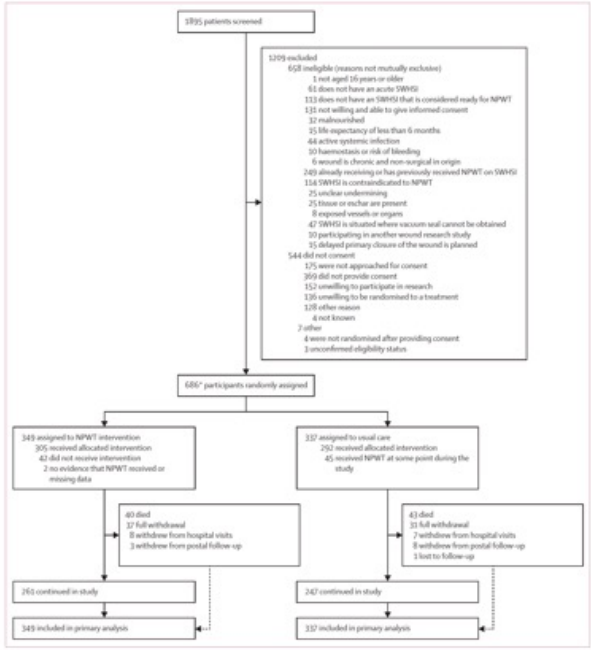

Figure 1: **Trial profile**
NPWT=negative pressure wound therapy. SWHSI=surgical wound healing by secondary intention. *There were six system randomisation errors where the same participant was randomised multiple times. These were removed from any analysis, leaving 686 participants.

	NPWT group	Usual care group	Treatment difference (95% CI)*	p value
Primary analysis population	n=349; median time to healing 187 days (95% CI 169 to 226)	n=337; median time to healing 195 days (95% CI 158 to 213)	HR 1·08 (0·88 to 1·32)	0·47
Time to healing as assessed by masked outcome assessment†	n=349; 157 days (95% CI 140 to 188)	n=337; 158 days (95% CI 134 to 203)	HR 1·13 (0·87 to 1·47)	0·36
Hospital admission‡	n=320; 63 (19·7%)	n=320; 58 (18·1%)	OR 1·13 (0·76 to 1·69)	0·54
Reoperation‡	n=320; 78 (24·4%)	n=320; 69 (21·6%)	OR 1·20 (0·82 to 1·74)	0·35
Amputation‡	n=320; 35 (10·9%)	n=320; 36 (11·2%)	OR 0·98 (0·60 to 1·62)	0·95
Wound infection‡	n=320; 102 (31·9%)	n=320; 100 (31·2%)	OR 1·05 (0·75 to 1·48)	0·77
Antibiotic use (for SWHSI)‡	n=320; 211 (65·9%)	n=320; 210 (65·6%)	OR 1·01 (0·70 to 1·45)	0·96
Death‡	n=349; 40 (11·5%)	n=337; 43 (12·8%)	OR 0·89 (0·56 to 1·41)	0·61
WHQ at 3 months§	n=195; mean 7·01 (5·08)	n=190; mean 7·15 (5·72)	Mean adjusted difference 0·29 (–1·01 to 1·58)	0·66
WHQ at 6 months§	n=132; mean 4·71 (4·33)	n=118; mean 4·94 (5·67)	Mean adjusted difference 0·29 (–1·19 to 1·77)	0·70
WHQ at 12 months§	n=86; mean 5·75 (5·76)	n=74; mean 5·52 (5·60)	Mean adjusted difference 1·09 (–0·65 to 2·83)	0·22
Wound pain at 3 months§	n=197; mean 18·9 (24·7)	n=202; mean 17·4 (23·1)	Mean adjusted difference –0·58 (–6·45 to 5·30)	0·85
Wound pain at 6 months§	n=139; mean 17·6 (27·3)	n=124; mean 15·3 (24·3)	Mean adjusted difference –0·28 (–7·11 to 6·54)	0·94
Wound pain at 12 months§	n=90; mean 15·9 (24·4)	n=83; mean 11·5 (18·3)	Mean adjusted difference 1·03 (–7·02 to 9·08)	0·80

HR=hazard ratio. NPWT=negative pressure wound therapy. OR=odds ratio. SWHSI=surgical wound healing by secondary intention. WHQ=Bluebelle Wound Healing Questionnaire. *Adjusted for wound size, duration of wound, and wound location as fixed effects and centre as a random effect. †Cox's proportional hazards regression. Data are 25th percentiles as fewer than half of the participants had healing confirmed in this analysis set so a median could not be reported. ‡Logistic regression using events over 12 months of follow-up. §Linear regression.

Table 2: **Primary and secondary outcomes for NPWT and usual care groups for the intention-to-treat population**

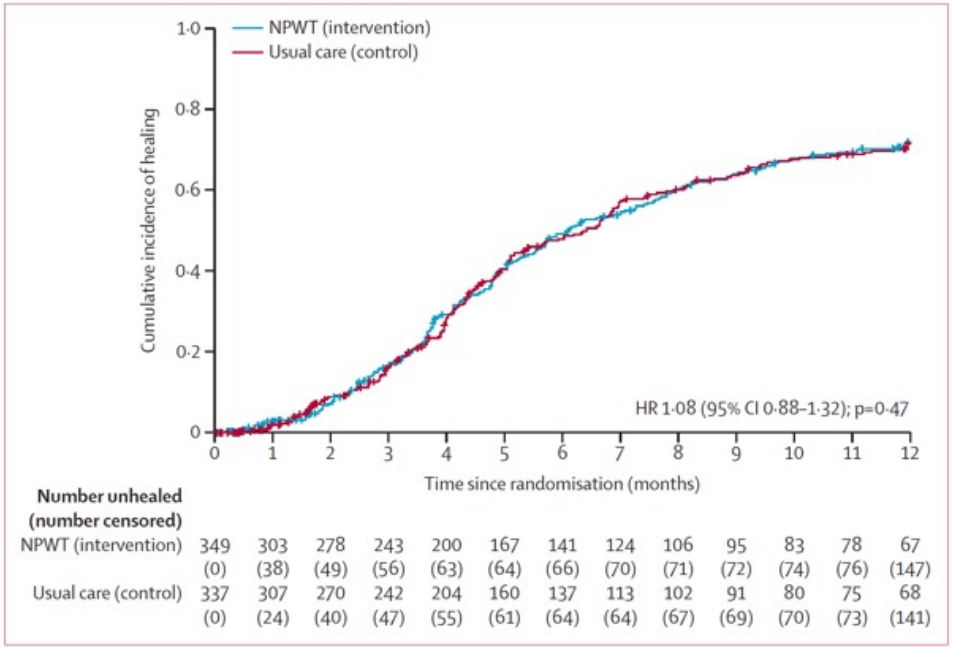

Number unhealed (number censored)													
NPWT (intervention)	349	303	278	243	200	167	141	124	106	95	83	78	67
	(0)	(38)	(49)	(56)	(63)	(64)	(66)	(70)	(71)	(72)	(74)	(76)	(147)
Usual care (control)	337	307	270	242	204	160	137	113	102	91	80	75	68
	(0)	(24)	(40)	(47)	(55)	(61)	(64)	(64)	(67)	(69)	(70)	(73)	(141)

***Figure 2*: Kaplan–Meier curve of time from randomisation to healing in SWHSI patients receiving NPWT or usual care treatments**

HR=hazard ratio. NPWT=negative pressure wound therapy. SWHSI=surgical wound healing by secondary intention.

	NPWT group (n=349)	Usual care group (n=337)	Risk difference (95% CI)
Number of participants with at least one adverse event	150 (43·0%)	139 (41·2%)	−1·7% (−9·1 to 5·7)
Number of patients with adverse events of special interest	48 (13·8%)	47 (13·9%)	0·2% (−5·0 to 5·4)
Amputation (major)*	33 (9·5%)	38 (11·3%)	..
Amputation (minor)*	7 (2·0%)	3 (0·9%)	..
Revascularisation, angioplasty	7 (2·0%)	5 (1·5%)	..
Revascularisation, angioplasty (unsuccessful)	0	1 (0·3%)	..
Revascularisation, surgical (common femoral artery endarterectomy)	1 (0·3%)	0	..
Number of participants with at least one serious adverse event	9 (2·6%)	4 (1·2%)	−1·3 (−3·4 to 0·6)
Serious adverse event category			
Death†	1 (11%)	0	..
Medication overdose	0	1 (20%)	..
Revascularisation, angioplasty	1 (11%)	1 (20%)	..
Wound bleeding	1 (11%)	0	..
Wound infection (major, debridement)	4 (44%)	0	..
Wound infection (major, endarterectomy)	0	1 (20%)	..
Wound infection (major, revascularisation)	0	2 (40%)	..
Wound infection (moderate)	1 (11%)	0	..
Wound infection (severe)	1 (11%)	0	..
Total deaths, including those recorded in other questionnaires	40 (11·5%)	43 (12·8%)	1·3% (−3·6 to 6·2)

NPWT=negative pressure wound therapy. SWHSI=surgical wound healing by secondary intention. *Amputations might not correspond exactly to those included in the secondary outcome as these are amputations at any location regardless of the SWHSI location and at any point during the study (rather than within 12 months of randomisation). †Deaths may not always have been recorded on serious adverse event forms but we have included all recorded deaths in the study in the table (including those reported in other case report forms).

***Table 3*: Adverse and serious adverse events**

Research in context

Evidence before this study

Healing by secondary intention refers to a strategy to heal wounds by leaving skin edges unopposed. This method requires the growth of granulation tissue from the base of the wound and might be preferred in areas where there is contamination, or inability to achieve primary skin cover. Healing by secondary intention is common, with an estimated prevalence of 4·1 per 10 000 population. Median time to healing for these wounds is prolonged (86 days [95% CI 75–130]), with wounds located on the foot or leg taking more than double the time to heal of those located elsewhere on the body. Additional treatments are often required, resulting in high health-care costs, and can affect patient quality of life. Alongside conventional wound dressings, an alternative called negative pressure wound therapy (NPWT) can be used as a dressing. This approach uses a controlled vacuum to remove wound fluid, which manufacturers claim results in a conducive wound healing environment. The use of NPWT for surgical wound healing by secondary intention (SWHSI) has increased rapidly in recent years, with a 23% increase in use reported between 2012 and 2014; however, there is an absence of robust supporting evidence regarding its clinical and cost-effectiveness. A Cochrane systematic review of NPWT for SWHSI identified two small, low-quality randomised controlled trials and recommended caution when interpreting the findings and that further high-quality randomised controlled trials be conducted.

Added value of this study

In this pragmatic, open-label, multicentre, parallel-group, randomised, controlled trial (SWHSI-2) we aimed to undertake the first robust evaluation of the clinical and cost-effectiveness of NPWT compared with usual care (no NPWT) in treating SWHSI. We found no evidence that NPWT reduced the time to wound healing compared with standard dressings in a population with predominantly lower limb wounds, including those with complications of diabetes. The time taken for the wounds to heal did not differ significantly between groups and there were no statistically significant differences between groups in the odds of relevant clinical secondary outcomes (readmission, reoperation, infections and antibiotic use, amputation, or death), patient-reported outcomes (Bluebelle Wound Healing Questionnaire and visual analogue scale pain scores), or masked outcome assessment using wound photographs.

After adjustment for baseline characteristics and EQ-5D-5L scores, NPWT was also found to increase patient quality of life and costs; however, these results were not statistically significant.

Implications of all the available evidence

Despite manufacturers' claims that NPWT promotes wound healing, the findings in our large study do not support this claim. NPWT does not confer an advantage in terms of time to healing or adverse events over standard care, particularly for patients with lower limb SWHSI, including those with complications of diabetes. This finding suggests that NPWT should not be considered as a first-line treatment for such patients in relation to wound healing and highlights the challenges that remain in wound care when new dressings are introduced without comparative evidence and the clear need to identify new candidate interventions for the healing of SWHSI.

PEPFAR, das ist der "U.S. President's Emergency Plan for AIDS Relief", ist die größte nationale Verpflichtung zur Bekämpfung einer einzelnen Krankheit weltweit. Es ist ein globales Programm der US-Regierung zur Bekämpfung der HIV/AIDS-Pandemie. PEPFAR ist in über 50 Ländern aktiv und hat Millionen von Menschenleben gerettet und Millionen von HIV-Infektionen verhindert.

Protecting Africa's children from extreme risk: a runway of sustainability for PEPFAR programmes

PEPFAR (President's Emergency Plan for AIDS Relief), a landmark US foreign health policy, is recognised for saving 26 million lives from HIV. PEPFAR investments have also had life-saving impacts for children across sub-Saharan Africa through childhood HIV prevention, care, and treatment, ensuring 7·8 million babies were born HIV-free, supporting 13 million orphaned and vulnerable children, and protecting 10·3 million girls from sexual abuse. In this Health Policy, we review data from UNAIDS, UNICEF, World Bank, Violence Against Children Surveys, SPECTRUM model data, and Population-based HIV Impact Assessments; synthesise PEPFAR reports; conduct in-depth interviews; search PubMed for programme effectiveness evidence; and review economic reports. PEPFAR support is associated with substantial collateral benefits for the USA and Africa, including a four-fold increase in export of US goods to Africa, and US$71·6 billion in total goods trade between the USA and Africa in 2024. PEPFAR-supported countries in Africa are committed to ownership of HIV responses by 2030—overall, PEPFAR-supported countries in sub-Saharan Africa have progressively increased their co-financing of their health systems through domestic government and private expenditure from $13·7 billion per year in 2004 to $42·6 billion per year in 2021. The feasibility of a 5-year transition to country-led sustainability is supported by evidence of innovative cost-saving models of delivery, including through faith-based and community-based organisations, and high return-on-investment for PEPFAR programmes. There are also collateral benefits of PEPFAR for US and Africa national security and health security, for example, reducing forced migration and increasing capacity to control emerging transborder infectious disease threats. Risks in sub-Saharan Africa remain acute: one in five girls (younger than 18 years) experience rape or sexual assault; one in ten children (younger than 18 years) are orphaned; and a child (younger than 15 years) is estimated to die from AIDS every 7 min. Without continued PEPFAR programmes, models predict that by 2030, an additional 1 million children will become infected with HIV, 0·5 million additional children will die of AIDS, and 2·8 million children will additionally become orphaned by AIDS. There is now an opportunity for a transformational partnership between the USA and Africa, to accelerate domestic government co-financing, private-sector investments, and charitable foundations. A 5-year progressive runway of transition can occur through continued authorisation of PEPFAR programmes, which can lead to the end of AIDS for children and families, an historic achievement.

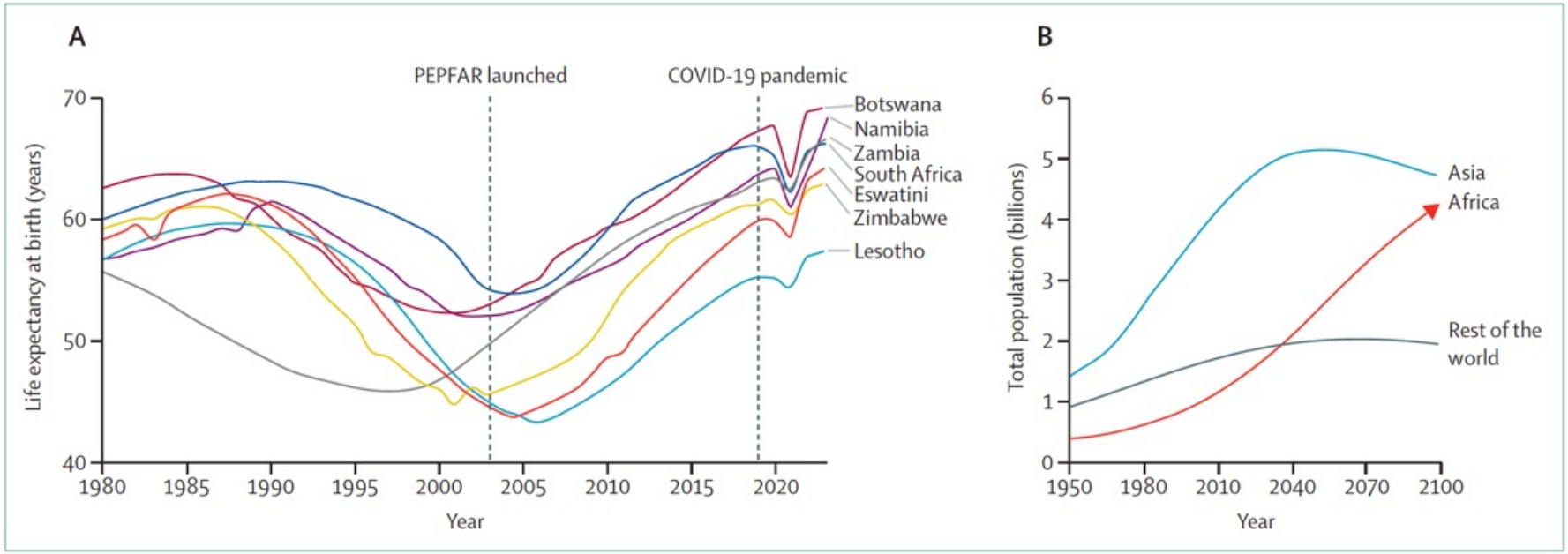

Figure 1: **Past and future demographic profiles in sub-Saharan Africa**

(A) Life expectancy at birth in seven countries in sub-Saharan Africa from 1980 to 2023, showing reductions linked to the HIV/AIDS pandemic, which rebounded following the launching of PEPFAR. Life expectancy again fell in 2019 due to the COVID-19 pandemic and rebounded. (B) Total population trends and projections from 1950 to 2100 by select global regions, with only Africa showing continued projected growth.[2] PEPFAR=President's Emergency Plan for AIDS Relief.

	Country	Programme	Design	Findings	Sustainability and reach
Economic strengthening					
Davis and Handa (2014)[15]	Kenya, Zambia, Zimbabwe, Malawi, Tanzania, Ghana Lesotho, and Ethiopia	Direct economic support (monetary transfers) for food and school	RCTs and quasi-experimental impact evaluations	Reduces child sexual abuse and exploitation; helps keep adolescents in school	Economic strengthening services including direct transfers, school fees, and microfinance programmes were provided for about 1·55 million girls (aged 10–24 years) in DREAMS and 4·35 million children (aged 0–17) in the OVC programme
Kim (2009)[16]	South Africa	Microfinance for mothers	Cluster RCT comparison of three randomly selected clusters: microfinance and gender norms, microfinance, and control	Microfinance and gender equity training reduce reoccurrence of intimate partner violence by 50%, reduces HIV risk, and improves household income	Scaled up as a component DREAMS programmes to adolescent girls and young women
Family strengthening					
Cluver (2018)[17]	South Africa and Tanzania	Parenting for lifelong health and ParentApp Digital	Cluster RCTs	Reduces child sexual abuse incidence by 57%; ten sessions cost of less than US$6; reduces abuse and substance use; improves parental supervision, household economic welfare, and adolescent sexual violence prevention	Over 5 years, DREAMS and OVC provided training for 448 000 people; overall, 8 million families were reached in more than 35 countries;[18] the Tanzanian Government has launched national programme
Vandenhoudt (2010)[19]	Kenya	Families Matter	Pre-design and post-design comparison of baseline measures for outcomes before programme with those after programme	Improves parent–child communication about sexual risk and abuse reduction and HIV prevention	Replicated in eight countries, reaching more than 400 000 people
Awareness, mentoring, or screening programmes					
Jewkes (2008)[20]	South Africa	Stepping Stones	Cluster RCT	Peer mentoring reduces herpes simplex virus-2 incidence (ie, sexually transmistted infections are an HIV cofactor) and intimate partner violence	DREAMS supported more than 10 000 adolescent girls and young women as mentors to deliver HIV prevention programmes to peers
Skevington (2013)[21]	India, Gambia, South Africa, Ethiopia, Angola, Tanzania, Uganda, Fiji	Stepping Stones	Systematic review	Peer mentoring reduces infection rates of herpes simplex virus-2 and stigma; improves communication about HIV risks	In 2023, DREAMS delivered HIV prevention programmes to 1·4 million girls in mentor-led safe spaces
Teaching boys and girls to use sexual violence prevention skills					
Baiocchi (2017)[22]	Kenya	No Means No Worldwide	Cluster RCT	Reduces child sexual abuse incidence by 42%	OVC and DREAMS reached more than 13 million girls in 5 years; support for programmes has transitioned to the Nigerian Government
Jones (2021)[23]	USA	Coaching Boys into Men	Cost-benefit analysis of two RCTs	Reduces perpetration of sexual violence, at cost-benefit of up to $2·4 million per 1000 participants	Tanzania National Institute of Education and Zambia Ministry of Health supports the programme; in 2023, Rwanda Ministry of Education committed to scale-up the programme over 3 years
Community protection					
Abramsky (2014)[24]	Uganda	SASA! Raising Voices and SASA! Faith	Cluster RCT	Community mobilisation of influencers reduced intimate partner violence by 52%	SASA! Raising Voices has been implemented by faith and community leaders in Uganda, Kenya, Zambia, Ethiopia, Malawi, and Tanzania
Kanagasabai (2023)[25]	Zambia	Faith Matters!	Pre-design and post-design comparison of baseline measures for outcomes before programme with those after programme	Faith leaders increased their conversations with youth about sexual abuse and HIV 3 months after the intervention, compared with baseline	Scaled within Zambia through interfaith network and expanded to Kenya, Uganda, and Zimbabwe

(Table 1 continues on next page)

	Country	Programme	Design	Findings	Sustainability and reach
(Continued from previous page)					
Accelerating HIV treatment adherence, viral load suppression, prevention for children and adolescents, and vertical transmission prevention					
Tafere et al (2023);[26] WHO (2019)[27]	Kenya and Ethiopia	Operation Triple Zero	Pre-design and post-design (Kenya) and comparison study (Ethiopia)	Kenya: VLS increased from 65% to 80% in children (aged 10–14 years) and 66% to 84% in adolescents (aged 15–19 years); Ethiopia: 92·4% in OTZ group *vs* 84·3% in VLS group	Ten countries with more than 1000 clinics serving more than 100 000 young people living with HIV
Willis et al (2019);[28] Mavhu et al (2020);[29] WHO (2019)[27]	Zimbabwe	CATS within the Zvandiri group-based support programme	Pre and post design, and RCT	Adherence to antiretrovirals increased from 42% to 72% after the CATS–Zvandiri programme; RCT shows CATS participants were 3·9 times more likely to adhere to antiretrovirals	Since 2004, Zimbabwe has scaled this programme from 51 of 63 districts, reaching 45 000 children and adolescents living with HIV; expanded to Eswatini, Mozambique, Rwanda, Uganda, Namibia, and Ghana
Makangila et al (2023)[30]	Zambia	Circle of Hope, faith-led and community-led posts	Non-randomised programme evaluation comparison	Faith-led and community-led community posts were more successful in identifying cases compared with provincial community posts in both men (32·5% *vs* 9·5%) and adolescent girls and young women (31·2% *vs* 7·3%); VLS was higher in faith and community-led community posts than in provincial community posts	Scaled in Zambia to seven of ten provinces by Zambian government; south-to-south replication in Zimbabwe, South Sudan, Kenya, Cote d'Ivoire; and adaptation into youth-friendly centres for girls (Malaika Houses) and boys (Destiny Houses)
Allison et al (2022)[31]	South Africa, Uganda, Kenya, Brazil, Thailand, and USA	Oral PrEP adherence	Systematic review of 29 studies (seven RCT, 19 cohort, and three other)	Adolescent and young adult adherence similar across countries, overall 64%	As of Dec 1, 2024, PEPFAR had newly enrolled 25 million people on PrEP (including oral or injectables)
Ford et al (2014)[32]	Included high-income, upper-middle-income, lower-middle-income, and low-income countries	HIV PEP adherence to 28-day course	Systematic review of 97 RCTs and non-randomised studies reporting PEP completion rates	PEP completion rates for were 36·6% for adolescents (95% CI 4·0–69·2), 64·0% for children (41·2–86·8), and 40·2% for sexual assault victims (31·2–49·2)	Adherence support is recommended for victims of sexual assault and adolescents as their adherence is poor; 2024 WHO Guidelines for Post-Exposure Prophylaxis of HIV[33] include regimens and considerations
Fonner et al (2023)[34]	Included countries in Africa, Asia, Latin America, and the USA	CAB-LA given every 2 months	Systematic review of safety and efficacy based on four double-blind RCTs	The pooled effect comparing CAB-LA with oral PrEP yielded a relative risk of 0·21 (0·07–0·061) showing a 79% reduction in HIV acquisition risk	WHO used Fonner et al (2023)[34] as basis for WHO guidelines on PrEP, determining CAB-LA to be safe and effective; PEPFAR has supported roll-out in Zimbabwe, Malawi, and Zambia
Johnson et al (2024)[35]	South Africa	CAB-LA given every 2 months for pregnant and breastfeeding women and their infants	Modelling study comparing CAB-LA, oral PrEP, and allowing choice between oral PrEP or CAB-LA	CAB-LA reduced risk of HIV acquisition during pregnancy and breastfeeding by 41·2% (95 CI 19·8–65·0); by 12·6% (6·0–19·4) in infants at or before birth; and by 29·5% (13·9–46·8) through breastmilk, performing substantially better than oral PrEP, but similar to the group given a choice	Increased use of CAB-LA to prevent vertical transmission during pregnancy and breastfeeding would be relevant for sub-Saharan Africa, where HIV acquisition during pregnancy and breastfeeding are important drivers of vertical transmission
Endershaw (2024)[36]	Sub-Saharan Africa	Consistent condom use among people living with HIV	Systematic review and meta-analysis of 33 studies	Pooled prevalence of 42·5% (95% CI 20·3–64·7) for consistent condom use	Study examined consistent condom use with non-marital partners

Examples chosen as primary PEPFAR interventions recommended in COP guidance from 2021–24. CAB-LA=long-acting injectable cabotegravir. CATS=Community Adolescent Treatment Supporters. COP=Country Operating Plan. DREAMS=determined, resilient, empowered, AIDS-free, mentored, and safe. OTZ= Operation Triple Zero. OVC=orphans and vulnerable children. PEPFAR=President's Emergency Plan for AIDS Relief. PEP=post-exposure prophylaxis. PrEP=pre-exposure prophylaxis. RCT=randomised controlled trials. VLS=viral load suppression.

Table 1: **Example evidence-based PEPFAR programmes**

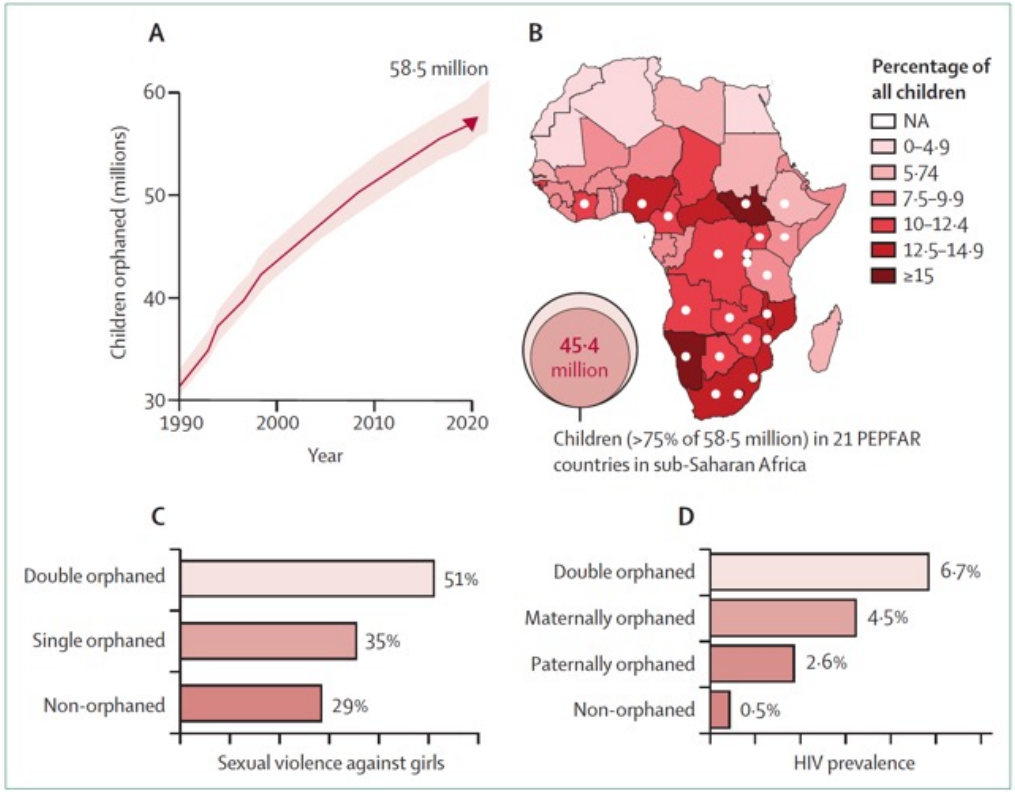

Figure 2: **Trends in all-cause orphanhood in sub-Saharan Africa, 2022**
(A) Distribution of orphanhood in sub-Saharan Africa shows 77·6% of orphans in countries with PEPFAR country offices. Grey area=95% CI.[14] (B) Orphanhood prevalence in 2022 (as shown by white circles). (C) Sexual abuse and violence among orphaned girls (age 13–24 years) in Kenya.[42] (D) HIV prevalence among orphaned children in high-burden locations. Includes Population-based HIV Impact Assessment Survey data from 14 countries (Cameroon [2017], Côte d'Ivoire [2017], Eswatini [2017], Ethiopia [2018], Kenya [2018], Lesotho [2017], Malawi [2016], Namibia [2017], Nigeria [2021], Rwanda [2019], Tanzania [2017], Uganda [2017], Zambia [2016], and Zimbabwe [2016]). Data were standardised using biomarker weights within each survey, the calculations used weighted proportion of type of orphan and pooled them across surveys to give an estimate representative across countries, then calculations used weighted HIV prevalence by orphanhood group pooled across surveys.[14] NA=not applicable. PEPFAR=President's Emergency Plan for AIDS Relief.

	Population (aged 0–17 years)[41]	Number of orphans (95% CI)[41]	Orphanhood prevalence (95% CI)*
Nigeria	108 864 080	13 900 000 (13 700 000–14 000 000)	12·77% (12·58–12·86)
Democratic Republic of the Congo	53 808 048	5 680 000 (5 580 000–5 770 000)	10·56% (10·37–10·72)
Ethiopia	58 480 672	2 990 000 (2 860 000–3 200 000)	5·11% (4·89–5·47)
Tanzania	32 182 156	2 660 000 (2 510 000–2 800 000)	8·27% (7·80–8·70)
Uganda	24 391 759	2 500 000 (2 280 000–2 680 000)	10·25% (9·35–10·99)
South Africa	19 566 105	2 480 000 (2 320 000–2 740 000)	12·67% (11·86–14·00)
Kenya	24 461 951	2 370 000 (2 210 000–2 560 000)	9·69% (9·03–10·47)
Mozambique	16 854 766	2 200 000 (2 020 000–2 410 000)	13·05% (11·98–14·30)
Angola	18 263 391	1 850 000 (1 800 000–1 890 000)	10·13% (9·86–10·35)
Côte d'Ivoire	14 609 980	1 680 000 (1 620 000–1 740 000)	11·50 % (11·09–11·91)
Cameroon†	13 458 393	1 420 000 (1 330 000–1 510 000)	10·56%
Malawi	10 127 604	1 270 000 (1 150 000–1 420 000)	12·54% (11·36–14·02)
Zambia	9 950 975	1 000 000 (930 000–1 140 000)	10·05% (9·35–11·46)
Zimbabwe	7 790 617	850 000 (760 000–1 010 000)	10·91% (9·76–12·96)
South Sudan	5 353 260	830 000 (810 000–860 000)	15·50% (15·13–16·06)
Burundi	7 049 655	630 000 (610 000–650 000)	8·94% (8·65–9·22)
Rwanda	6 168 602	480 000 (450 000–530 000)	7·78% (7·30–8·59)
Namibia	1 247 982	210 000 (190 000–240 000)	16·83% (15·22–19·23)
Lesotho	949 146	180 000 (190 000–240 000)	18·96% (16·86–22·13)
Eswatini	491 984	120 000 (110 000–140 000)	24·39 (22·36–28·46)
Botswana	940 827	100 000 (94 000–130 000)	10·63 (9·99–13·82)
Total	435 011 958	45 400 000 (45 100 000–45 700 000)	10·44 (10·31–10·56)

PEPFAR=President's Emergency Plan for AIDS Relief. *Orphanhood prevalence was calculated by dividing number of orphans by population of children aged 0–17 years. Totals were calculated by summing country central estimates, with the confidence interval for the total calculated assuming independent normal distributions for each country. †Estimates for Cameroon are not reported in the UNICEF dataset; therefore, the central estimate was obtained from the SPECTRUM model. Totals were calculated by summing up the country's central estimates, with the confidence interval for the total calculated assuming independent normal distributions for each country.

Table 2: **Orphanhood prevalence due to all causes for 21 countries in sub-Saharan Africa with PEPFAR Country Offices, 2022**

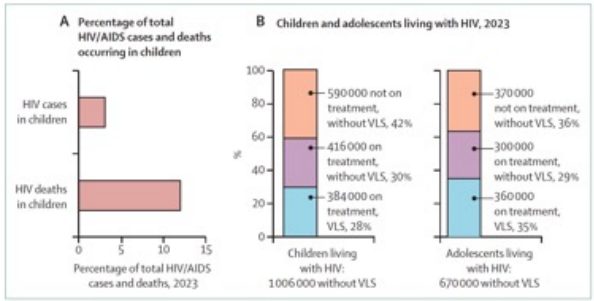

Figure 3: **HIV risks among children**
(A) Percentage of total HIV/AIDS cases and deaths in children (aged 0–14 years) globally. (B) Children and adolescents living with HIV. There are high numbers of children (aged 0–14 years) and adolescents (aged 15–19 years) living with HIV who are not virally suppressed (including both those not on treatment and those reported to be on treatment), with a total of more than 1·5 million children and adolescents.[30] VLS=viral load suppression.

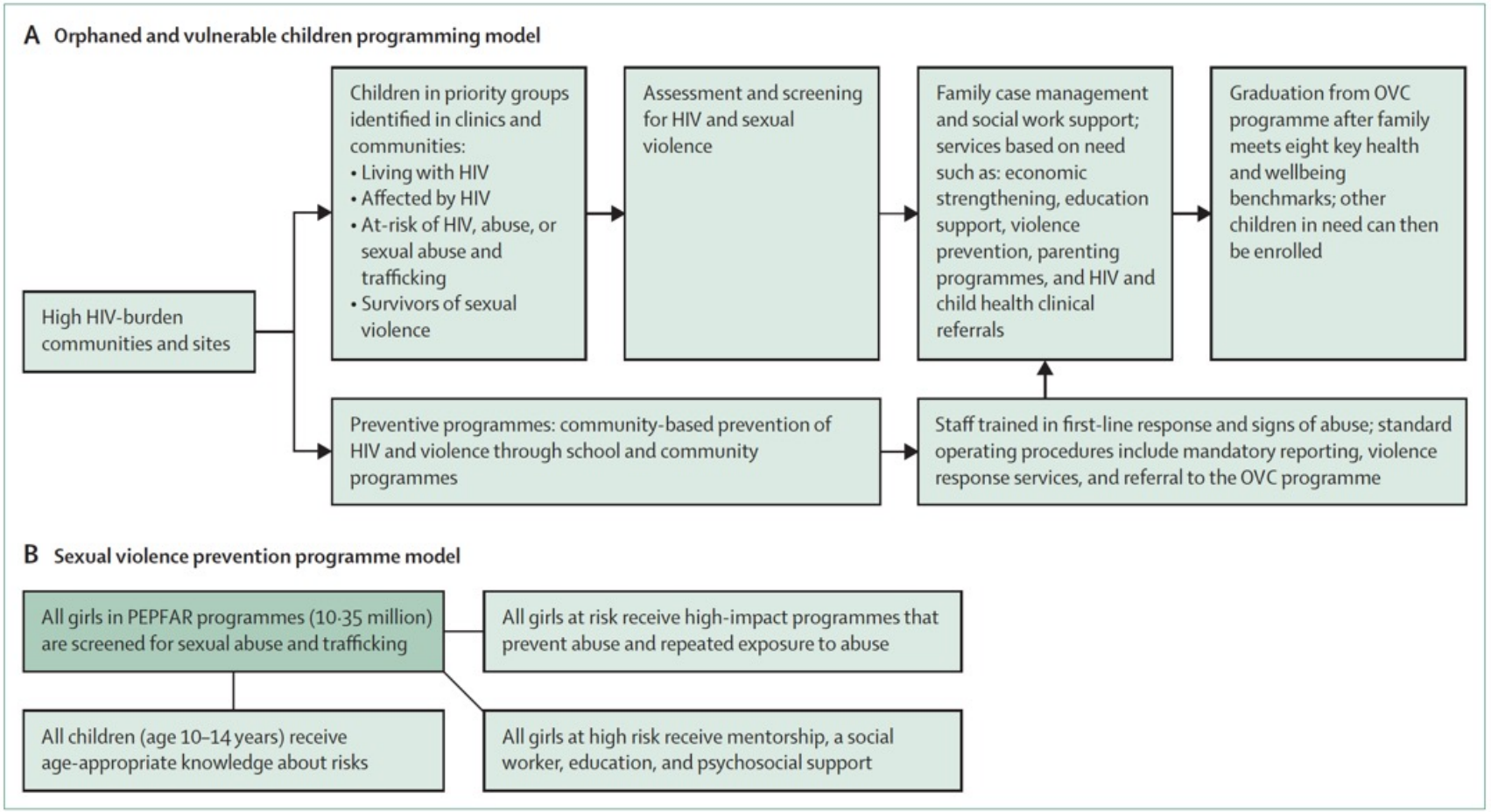

Figure 4: **PEPFAR models for OVC services and sexual violence and HIV prevention for girls, youth, and children**

(A) PEPFAR OVC screening and service model that guides identification, care, and graduation of beneficiaries. (B) PEPFAR's model for protecting adolescent girls, youth, and children from sexual violence and HIV through the DREAMS and OVC programmes. PEPFAR's system is one of screening, referral, prevention of repeated abuse, and support for children and adolescents through faith and community-based organisations (appendix). DREAMS=determined, resilient, empowered, AIDS-free, mentored, and safe. OVC=orphans and vulnerable children. PEPFAR=President's Emergency Plan for AIDS Relief.

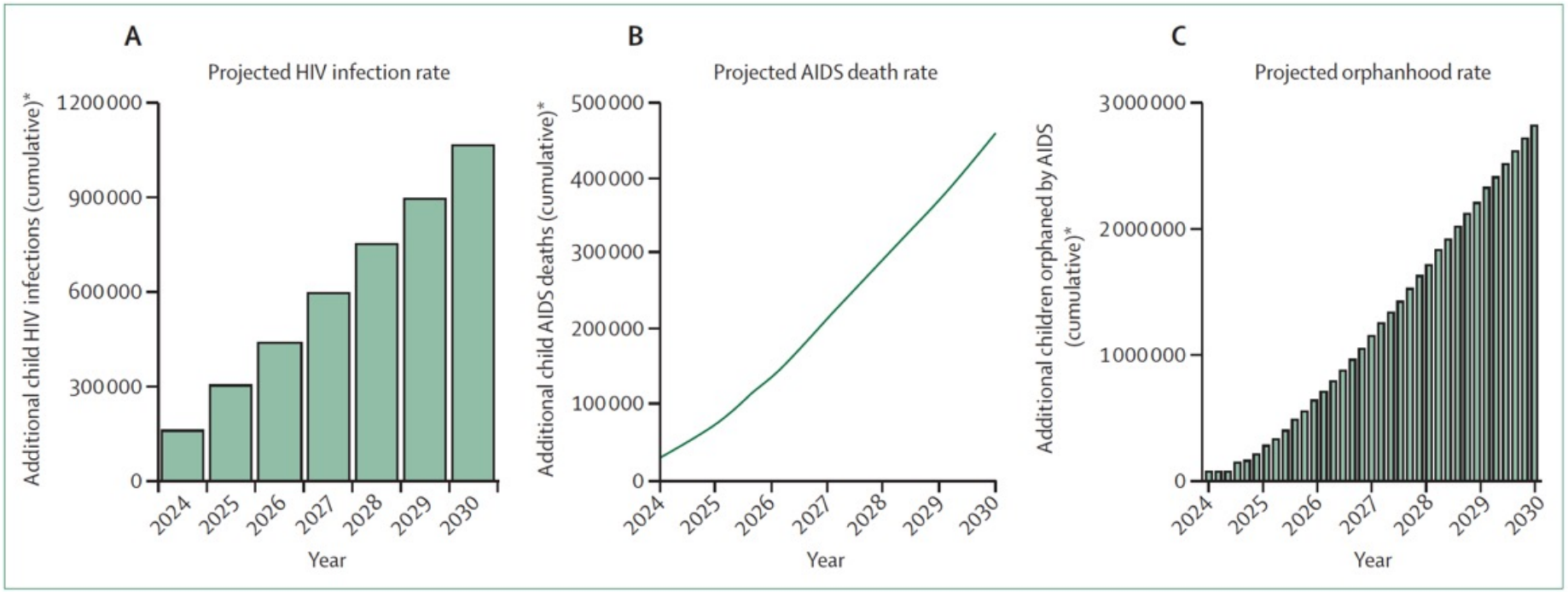

Figure 5: **Children are at extreme risks of HIV infection without PEPFAR**

(A) Without PEPFAR, 1 million more new child HIV infections, (B) 460 000 more child deaths caused by AIDs, and (C) 2·8 million more children orphaned by AIDS, are all projected by 2030. Projection scenarios for 2024–2030 were based on modelling the complete cessation of PEPFAR in 2024 against the counterfactual of constant coverage of five interventions (preventing perinatal transmission to reduce child infections; paediatric antiretroviral therapy to reduce child death; adult antiretroviral therapy to reduce adult death and AIDS orphans; voluntary medical male circumcision; and key populations services to reduce adult prevalence of HIV) at the 2022 level (a combination of both PEPFAR and non-PEPFAR interventions). To model the number of children affected by the immediate and complete cessation of PEPFAR, the PEPFAR 2022 services were subtracted from the anticipated 2024 coverage in the absence of PEPFAR for the modelled interventions and carried that coverage level forward through 2030.[5] PEPFAR=President's Emergency Program for AIDS Relief. *Cumulative deaths 2024–30 among children aged 0–14 years.

Conclusion: a 5-year runway to sustainability for PEPFAR can protect the health and future of the USA's and Africa's children and adolescents

The findings of this Health Policy lead to one overwhelming conclusion: that continuation of PEPFAR programmes, and investment in a runway of sustainability through progressively increased domestic co-financing of PEPFAR, are crucially important for both the USA and Africa. PEPFAR brings multiple benefits. First, the direct benefits of the programme in saving families with children, protecting orphaned children, preventing devastating consequences for women who are pregnant and breastfeeding, as well as their babies, and protecting girls and adolescents from sexual trafficking and abuse. Second, the indirect benefits within each country in short-term and long-term economic gains, and in stronger responses to transborder disease outbreaks. Third, the reciprocal benefits of soft power—strong trade partners and geopolitical stability within a context of the largest youth cohort in Africa's history. Now is the time to capitalise on unified leadership, and on PEPFAR's unparallelled success, to ensure prosperity, strength, and safety for both the USA and Africa.

While there were concerns raised by some within the Trump administration and in Congress about PEPFAR's future, PEPFAR is a permanent part of U.S. law and has been repeatedly reauthorized. PEPFAR continues to operate as long as funding is appropriated, and it has been included in recent appropriations acts. Therefore, it is unlikely that Trump will completely eliminate PEPFAR.

nature

How we taste sweetness: long-sought structure of human receptor mapped at last

3D structure of the tongue's sweet-sensing protein could guide future food designs.

The structure of human sweetness

Highlights

- Two GPCR subunits assemble to recognize sweet ligands
- The TAS1R2 subunit binds the ligands and couples to the G protein
- A common binding pocket recognizes sucralose and aspartame
- 3D variability analysis shows coordinated structural changes between the subunits

Summary

In humans, the detection and ultimately the perception of sweetness begin in the oral cavity, where taste receptor cells (TRCs) dedicated to sweet-sensing interact with sugars, artificial sweeteners, and other sweet-tasting chemicals. Human sweet TRCs express on their cell surface a sweet receptor that initiates the cascade of signaling events responsible for our strong attraction to sweet stimuli. Here, we describe the cryo-electron microscopy (cryo-EM) structure of the human sweet receptor bound to two of the most widely used artificial sweeteners—sucralose and aspartame. Our results reveal the structural basis for sweet detection, provide insights into how a single receptor mediates all our responses to such a wide range of sweet-tasting compounds, and open up unique possibilities for designing a generation of taste modulators informed by the structure of the human receptor.

Human Sweet Taste Receptor

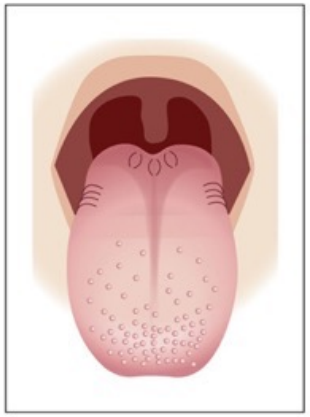

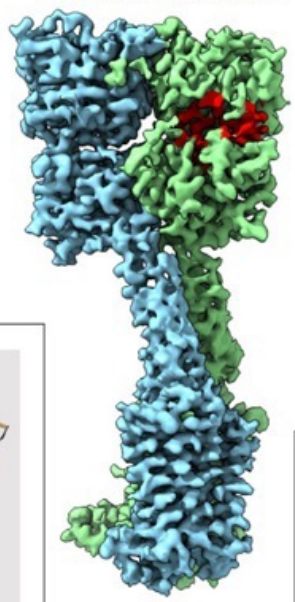

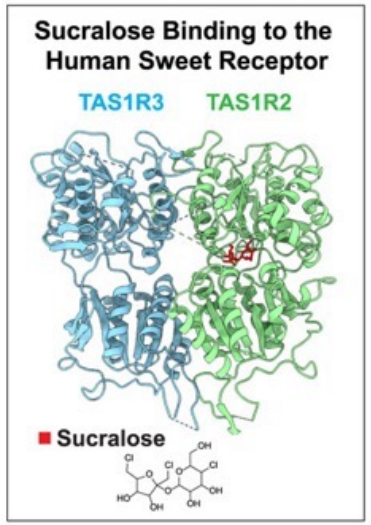

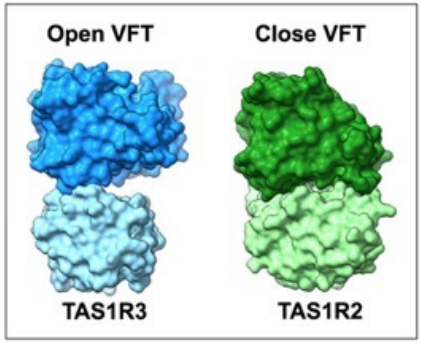

Discussion

The taste of sweet permeates every aspect of human experience, from the taste of a mother's milk to the current impact of sugar in packaged products and drinks in human health. Notably, a single receptor (TAS1R2+3) expressed in sweet taste receptor cells (TRCs) in the tongue and oral cavity mediates the taste of sweet in humans and other mammals.

The receptor, composed of two GPCR subunits, one unique (TAS1R2) and one shared with the umami receptor (TAS1R3), has the essential role of detecting and driving appetitive and consummatory responses to the most basic sources of metabolic energy (e.g., glucose, sucrose, lactose, and other sugars). Consequently, its primary structure is conserved among mammals, including in humans. Not surprisingly, there is significant polymorphism in the receptor in the human population, perhaps accounting for some of the variability in our "sweet-tooth" (i.e., the unique differences in sensitivity to sweet stimuli between subjects). While studies attempting to link polymorphic variants to differences in human sweet sensitivity are still very limited, a number of promising studies may provide additional insights.

We discovered and de-orphaned the TAS1R2+3 mammalian sweet taste receptor over 20 years ago and validated its essential role in sweet detection and sweet-evoked responses using a combination of genetics, cell-based assays, and physiological and behavioral studies. Non-caloric artificial sweeteners entered consumer products over 60 years ago. Artificial sweeteners can be 100× (e.g., saccharin, aspartame, and sucralose) to over 10,000× (e.g., neotame) more potent than sucrose.

5 surprising things linked to cancer — and what to know about them

Almost one-third of Americans have a tattoo, and 22 percent have more than one, according to the Pew Research Center. Women and people under 50 are more likely than other people to get inked.

But if you're debating between a discreet flower near your ankle or a full-sleeve homage to "Game of Thrones," you should also know about a recent study.

In an analysis of about 5,600 people in Sweden, those with lymphoma were 21 percent more likely to have received a tattoo in the past compared with those who did not have lymphoma. The size and color of the tattoo did not appear to make a difference.

A small Danish study of twins also found an association between tattoos and lymphoma as well as between tattoos and skin cancer, possibly because the tattoo ink could make it harder to spot smaller cancers.